Option Pricing on Backward-Looking Rates

Lisa de Miranda

In corporation with
ING Bank, Amsterdam

Faculty EEMCS, Delft University of Technology

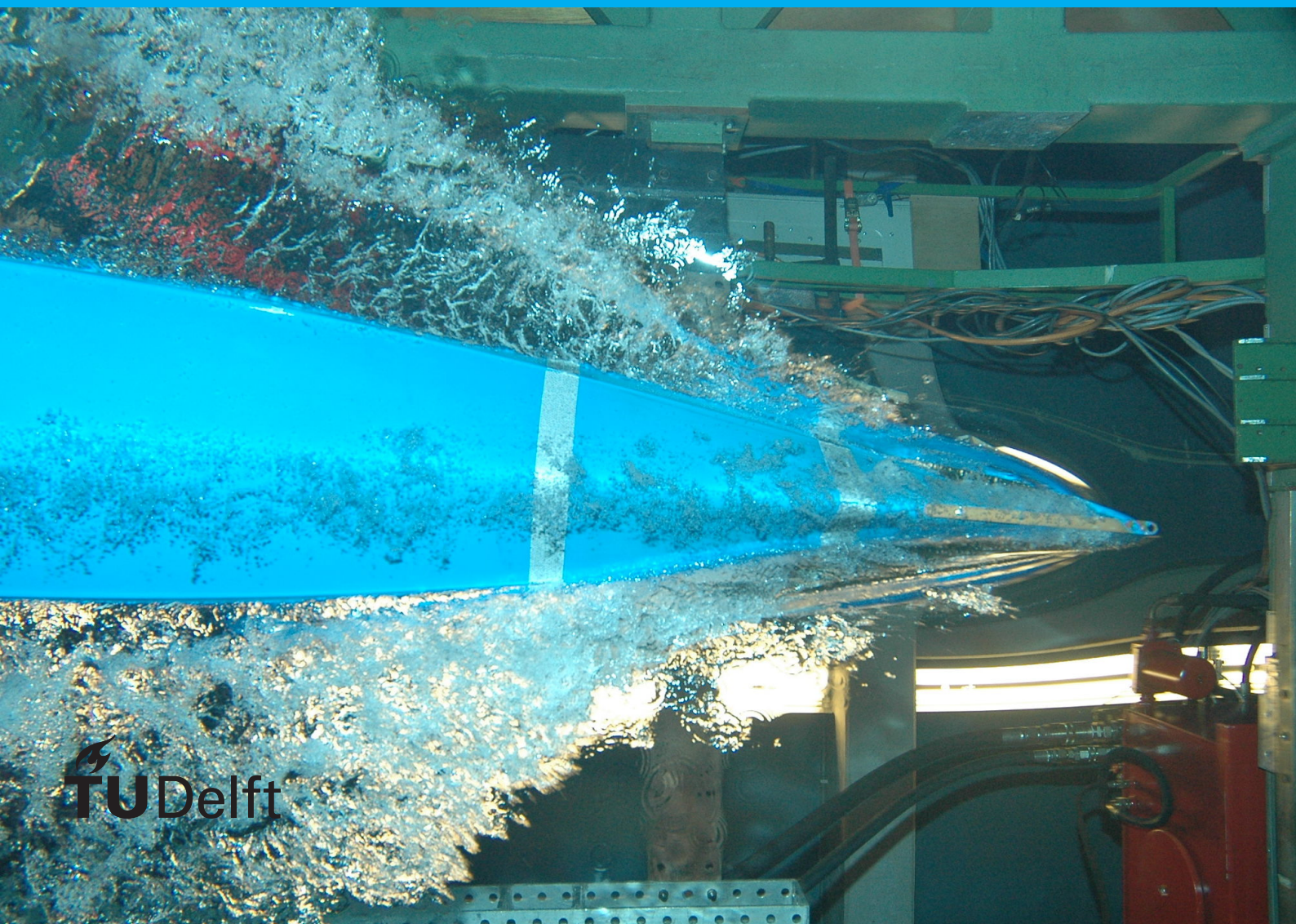

Option Pricing on Backward-Looking Rates

by

Lisa de Miranda

to obtain the degree of Master of Science
at the Delft University of Technology,
to be defended publicly on Friday March 19, 2021 at 15:00.

Student number:	4484576	
Project duration:	May 6, 2020 – March 19, 2021	
Thesis committee:	Prof. dr. ir. C.W. Oosterlee,	TU Delft, supervisor
	Dr. ir. M. Keijzer,	TU Delft
	Dr. M. Möller,	TU Delft
	Ir. B. Hoorens,	ING Bank, Amsterdam
	Dr. A. Kostiuk,	ING Bank, Amsterdam

TU Delft

Abstract

This thesis is devoted to option pricing on backward-looking rates. For the last decades, interest rate products were often linked to IBOR rates. IBORs are short-term borrowing rates charged between global banks in the unsecured interbank market. The purpose of this thesis is to compare the Hull-White model to the Black-Karasinski model for the pricing of caps/floors on compounded rates. Both models are so-called short-rate models, which are widely used for interest rate modelling. Due to the IBOR reform, new products are expected to appear in the market. One type of these products is caps/floors linked to the new Risk-Free Rate (RFR). The new RFRs will be in-arrears backward-looking rates and, as a consequence, have an impact on the choice of pricing models.

This thesis considers caps/floors on the new compounded RFR rates. For both models various pricing techniques for caps/floors on compounded rates are investigated. For the Hull-White model, the pricing kernel approach and a Monte Carlo simulation are explored. The pricing kernel approach yields an analytic formula for caps/floors on compounded rates. This formula is also used for the comparison. For the Black-Karasinski model, the pricing kernel approach, the trinomial tree method and the Monte Carlo simulation are considered. The pricing kernel approach yields a semi-analytic formula for caps/floors on compounded rates. However, in practice the computation time of this semi-analytic formula turned out to be substantial. Further, despite the fast computation time of the trinomial tree for LIBOR caps/floors, the trinomial tree method is rather slow for the caps/floors on compounded rates. As a result, the Monte Carlo simulation is the most suitable pricing technique, along the three explored methods, for caps/floors on compounded rates under the Black-Karasinski model. Therefore, the Monte Carlo simulation is used for pricing caps on compounded rates in the model comparison.

Since there exists no liquid market yet for caps/floors linked to the new RFR, the models are calibrated to a proxy market. First, the Black-Karasinski model is calibrated to the proxy market using a heuristic approach. This heuristic approach is chosen as a compromise between computation time and accuracy. Then, the Hull-White model is calibrated to the Black-Karasinski model using the stripping method. Having both models calibrated, the price of caplets/floorlets on compounded rates are calculated. Thereafter, these prices are inverted to Bachelier implied volatilities for a uniform comparison. From the comparison of the two models, a difference in Bachelier implied volatility is observed in a range of -4 to 4 bps. This is of one order less than the volatility itself.

Preface

This thesis has been submitted for the degree of Master of Science in Applied Mathematics from the Delft University of Technology. First of all, I would like to thank professor Kees Ooslerlee of the Numerical Analysis group of DIAM. With the help of Kees I got in contact with ING and was able to do my thesis in the Risk Trading Quants team of ING Bank, Amsterdam. Moreover, his feedback and insights were extremely valuable and helpful for writing this thesis. Second, I would like to thank Anton Kostiuk and Bart Hoorens for the great supervision at ING. Without your help this thesis would not have been a success. Further, Anton and Bart made me feel welcome in the team, even though everything was online due to COVID. Moreover, their positivity helped me to get through my thesis. Third, I would like to thank Colin Turfus for providing relevant chapters of his book before it was published. Furthermore, I would like to thank Marleen Keijzer and Matthias Möller for being part of my thesis committee. Last, but certainly not least, I would like to thank my friends and family for their support during this period.

Lisa de Miranda
Delft, March 2021

Contents

Acronyms

ATM At the Money.

bps Basis Points.

EONIA Euro OverNight Index Average.

ESTR Euro Short Term Rate.

IBOR Inter-Bank Offered Rate.

ITM It the Money.

LIBOR London Inter-Bank Offered Rate.

MC Monte Carlo.

ODE Ordinary Differential Equation.

OIS Overnight Index Swap.

OTM Out of the Money.

PDE Partial Differential Equation.

RFR Risk-Free Rate.

SABR Stochastic Alpha, Beta, Rho.

SDE Stochastic Differential Equation.

USD SOFR United States Dollar Secured Overnight Financing Rate.

1 Introduction

This thesis is devoted to option pricing on backward-looking rates. For the last decades, interest rate products were often linked to Inter-Bank Offered Rate (IBOR) rates. IBORs are short-term borrowing rates charged between global banks in the unsecured interbank market. One of the well known IBORs is the London Inter-Bank Offered Rate (LIBOR). The LIBOR rates are calculated for various currencies and borrowing periods, ranging from one day to one year. The calculation of the LIBORs is based on the quotes of a set of panel banks. The LIBOR rates were traditionally used as reference rates for different interest rate products. The LIBOR rates are forward-looking rates and, thus, are fixed at the beginning of the period.

LIBOR rates have been subject to manipulations. In the past, some banks have already paid large fines for manipulating LIBOR rates for their own gain. As a consequence, the LIBOR rates will be reformed and replaced by the new Risk-Free Rate (RFR). In general, LIBOR rates were planned to be discontinued at the end of 2021. The new RFR will become the main reference rate for new interest rate products. Moreover, the new RFR will have to replace the LIBOR for legacy contracts. In the Eurozone, this new RFR is called the Euro Short Term Rate (ESTR) and will replace the current Euro OverNight Index Average (EONIA) rate. The ESTR will be based on unsecured overnight transactions. The compounded rate linked to the new RFR will thus be an in-arrears backward-looking rate. In contrast to the LIBOR rate, this compounded rate is only known at the end of the period since it is based on the new RFR, which is published daily.

Chapter 2 provides an introduction to derivatives pricing and is recommended for people who are not familiar with interest rate derivatives. Within this chapter the definition of the zero-coupon bond and different interest rates are introduced. Furthermore, a number of plain vanilla interest rate derivatives and their pricing formulae are discussed. These pricing formulae can, for example, be obtained with the Black and Bachelier models.

In this thesis, we focus on interest rate caps/floors. The LIBOR caps/floors provide an insurance against the LIBOR rate rising above/falling below a certain level. However, since the LIBOR rate will cease to exist, new products are expected to appear in the market. One of these products will be caps/floors on compounded rates linked to the new RFR. These caps/floors linked to the new RFR will provide an insurance against the compounded average of the new RFR rising above/falling below a certain level. The IBOR reform has implications for the existing derivatives linked to the LIBOR rate, as they will be amended to reference to compounded new RFRs. Moreover, the IBOR reform has implications for new derivatives linked to the new RFR and their pricing models. The LIBOR rates are forward-looking and are fixed at the beginning of the accrual period. The compounded rates linked to the new RFRs, however, are in-arrears backward-looking and are calculated at the end of the accrual period. This is graphically illustrated in Figure 1.1. The compounded rate linked to the new RFR rate fixes gradually during the whole accrual period, and therefore violates the assumptions of the Black and Bachelier type models. As a consequence, standard models like the Black and Bachelier models cannot directly be used anymore. Therefore, in this thesis, term structure models are used to price derivatives linked to the new RFRs. In general, numerous models can be applied for this purpose. However, this thesis focuses only on the so-called short-rate models.

There are two main research objectives. The first main research objective is how to price options

on backward-looking rates efficiently under various models. The second main research objective is a model comparison to determine model risk. In this thesis, two different short-rate models are considered. For this comparison, pricing techniques are required to calculate the price of caps/floors on compounded rates. Based on the first main research objective, two pricing techniques are used for the comparison between the models.

The first model is the one-factor Hull-White model. An advantage of the Hull-White model is the existence of an analytical zero-coupon bond price formula due to the affine nature of the model. Further, the Hull-White model exhibits mean reversion, which is desirable in interest rate modelling. Moreover, the Hull-White model is a normally distributed model and has an analytical formula for caps/floors. The model is chosen since it can be used as a potential interpolation model for cap/floor volatilities. Since the market generally quotes vanilla options on a grid of strikes and maturities, prices of other options have to be inferred from them based on interpolation. Therefore, one prefers an analytically tractable model, which is the case for the one-factor Hull-White model. A detailed discussion about the Hull-White model can be found in Chapter 3.

The second model we consider, is the Black-Karasinski model. This is a log-normally distributed model that also exhibits mean reversion. A drawback of the Black-Karasinski model in comparison to the Hull-White model is the absence of an analytical formula for the zero-coupon bond prices. This model is considered because of the existence of a semi-analytic pricing formula for caps/floors derived by Turfus, 2021 using the pricing kernel approach. However, it turns out that in practice the computation time is substantial. Therefore, we also consider numerical methods. More details about the Black-Karasinski model and the pricing methods are presented in Chapter 4.

Chapter 5 is dedicated to a model comparison between the Hull-White and Black-Karasinski models. As mentioned before, the Hull-White model might be used for interpolation, which can lead to potential model risk. Therefore, this model comparison is done to infer the model risk. The foundations of this comparison, like pricing techniques, etc., are laid down in Chapters 3 and 4 corresponding to the Hull-White and Black-Karasinski models, respectively. In order to make a comparison, the models have to be calibrated to market data. However, at the moment, there exists no liquid market for derivatives linked to the new RFR. Therefore, a quasi-calibration to a proxy market is used, in order to obtain realistic option prices for the model comparison. For more details, we refer to Chapter 5.

Lastly, a conclusion about the two models is given in Chapter 6. This chapter also includes recommendations for further research.

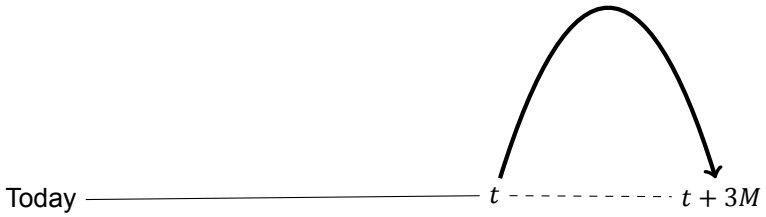

(a) Rate definition of the $3M$ LIBOR rate.

(b) Rate definition of the $3M$ compounded rate linked to the new RFR.

Figure 1.1: For a derivative linked to the $3M$ LIBOR rate, the payoff is known at time t since the LIBOR fixes at the beginning of the period. For a derivative linked to a compounded rate, the payoff is only known at the end of the period.

2

Introduction to interest rate derivatives

In this chapter we give an introduction to interest rates, interest rate derivatives, pricing techniques and numerical methods for the derivative pricing. Below we focus on notions and tools needed for our further considerations, a more extensive introduction can be found in e.g. Andersen and Piterbarg, 2010. We begin with the definition of a zero-coupon bond and different interest rates in Section 2.1, which we use during this thesis. In Section 2.2 we present the basics of derivative pricing and Section 2.3 is devoted to various basic interest rate products and their pricing formulae. Last, Section 2.4 introduces various pricing techniques that can be used for option pricing.

2.1. Definitions

We start with the definition of the simplest product, namely a zero-coupon bond.

Definition 2.1. *A **zero-coupon bond** is a product without coupon payments which pays 1 at maturity. The t-value of a zero-coupon bond with maturity T is denoted by $P(t,T)$. Since a zero-coupon bond pays 1 at maturity $P(T,T) = 1$.*

Below we introduce some notions of the interest rates that are used in this thesis.

Definition 2.2. *Let $0 \leq t \leq S < T$ be in year fractions, we define the following:*

1. *The **spot LIBOR rate** for the interval $[S,T]$ is given by:*

$$L(S,T) = \frac{1}{T-S}\left(\frac{1}{P(S,T)} - 1\right).$$

2. *The **simple compounded forward LIBOR rate** for the interval $[S,T]$ at time t is defined as:*

$$F_{lib}(t,S,T) = \frac{1}{T-S}\left(\frac{P(t,S)}{P(t,T)} - 1\right).$$

3. *The **instantaneous forward rate** at time t with maturity T is given by:*

$$f(t,T) = -\frac{\partial \log(P(t,T))}{\partial T}.$$

   The instantaneous forward rate is the interest at time t for an investment from time T to $T+\Delta$ where $\Delta \downarrow 0$.

4. *The **short-rate** at time t is defined as:*

$$r(t) = f(t,t).$$

5. *The **compounded rate** linked to an overnight rate over the period* $[S = t_1, t_1, \dots, t_M = T]$ *is given by:*

$$CR(S,T) = \frac{1}{\tau}\left(\prod_{i=1}^{M}(1+\tau_i R_i) - 1\right),$$

where the product is over all business days in the period $[S,T]$*,* τ *is the year fraction from* S *to* T*,* τ_i *is the year fraction from* t_i *to* t_{i+1} *and* R_i *is the overnight rate, for example EONIA, for time* t_i*.*

2.2. Derivative pricing

As a brief introduction to the derivative pricing, we describe some general pricing theorems in Section 2.2.1. Moreover, the concept of change of measure is explained in Section 2.2.2. The measure change is a useful tool that can help to simplify derivative pricing, especially for interest rate derivatives.

2.2.1. Pricing theorem

Most derivatives considered in this thesis are defined by their payoff paid at maturity time T. The derivative pricing answers the question what the value of the derivative at any time $t < T$ is. In order to give a general result for the derivative pricing we have to start with some notions. We introduce the risk-neutral measure $\mathbb{Q}$ with the money-market account as numeraire. Further, we define the money-market account as $M(t)$ with dynamics:

$$dM(t) = r(t)M(t)dt, \tag{2.1}$$

where $r(t)$ is a short-rate, see Definition 2.2. Solving this differential equation gives us:

$$M(t) = M(0)e^{\int_0^t r(u)du}.$$

Usually, $M(0) = 1$ such that we end up with:

$$M(t) = e^{\int_0^t r(u)du}.$$

For a general numeraire, the following theorem gives the price of a derivative at time t.

Theorem 2.1. *Let* $\hat{V}(T)$ *be the payoff at time* T *of a derivative. Let us assume* $\hat{V}(T)$ *is a* $\mathcal{F}_T$*-measurable random variable. Then, for any* $t < T$ *the time* t*-value of the derivative under the measure* $\mathbb{Q}^{\hat{N}}$*, with general numeraire* $\hat{N}$*, can be calculated as:*

$$\hat{V}(t) = \mathbb{E}^{\mathbb{Q}^{\hat{N}}}\left[\frac{\hat{N}(t)}{\hat{N}(T)}\hat{V}(T)\middle|\mathcal{F}_t\right],$$

where $\mathbb{E}^{\mathbb{Q}^{\hat{N}}}$ *is the expectation under the measure* $\mathbb{Q}^{\hat{N}}$*.*

Proof. For the proof of this theorem, we refer to Shreve, 2004, p. 218. □

Notice, when the money-market account is considered as numeraire, according to Theorem 2.1, the time t-value of a derivative can be calculated with:

$$\hat{V}(t) = \mathbb{E}^{\mathbb{Q}}\left[\frac{M(t)}{M(T)}\hat{V}(T)\middle|\mathcal{F}_t\right],$$

where $\mathbb{E}^{\mathbb{Q}}$ is the expectation under the risk-neutral measure with the money-market account as numeraire. Alternatively, if a derivative with maturity T depends on an underlying $X(T)$, one can use the Feynman-Kac Theorem 2.2 to obtain the value of the derivative at time $t < T$.

Theorem 2.2 (Feynman-Kac)**.** *Let us assume that the money-market account is defined by* (2.1) *with constant interest rate* $r(t) = r$*. Let* $V(t,X)$ *be the value of a derivative depending on underlying* $X = X(t)$ *with dynamics:*

$$dX(t) = \mu(t,X)dt + \sigma(t,X)dW^{\mathbb{Q}}.$$

Suppose that $V(t,X)$ satisfies the following Partial Differential Equation (PDE):

$$\frac{\partial V}{\partial t} + \mu(t,X)\frac{\partial V}{\partial X} + \frac{1}{2}\sigma^2(t,X)\frac{\partial^2 V}{\partial X^2} - rV = 0,$$

with final condition given by $V(T,X) = H(T,X)$. The solution $V(t,X)$ of this PDE at any time $t < T$ is then given by:

$$V(t,X) = e^{-r(T-t)}\mathbb{E}^{\mathbb{Q}}\left[H(T,X)|\mathcal{F}_t\right],$$

where the expectation is under the risk-neutral measure with the money-market account as numeraire.

Proof. For the proof, we refer to Oosterlee and Grzelak, 2020, p. 61. □

Using either Theorem 2.1 or 2.2 one can price derivatives at time t. In particular, in the case of European call and put options under the Black or Bachelier models, there exist analytic expressions for the prices. More specifically, if the underlying is log-normally distributed, Black's formula given in Theorem 2.3 can be used. If the underlying is normally distributed Bachelier's formula given in Theorem 2.4 can be used.

Theorem 2.3 (Black's formula for European call and put options)**.** *Let $X(t)$ be the value of an underlying asset at time $0 \leq t \leq T$, $\hat{F}(t)$ be the forward price at time t of $X(T)$, i.e., $\hat{F}(t) = \mathbb{E}^{\mathbb{Q}^T}\left[X(T)|\mathcal{F}_t\right]$ where the expectation is under the T-forward measure. The T-forward measure is the measure with zero-coupon bond $P(\cdot,T)$ as numeraire. Further, let σ be the volatility of the forward price. Assume that $X(T)$ conditional on the information at time t is log-normally distributed with mean $\hat{F}(t)$ and standard deviation $\sigma\sqrt{T-t}$. Then, the price of a European call and put option with maturity T, strike K and underlying $X(t)$ is given by:*

$$\begin{aligned}\hat{V}^C(t) &= P(t,T)\left(\hat{F}(t)\Phi(d_1) - K\Phi(d_2)\right),\\ \hat{V}^P(t) &= P(t,T)\left(K\Phi(-d_2) - \hat{F}(t)\Phi(-d_1)\right),\end{aligned}$$

where $\Phi(\cdot)$ is the cumulative distribution function of a standard normal distribution, $\hat{V}^C(t)$ and $\hat{V}^P(t)$ denote respectively the value of the call and put option and

$$\begin{aligned}d_1 &= \frac{\log\left(\frac{\hat{F}(t)}{K}\right) + \frac{1}{2}\sigma^2(T-t)}{\sigma\sqrt{T-t}},\\ d_2 &= d_1 - \sigma\sqrt{T-t}.\end{aligned}$$

Proof. Following the proof of the general pricing theorem of Geman-El Karoui-Rochet, see Björk, 2004, p. 361, we obtain for a European call option:

$$\hat{V}^C(t) = X(t)\Phi(d_1) - P(t,T)K\Phi(d_2).$$

With this expression for a European call option the following can be derived:

$$\begin{aligned}\hat{V}^C(t) &= X(t)\Phi(d_1) - P(t,T)K\Phi(d_2)\\ &= P(t,T)\left(\frac{X(t)}{P(t,T)}\Phi(d_1) - K\Phi(d_2)\right)\\ &= P(t,T)\left(\mathbb{E}^{\mathbb{Q}^T}\left[\frac{X(T)}{P(T,T)}|\mathcal{F}_t\right]\Phi(d_1) - K\Phi(d_2)\right)\\ &= P(t,T)\left(\hat{F}(t)\Phi(d_1) - K\Phi(d_2)\right).\end{aligned}$$

Similarly, with the general pricing theorem of Geman-El Karoui-Rochet the following expression for a European put option can be obtained:

$$\begin{aligned}\hat{V}^P(t) &= P(t,T)K\Phi(-d_2) - X(t)\Phi(-d_1)\\ &= P(t,T)\left(K\Phi(-d_2) - \hat{F}(t)\Phi(-d_1)\right).\end{aligned}$$

□

Theorem 2.4 (Bachelier formula for European call and put options)**.** *Consider an underlying asset $X(t)$, $0 \leq t \leq T$. Let $\hat{F}(t)$ be the forward price at time t of $X(T)$ under the T-forward measure and σ the volatility of the forward price. Assume that $X(T)$ conditional on the information at time t is normally distributed with mean $\hat{F}(t)$ and standard deviation $\sigma\sqrt{T-t}$. The price of a European call and put option with maturity T, strike K and underlying $X(t)$ is then given by:*

$$\begin{aligned}\hat{V}^C(t) &= P(t,T)\Big[(X(t)-K)\Phi(d_1) - \sigma\sqrt{T-t}\varphi(d_1)\Big],\\ \hat{V}^P(t) &= P(t,T)\Big[(K-X(t))\Phi(-d_1) + \sigma\sqrt{T-t}\varphi(d_1)\Big],\end{aligned}$$

where $\Phi(\cdot)$ is the cumulative distribution function of a standard normal distribution, $\varphi(\cdot)$ is the standard normal density function and d_1 is given by:

$$d_1 = \frac{X(t)-K}{\sigma\sqrt{T-t}}.$$

Proof. For a proof of the Bachelier formula for European put and call options, we refer to Delbaen and Schachermayer, 2006. □

2.2.2. Change of measure

The numeraire is a standard, or in other words a unit, which one uses to express the value of other tradable assets. In the very basic formulation, pricing is done under the risk-neutral measure $\mathbb{Q}$ corresponding to the money-market account as numeraire, see Section 2.2.1. However, sometimes it is more convenient to use another numeraire, as it might simplify the expression to be calculated under the conditional expectation. As an alternative numeraire one can take any positive non-dividend-paying asset. Then, for each eligible numeraire there exists a corresponding equivalent martingale measure.

Before proceeding, we give a number of definitions and theorems relevant for the measure change toolbox where we follow Seifried, 2013 and Brigo and Mercurio, 2007.

Definition 2.3. *A **numeraire** is any positive non-dividend-paying asset.*

When changing the numeraire, the definition of the Radon-Nikodym derivative is often used. This definition is stated below.

Definition 2.4. *Let $(\Omega, \mathcal{F}, \mathbb{Q})$ be a probability space, let $\tilde{\mathbb{Q}}$ be another probability measure on $(\Omega, \mathcal{F})$ that is equivalent to $\mathbb{Q}$, and let Z be an almost surely positive random variable with $\mathbb{E}[Z] = 1$ that relates $\mathbb{Q}$ and $\tilde{\mathbb{Q}}$ via:*

$$\tilde{\mathbb{Q}}(A) = \int_A Z(w)d\mathbb{Q}(w) \text{ for all } A \in \mathcal{F}.$$

*Then Z is called the **Radon-Nikodym derivative** of $\tilde{\mathbb{Q}}$ with respect to $\mathbb{Q}$, and we write:*

$$Z = \frac{d\tilde{\mathbb{Q}}}{d\mathbb{Q}}.$$

To change the numeraire, the following theorem can be used.

Theorem 2.5 (Change of numeraire)**.** *Suppose that $X(t)$ is a price process on $[0,T]$ such that $\frac{X(t)}{M(t)}$ is a $\mathbb{Q}$-martingale on $[0,T]$, where $M(t)$ is the money-market account. Then, there exists a uniquely determined probability measure $\tilde{\mathbb{Q}}$ equivalent to $\mathbb{Q}$ on $\mathcal{F}_T$ such that for every asset $S(t)$ the $X(t)$-discounted price process is a $\tilde{\mathbb{Q}}$-martingale on $[0,T]$ with $X(t)$ as numeraire, i.e.,*

$$\frac{S(t)}{X(t)} \text{ is a } \tilde{\mathbb{Q}}\text{-martingale on } [0,T].$$

Moreover, the Radon-Nikodym derivative defining the measure $\tilde{\mathbb{Q}}$ is given by:

$$\frac{d\tilde{\mathbb{Q}}}{d\mathbb{Q}} = \frac{M(t)X(T)}{M(T)X(t)}. \tag{2.2}$$

Proof. For a proof, we refer to Seifried, 2013, p. 47. □

There are two facts about the change of numeraire which are stated below without a proof. For more details about these facts we refer to Brigo and Mercurio, 2007, p. 29.
Fact 1: The price of any asset divided by the numeraire is a martingale under the measure associated with that numeraire.
Fact 2: The time t risk-neutral price under the measure $\mathbb{Q}$ is invariant by change of measure. Let $\tilde{\mathbb{Q}}$ be another equivalent measure with $X(t)$ as numeraire. The Radon-Nikodym derivative of $\tilde{\mathbb{Q}}$ with respect to $\mathbb{Q}$ is given by Equation (2.2). This gives:

$$\hat{V}(t) = \mathbb{E}^{\mathbb{Q}}\left[\frac{M(t)V(T)}{M(T)}\middle|\mathcal{F}_t\right] = \mathbb{E}^{\tilde{\mathbb{Q}}}\left[\frac{M(t)V(T)}{M(T)}\frac{M(T)X(t)}{M(t)X(T)}\middle|\mathcal{F}_t\right] = \mathbb{E}^{\tilde{\mathbb{Q}}}\left[\frac{X(t)V(T)}{X(T)}\middle|\mathcal{F}_t\right].$$

When changing the numeraire, sometimes the dynamics of an underlying asset need to be changed as well. To change the dynamics under the measure of another numeraire Girsanov's theorem, presented below, can be used.

Theorem 2.6 (Girsanov)**.** *Consider the Stochastic Differential Equation (SDE) with Lipschitz coefficients:*

$$dX(t) = \hat{\mu}(X(t))dt + \sigma(X(t))dW^{\mathbb{Q}}(t),$$

under $\mathbb{Q}$. Let $\bar{\mu}(x)$ be a new drift and assume $\frac{\bar{\mu}(x)-\hat{\mu}(x)}{\sigma(x)}$ to be bounded. Define the measure $\tilde{\mathbb{Q}}$ by:

$$\left.\frac{d\tilde{\mathbb{Q}}}{d\mathbb{Q}}\right|_{\mathcal{F}_t} = \exp\left(-\frac{1}{2}\int_0^t\left(\frac{\tilde{\mu}(X(s))-\hat{\mu}(X(s))}{\sigma(X(s))}\right)^2 ds + \int_0^t \frac{\tilde{\mu}(X(s))-\hat{\mu}(X(s))}{\sigma(X(s))}dW^{\mathbb{Q}}(s)\right).$$

Then $\tilde{\mathbb{Q}}$ is equivalent to $\mathbb{Q}$. Moreover, the process $W^{\tilde{Q}}(t)$ defined by:

$$dW^{\tilde{Q}}(t) = -\left(\frac{\tilde{\mu}(X(t))-\hat{\mu}(X(t))}{\sigma(X(t))}\right)dt + dW^{\mathbb{Q}}(t),$$

is a Brownian motion under $\tilde{\mathbb{Q}}$ and

$$dX(t) = \tilde{\mu}(X(t))dt + \sigma(X(t))dW^{\tilde{Q}}(t).$$

Proof. For a proof, we refer to Brigo and Mercurio, 2007, p. 911. □

2.3. Interest rate derivatives

In this section we describe some plain vanilla interest rate derivatives, which are relevant for this thesis, and their pricing formulae. We start with a zero-coupon bond. Thereafter, fixed and floating rate bonds, swaps and caps/floors are discussed. For the definitions below, let us define a set of payment dates $\mathcal{T}_m = \{T_0, T_1, \dots, T_m\}$ and the corresponding year fractions $\tau_i = T_i - T_{i-1}$, for $i = 1, \dots, m$. For this section a single curve framework is considered.

2.3.1. Zero-coupon bond

As mentioned before, a zero-coupon bond is a contract which pays 1 at maturity T. The zero-coupon bond is the simplest contract and is a building block for our further definitions and discussions.

The below corollary of Theorem 2.1 gives a formula for the zero-coupon bond price.

Corollary 2.6.1. *The value of a zero-coupon bond at time t with maturity T is given by:*

$$P(t,T) = \mathbb{E}^{\mathbb{Q}}\left[e^{-\int_t^T r(u)du}P(T,T)\middle|\mathcal{F}_t\right] = \mathbb{E}^{\mathbb{Q}}\left[e^{-\int_t^T r(u)du}\middle|\mathcal{F}_t\right].$$

2.3.2. Fixed and floating rate bonds

Let N be the notional and K be a fixed rate. Consider the payment dates $\mathcal{T}_m \backslash T_0$. A fixed rate bond is a financial contract with the following coupon payments:

$$C_i^{fix} = \begin{cases} NK\tau_i & \text{for } i \in \{1, \dots, m-1\}, \\ N + NK\tau_i & \text{for } i = m. \end{cases}$$

Since a fixed rate bond can be seen as m zero-coupon bonds with notional C_i^{fix} for $i = 1, \dots, m$, a replication argument can be used to obtain a pricing formula for the coupons of a fixed rate bond:

$$\hat{V}_i^{fix}(t) = P(t, T_i) C_i^{fix}.$$

The total t-value of a fixed rate bond is then given by:

$$\hat{V}^{fix}(t) = \sum_{i=1}^{m} \hat{V}_i^{fix}(t) = P(t, T_m)N + \sum_{i=1}^{m} P(t, T_i) NK\tau_i. \tag{2.3}$$

Let N be the notional and consider the payment dates $\mathcal{T}_m \backslash T_0$. A floating rate bond is a contract with the following coupon payments:

$$C_i^{fl} = \begin{cases} N\tau_i L(T_{i-1}, T_i) & \text{for } i \in \{1, \dots, m-1\}, \\ N\tau_i L(T_{i-1}, T_i) + N & \text{for } i = m, \end{cases}$$

where $L(t_{i-1}, T_i)$ is the LIBOR rate as defined in Definition 2.2. Using the zero-coupon bond $P(t, T_i)$ as numeraire the following holds:

$$\frac{\hat{V}_i^{fl}(t)}{P(t, T_i)} = \mathbb{E}^{\mathbb{Q}^{T_i}} \left[\frac{C_i^{fl}}{P(T_i, T_i)} \middle| \mathcal{F}_t \right],$$

which gives the value at time $t < T_0$ of a payment at time T_i:

$$\hat{V}_i^{fl}(t) = P(t, T_i) \mathbb{E}^{\mathbb{Q}^{T_i}} \left[C_i^{fl} | \mathcal{F}_t \right].$$

Since the expectation of the LIBOR rate, $L(T_{i-1}, T_i)$, under the T_i forward measure is equal to $F_{lib}(t, T_{i-1}, T_i)$, given in Definition 2.2, we can write the following in a single curve framework:

$$\begin{aligned} \hat{V}_i^{fl}(t) &= \begin{cases} P(t, T_i) \left(N\tau_i \frac{1}{\tau_i} \left(\frac{P(t, T_{i-1})}{P(t, T_i)} - 1 \right) \right) & \text{for } i \in \{1, \dots, m-1\} \\ P(t, T_i) \left(N\tau_i \frac{1}{\tau_i} \left(\frac{P(t, T_{i-1})}{P(t, T_i)} - 1 \right) + N \right) & \text{for } i = m \end{cases} \\ &= \begin{cases} N \left(P(t, T_{i-1}) - P(t, T_i) \right) & \text{for } i \in \{1, \dots, m-1\} \\ NP(t, T_{i-1}) & \text{for } i = m. \end{cases} \end{aligned}$$

The value of the floating rate bond in a single curve framework at time t is given by:

$$\hat{V}^{fl}(t) = \sum_{i=1}^{m} \hat{V}_i^{fl}(t) = NP(t, T_0). \tag{2.4}$$

2.3.3. Swaps

In this section two different interest rate swaps are described: the LIBOR interest rate swaps and the Overnight Index Swap (OIS). Swaps are commonly used derivatives. We mention OIS swaps separately, since the structure of the underlying for the new RFR has similarities with the OIS swap. More specifically, they are both referencing daily compounding rates.

2.3.3.1. Interest rate swaps

Let N be the notional and K be a fixed rate and consider the payment dates $\mathcal{T}_m \backslash T_0$. A payer interest rate swap is a financial contract in which the holder pays the fixed coupons $\tau_i NK$ and receives the floating coupons $\tau_i NL(T_{i-1}, T_i)$ at time T_i. A receiver interest rate swap is a financial contract in which the holder receives the fixed coupons $\tau_i NK$ and pays the floating coupons $\tau_i NL(T_{i-1}, T_i)$ at time T_i.

When dealing with a plain vanilla interest rate swap, the payments are in the same currency. The notional amounts are not exchanged between the parties. To derive the pricing formula for an interest rate swap, we assume that both parties exchange the notional at time T_m. This does not change the value of the contract. With this assumption, a payer interest rate swap can be seen as the difference between a floating rate bond and a fixed rate bond. Analogously, the value of the receiver interest rate swap is the difference between the values of a fixed rate bond and a floating rate bond. This results in the following pricing formula in a single curve framework:

$$\hat{V}^S(t) = \omega \left(\hat{V}^{fl}(t) - \hat{V}^{fix}(t) \right), \tag{2.5}$$

where ω equals 1 in case of a payer interest rate swap and -1 in case of a receiver interest rate swap. Further, $\hat{V}^{fix}(t)$ and $\hat{V}^{fl}(t)$ denote the values of the fixed rate bond and the floating rate bond at time t, respectively.

Swap rate Consider a payer or receiver interest rate swap. By substituting Equations (2.3) and (2.4) into Equation (2.5) the values of such swaps at time t are given by:

$$\hat{V}^S(t) = \omega N \left(P(t, T_0) - P(t, T_m) - \sum_{i=1}^{m} P(t, T_i) \tau_i K \right). \tag{2.6}$$

An interest rate swap is usually traded to par at the inception. The fixed rate K is chosen such that the value of the swap at the time of issue is equal to zero. Such a fixed rate is called the swap rate. From Equation (2.6) the swap rates at time t for both payer and receiver interest rate swaps are given by:

$$S_{0,m}(t) = \frac{P(t, T_0) - P(t, T_m)}{\sum_{i=1}^{m} P(t, T_i) \tau_i}.$$

The swap rate is usually defined as:

$$S_{0,m}(t) = \frac{P(t, T_0) - P(t, T_m)}{A_{0,m}(t)},$$

where $A_{0,m}(t)$ is called the annuity and is defined as:

$$A_{0,m}(t) := \sum_{i=1}^{m} P(t, T_i) \tau_i.$$

2.3.3.2. OIS swaps

An OIS swap is an agreement between two parties to exchange floating and fixed payments. The fixed coupon payments are the same as for a LIBOR interest rate swap, but the floating coupon payments are linked to a compounding overnight index. With a notional of N and payment dates $\mathcal{T}_m \backslash T_0$, the floating coupon payments are given by:

$$C_i^{OIS} = \tau_i N R_i^{OIS},$$

with

$$R_i^{OIS} = \frac{1}{\tau_i} \left(\prod_{j=1}^{n_i} (1 + \tau_{ij} e_{ij}) - 1 \right),$$

where the product includes all overnight fixings of the i-th coupon, e_{ij} is the j-th overnight rate fixing of the i-th coupon and τ_{ij} is the year fraction between the $(j-1)$-th and j-th fixing of the i-th coupon.

Notice, R_i^{OIS} is a stochastic variable and known at the end of the coupon. To make the notation a bit easier, we get rid of the index i corresponding to the coupon. The forward rate is given by:

$$F_{OIS}(t, T_{begin}, T_{end}) = \frac{1}{\tau}\left(\frac{P(t, T_{begin})}{P(t, T_{end})} - 1\right),$$

where T_{begin} and T_{end} denote the start and end date of the coupon, respectively. For the derivation of this forward rate, we refer to Appendix A.

In order to calculate the expected value of a floating coupon, we use the T_{end}-forward measure. We assume that the pay date is the same as the end date. The start and end date of the j-th fixing of the coupon are denoted by T_{begin}^j and T_{end}^j, respectively. We consider two types of OIS coupons: coupons that start in the future, i.e., $t < T_{begin}$, and running coupons. For a coupon that starts in the future the following holds:

$$\mathbb{E}^{\mathbb{Q}^{T_{end}}}\left[P(t, T_{end}) N \tau R^{OIS} | \mathcal{F}_t\right] = P(t, T_{end}) N \tau F_{OIS}(t, T_{begin}, T_{end}).$$

For a running coupon, the expectation of the OIS leg is given by:

$$\mathbb{E}^{\mathbb{Q}^{T_{end}}}\left[P(t, T_{end}) N \tau R^{OIS} | \mathcal{F}_t\right] = P(t, T_{end}) N \left(\prod_{j=1}^{m}(1 + \tau_j e_j)\bar{\tau} F_{OIS}(t, T_{begin}^{m+1}, T_{end})\right),$$

where m corresponds to the day of the last available historical overnight fixing rate of the running coupon and $\bar{\tau}$ is the year fraction from T_{begin}^{m+1} to T_{end}. For the derivations of these two coupons, we refer to Appendix A.

2.3.4. Caps and Floors

An interest rate cap is a product which provides insurance against the floating interest rate rising above a certain level. This level is called the cap rate or strike. On the other hand, an interest rate floor provides insurance against the floating interest rate falling below a certain level. This level is called the floor rate or strike. We make a distinction between LIBOR caps/floors and caps/floors on compounded rates. Historically, there were only caps/floors linked to the LIBOR rate. However, since the IBOR rates will disappear, the market will develop new products and one of them are caps/floors linked to the new RFR. Those rates are based on an in-arrears compounding.

2.3.4.1. LIBOR caps and floors

A LIBOR caplet/floorlet is a European call/put option with notional N_i and strike K_i on the LIBOR rate $L(T_{i-1}, T_i)$ that is fixed on T_{i-1}. At time T_i the payoff of the LIBOR caplet/floorlet is:

$$\hat{V}_i(T_i) = N_i \tau_i \max\left(\omega\left[L(T_{i-1}, T_i) - K_i\right], 0\right), \text{ for } i = 1, \ldots, m,$$

where ω equals 1 in case of a caplet and -1 in case of a floorlet and $\tau_i = T_i - T_{i-1}$ is a year fraction. A cap/floor is a sum of m caplets/floorlets with the same notional and strike, i.e., $N = N_i$ and $K = K_i$ for $i = 1, \ldots, m$. The value of a cap/floor at time $t < T_0$ is the sum of the values of the individual caplets/floorlets at time t.

Since the LIBOR caplet/floorlet is a European call/put option with the LIBOR rate as underlying, both the Black and the Bachelier model can be used to value a LIBOR caplet/floorlet at time t. Both models are in principal the same, only the assumption of the distribution of the underlying at the fixing time is different. The Black model assumes the LIBOR rate $L(T_{i-1}, T_i)$ conditional on the information at time t to be log-normally distributed with mean $F_{lib}(t, T_{i-1}, T_i)$ and standard deviation $\sigma_i\sqrt{T_i - t}$. Where σ_i is the volatility of the forward LIBOR rate. This gives

$$\begin{aligned}
\hat{V}_i^C(t) &= N_i \tau_i P(t, T_i)\left(F_{lib}(t, T_{i-1}, T_i)\Phi(d_1) - K_i\Phi(d_2)\right), \\
\hat{V}_i^P(t) &= N_i \tau_i P(t, T_i)\left(K_i\Phi(-d_2) - F_{lib}(t, T_{i-1}, T_i)\Phi(-d_1)\right), \\
d_1 &= \frac{\log\left(\frac{F_{lib}(t, T_{i-1}, T_i)}{K_i}\right) + \frac{1}{2}\sigma_i^2(T_i - t)}{\sigma_i\sqrt{T_0 - t}}, \\
d_2 &= d_1 - \sigma_i\sqrt{T_i - t},
\end{aligned}$$

where $\hat{V}_i^C(t)$ and $\hat{V}_i^P(t)$ denote the value of the caplet and floorlet at time t, respectively. On the other hand, the Bachelier model assumes the LIBOR rate $L(T_{i-1}, T_i)$ conditional on the information at time t to be normally distributed with mean $F_{lib}(t, T_{i-1}, T_i)$ and standard deviation $\sigma_i\sqrt{T_i - t}$. Where σ_i is the volatility of the forward LIBOR rate. This gives:

$$\begin{aligned}
\hat{V}_i^C(t) &= N_i\tau_i P(t,T_i)\left((F_{lib}(t,T_{i-1},T_i) - K)\Phi(d_1) + \sigma\sqrt{T_i - t}\varphi(d_1)\right),\\
\hat{V}_i^P(t) &= N_i\tau_i P(t,T_i)\left((K - F_{lib}(t,T_{i-1},T_i))\Phi(-d_1) + \sigma\sqrt{T_i - t}\varphi(d_1)\right),\\
d_1 &= \frac{F_{lib}(t,T_{i-1},T_i) - K}{\sigma\sqrt{T_i - t}}.
\end{aligned}$$

With these values of a caplet/floorlet at time t, the value of a cap/floor at time $t < T_0$ can be obtained by:

$$\begin{aligned}
\hat{V}^{Cap}(t) &= \sum_{i=1}^{m} \hat{V}_i^C(t),\\
\hat{V}^{Floor}(t) &= \sum_{i=1}^{m} \hat{V}_i^P(t),
\end{aligned}$$

where $\hat{V}_i^C(t)$ and $\hat{V}_i^P(t)$, dependent on the distribution of the underlying, are given by the above Black or Bachelier model.

2.3.4.2. Caps and floors on compounded rates

As a result of the IBOR reform, the IBOR rates will cease to exist and will be replaced by the new RFR. New market instruments will reference a compounding RFR rate similar to the floating rates of the already existing OIS swaps. To be more precise, the compounded underlying rates over the period $[S, T]$ are as defined in Definition 2.2, and denoted by $CR(S, T)$.

The caps/floors on compounded rates have a similar payoff as the LIBOR caps/floors. The same as the LIBOR caps/floors, the caps/floors on the compounded rates provide an insurance against the compounded average of the new RFR rising above or falling below a certain level. Namely, the payoff of a caplet/floorlet linked to the new RFR over the period $[T_{i-1}, T_i]$ with strike K_i and notional N_i is given by:

$$\hat{V}_{CR}(T_i) = N_i\tau_i \max\left(\omega\left[CR(T_{i-1},T_i) - K_i\right], 0\right), \text{ for } i = 1, \ldots, m,$$

where ω equals 1 in case of a caplet and -1 in case of a floorlet. Similar to LIBOR caps/floors, caps/floors on compounded rates are the sum of caplets/floorlets on compounded rates. However, note that in case of the LIBOR caplets/floorlets the underlying rate is fixed at the beginning of the caplet/floorlet, but in case of the compounding rate it will be fixed and paid at the end of the caplet/floorlet.

Due to the compounding property of the compounded rate linked to the new RFR, a Black or Bachelier model cannot directly be applied. The Black and Bachelier models assume a quantity which fixes from one to another time instance. The new RFR rate fixes gradually during the whole coupon period, and thus violates the assumptions of the Black/Bachelier type models. Therefore, in this thesis, we look into various pricing techniques to price these options on backward-looking rates, which follow the compounding mechanism as described above.

2.4. Pricing techniques

In this section, an introduction of various pricing techniques in option pricing is given. First, the Monte Carlo (MC) simulation is described in Section 2.4.1. Thereafter, Section 2.4.2 is dedicated to the tree method. Last, Green functions are considered in Section 2.4.3.

2.4.1. Monte Carlo methods

This section provides a brief summary of MC methods for completeness, but we expect the reader to be familiar with the concept. MC methods are numerical methods used to calculate expectations of

random quantities. They rely on the Law of Large Numbers and the Central Limit Theorem. In particular, MC methods are used in option pricing. For this introduction we follow Kostiuk, 2004 and Oosterlee and Grzelak, 2020, for more details about MC methods we refer to Korn et al., 2010 or Glasserman, 2004.

With a MC simulation the expectation $\mathbb{E}[X]$ can be estimated where X is a random variable. The idea behind this calculation is simulating $\tilde{N}$ independent identically distributed (i.i.d.) realisations of the random variable X denoted by X_i for $i = 1, \dots, \tilde{N}$. The MC approximation of this expectation is then given by:

$$\hat{X} = \frac{1}{\tilde{N}} \sum_{i=1}^{\tilde{N}} X_i.$$

According to the Law of Large Numbers, see Rice, 2007, p. 178, this approximation is accurate for large $\tilde{N}$.

With this MC approximation an error is made. Here we assume that no time-discretisation is used to simulate X_i. Under this assumption, the statistical error is the only error which is made by the MC estimator. By the Central Limit Theorem, the size of the statistical error can be determined. From the Central Limit Theorem, see Rice, 2007, p. 184, it follows that the MC approximation is $\mathcal{N}(\mathbb{E}[X], Var[X])$ distributed. In practice the variance is often unknown. However, the sample variance, denoted by $\bar{v}_{\tilde{N}}^2$, can be used to estimate the variance:

$$\bar{v}_{\tilde{N}}^2 := \frac{1}{\tilde{N} - 1} \sum_{j=1}^{\tilde{N}} (X_i - \bar{X})^2.$$

The standard error is then defined by:

$$\epsilon_{\tilde{N}} := \frac{\bar{v}_{\tilde{N}}}{\sqrt{\tilde{N}}}.$$

Notice, that if the number of MC paths increases with a factor 4, the standard error decreases with a factor 2.

Sometimes, in order to price derivatives, an expectation of a function of a solution of a differential equation has to be computed. For example, the price of an Asian call option with arithmetic continuous averaging, maturity T and strike K is given by:

$$V_{Asian}^{C}(t, X(\cdot)) = \mathbb{E}^{\mathbb{Q}}\left[e^{-rT} \left(\frac{1}{T} \int_0^T X(u) du - K \right)^+ \middle| \mathcal{F}_t \right],$$

where the dynamics of $X(t)$ is given by the following SDE:

$$dX(t) = \mu(t, X) dt + \sigma(t, X) dW^{\mathbb{Q}}(t). \tag{2.7}$$

For simplifications, we consider a constant interest rate. When using a MC simulation in order to obtain the price of this Asian option, a number of i.i.d. realisations of $e^{-rT} \left(\frac{1}{T} \int_0^T X(u) du - K \right)^+$ have to be drawn. However, this is not possible straightaway, since there is no closed form solution of the integral of $X(t)$. Moreover, the solution of the SDE is not known. Therefore, a discretisation scheme needs to be used to simulate the path of the process $X(t)$ and this causes a discretisation error.

Consider a derivative with payoff $V(T, X(\cdot))$ dependent on underlying $X(t)$ with dynamics defined by (2.7). With the following MC algorithm the t_0-value of this derivative can be determined for $t_0 < T$, Oosterlee and Grzelak, 2020, p. 249.

Step 1: Define a grid on the interval $[0, T]$, $0 = t_0, t_1, \dots, t_m = T$, where $t_i = \frac{iT}{m}$. The number of time steps is defined by $m + 1$.

Step 2: Generate asset values, denoted by $x_{i,j}$, on $\tilde{N}$ MC paths taking the risk-neutral dynamics of the underlying model. $x_{i,j}$ has two indices, the time step i, when a discretisation scheme is used, and the MC path j. Two well known discretisation schemes are the Euler and Milstein schemes given below.

Step 3: Compute the $\tilde{N}$ payoff values, V_j. In the case of European options, $V_j = V(T, x_{m,j})$, in the case

of path-dependent options, $V_j = V(T, \{x_{i,j}\}_{i=0}^m)$.
Step 4: Calculate the value of the option with:

$$V(t_0, X(t_0)) = e^{-r(T-t_0)}\mathbb{E}^{\mathbb{Q}}\left[V(T, X(T))|\mathcal{F}_{t_0}\right] \approx e^{-r(T-t_0)}\frac{1}{\tilde{N}}\sum_{i=1}^{\tilde{N}} V_j.$$

Step 5: Determine the standard error obtained by this MC simulation.

The Euler scheme is a basic integration method to solve the dynamics of (2.7). The solution of $X(t_{i+1})$ at time t_{i+1}, denoted by x_{i+1} is approximated by:

$$\begin{aligned} x_{i+1} &\approx x_i + \int_{t_i}^{t_{i+1}} \mu(t_i, x_i)dt + \int_{t_i}^{t_{i+1}} \sigma(t_i, x_i)dW^{\mathbb{Q}}(t) \\ &\approx x_i + \mu(t_i, x_i)\Delta t + \sigma(t_i, x_i)W^{\mathbb{Q}}(\Delta t), \end{aligned}$$

where $\Delta t = t_{i+1} - t_i$.

The Milstein scheme has a higher rate of convergence. Discretisation with the Milstein scheme is given by the Euler scheme with an extra term:

$$x_{i+1} \approx x_i + \int_{t_i}^{t_{i+1}} \mu(t_i, x_i)dt + \int_{t_i}^{t_{i+1}} \sigma(t_i, x_i)dW^{\mathbb{Q}}(t) + \frac{1}{2}\sigma(t_i, x_i)[(W^{\mathbb{Q}}(\Delta t))^2 - \Delta t]\frac{\partial \sigma}{\partial x}(t_i, x_i).$$

In the case of $\sigma(t, X(t)) = \bar{\sigma}X(t)$, the Milstein scheme is given by:

$$x_{i+1} \approx x_i + \mu(t_i, x_i)\Delta t + \bar{\sigma}x_i W^{\mathbb{Q}}(\Delta t) + \frac{1}{2}\bar{\sigma}^2 x_i\left[(W^{\mathbb{Q}}(\Delta t))^2 - \Delta t\right].$$

2.4.2. Trees

Trees provide another method to numerically calculate the price of options. In this section, a short introduction is given about option pricing with trees, for more details we refer to Korn and Stefanie, 2010. Consider an option on an underlying asset denoted by $X(t)$. A discretisation of the time $0 = t_0, t_1, \dots, t_{\tilde{N}}$ is needed if one wants to determine the price of this option at time t_0 with trees. For each time the representative values of the underlying asset are determined iteratively. Start at time t_0, for this time the value of the underlying asset is known. When a trinomial tree is considered, three possible values of asset $X(t)$ are assumed for time t_1. More specifically, the value of the asset can make a jump with size u, d or m with corresponding probabilities p_u, p_d and p_m. This is shown in Figure 2.1. From each node at time t_1 the asset can again take three possible values for the next time step. The trinomial trees is then defined by:

$$X(t_{i+1}) = \begin{cases} X(t_i)u & \text{with probability } p_u \\ X(t_i)m & \text{with probability } p_m \\ X(t_i)d & \text{with probability } p_d \end{cases}.$$

The probabilities p_u, p_d and p_m have to sum up to 1. Figure 2.2 illustrates an example of a trinomial tree. We denote the nodes of the tree by (i, j), where i corresponds to the time step and j corresponds to the state in that time step.

With a trinomial tree, the price of an option at time t_0 with maturity T and underlying $X(t)$ can be obtained in the following way:

- Construct a trinomial tree from time t_0 to time T. Discretise the time in $\tilde{N} + 1$ time steps.
- Calculate the payoff of the option at each leaf of the tree. Denote the value of the option on node (i, j) by $V_{i,j}$.
- Calculate the value of the option on the other nodes of the tree with a backward iteration. The value of the option on node (i, j) is obtained using the formula:

  $$V_{i,j} = e^{-r(t_{i+1}-t_i)}\left[p_u V_{i+1,j+1} + p_m V_{i+1,j} + p_d V_{i+1,j-1}\right].$$

  For simplification, the short-rate r is assumed to be constant.

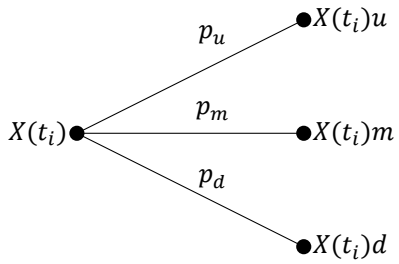

Figure 2.1: Possible values for asset $X(t)$ at time t_{i+1} evolving from asset $X(t)$ at time t_i.

With the steps described above, we give present how trees can be used for option pricing. Moreover, there is a relation between the tree method and finite difference method. More precisely, the tree method corresponds to an explicit finite difference method applied on a transformed version of the pricing PDE. For details, we refer to Higham, 2004, p.261.

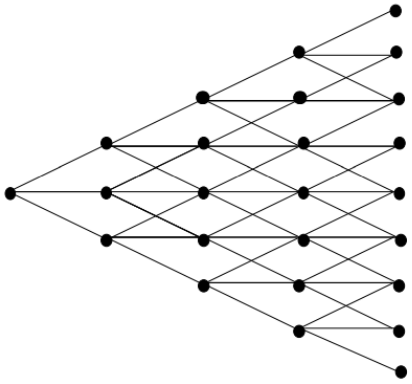

Figure 2.2: Trinomial tree Clifford et al., 2010, p. 3.

2.4.3. Green functions

Another pricing technique is based on Green functions. With the Feynman-Kac Theorem 2.2, the pricing PDE of a derivative can be written. In order to determine the t-value of this derivative, one needs to solve this differential equation. In this section we give briefly describe the idea behind the application of the Green function technique to solve differential equations. For details see Kirkwood, 2003. We would like to stress that we do not give a proof, but rather a brief motivation while omitting technicalities. Moreover, for simplification, an Ordinary Differential Equation (ODE) is used for this brief sketch.

Consider a second-order linear differential equation:

$$\mathcal{L}(y(x)) := a_2(x)\frac{\partial^2 y(x)}{\partial x^2} + a_1(x)\frac{\partial y(x)}{\partial x} + a_0(x)y(x) = h(x), \tag{2.8}$$

for $b \leq x \leq c$.

Fix z, $b \leq z \leq c$ and let us assume that there is a parametric function $\hat{G}(x,z)$ that solves the following parametric differential equation:

$$\mathcal{L}(\hat{G}(x,z)) = \delta(x-z), \tag{2.9}$$

where δ is the Dirac delta function. This function $\hat{G}(x,z)$ is called the Green function.

If both sides in Equation (2.9) are first multiplied by $h(z)$ and then integrated with respect to z, the following is obtained:

$$\int_b^c \mathcal{L}(\hat{G}(x,z))h(z)dz = \int_b^c \delta(x-z)h(z)dz = h(x),$$

where for regular enough $h(x)$ the second equal sign holds because of the Dirac delta function properties. Then, under some sufficient conditions, the integral and differential operator $\mathcal{L}(\cdot)$ can be swapped:

$$\int_b^c \mathcal{L}(\hat{G}(x,z))h(z)dz = \mathcal{L}\left(\int_b^c \hat{G}(x,z)h(z)dz\right).$$

This gives:

$$\mathcal{L}\left(\int_b^c \hat{G}(x,z)h(z)dz\right) = h(x),$$

which in turn implies that

$$y(x) = \int_b^c \hat{G}(x,z)h(z)dz$$

is a solution of Equation (2.8).

To conclude, Green functions that solve the pricing PDE are related to the density function of the asset price. More precisely, the discounted transition probability density function can be seen as the Green function and is called Arrow-Debreu security in finance. For more details, we refer to Oosterlee and Grzelak, 2020.

3

One-factor Hull-White model

This chapter is dedicated to the one-factor Hull-White short-rate model. For the sake of notational simplicity, we refer to it as the Hull-White model. The Hull-White model belongs to the class of affine models that have the useful result, presented in Section 3.1, that the zero-coupon bond price is analytically tractable. Furthermore, a brief introduction to the Vasicek short-rate model is given. Thereafter, the one-factor Hull-White model, which is an extension of the Vasicek model, is described. Moreover, the prices of LIBOR caps/floors and caps/floors on compounded rates are investigated. Both types of the caps/floors will be priced using two different pricing methods: closed form formulae and a MC approach. In Section 3.3.1 the pricing formula for caps/floors using the pricing kernel is derived. Thereafter, in Section 3.3.2 the cap/floor prices are calculated using a MC simulation. Moreover, a comparison of the various pricing methods is presented in Section 3.4. Last, the chapter is concluded in Section 3.5.

3.1. Affine model

If the dynamics of a short-rate model are given as in Proposition 3.1, the model belongs to the class of affine short-rates models Andersen and Piterbarg, 2010. These models have an affine term structure which can be found by solving two differential equations. This useful result is presented in Proposition 3.1.

Proposition 3.1. *Suppose the dynamics of $r(t)$ are given by:*

$$dr(t) = \mu(t, r(t))dt + \sigma(t, r(t))dW(t),$$

and $\mu(t, r(t))$ and $\sigma(t, r(t))$ are of the form:

$$\begin{aligned} \mu(t, r(t)) &= \lambda(t)r(t) + \nu(t), \\ \sigma^2(t, r(t)) &= \gamma(t)r(t) + \delta(t). \end{aligned}$$

Then the model has an affine term structure of the form:

$$P(t, T) = A(t, T)\exp(-B(t, T)r(t)),$$

where A and B satisfy the following Riccati differential equations:

$$\begin{aligned} \frac{\partial}{\partial t}B(t, T) + \lambda(t)B(t, T) - \frac{1}{2}\gamma(t)B^2(t, T) + 1 &= 0, \\ \frac{\partial}{\partial t}\log A(t, T) - \nu(t)B(t, T) + \frac{1}{2}\delta(t)B^2(t, T) &= 0, \end{aligned}$$

with $B(T, T) = 0$ and $A(T, T) = 1$.

Proof. For a proof, we refer to Björk, 2004, par 22.3. □

3.2. Short-rate models

At first, an introduction to the Vasicek short-rate model is briefly presented. Thereafter, the Hull-White model, an extension of the Vasicek model, is discussed in more detail. As mentioned before, due to the affine nature of the model, there exists an analytic formula for zero-coupon bond prices under the Hull-White model. Section 3.1 provides a proposition for affine models, which is used to obtain the zero-coupon bond price for the Hull-White model. The existence of an analytic formula for the zero-coupon bond is one of the advantages of the Hull-White model. These formulae for both constant and piecewise constant volatilities will be derived. In this section we follow Sterling and Hári, 2007.

3.2.1. Vasicek Model

Empirical studies show that interest rates exhibit mean reversion, see e.g. Andersen and Piterbarg, 2010. In the Vasicek model the mean reversion is, under the risk-neutral measure $\mathbb{Q}$, captured by following the Ornstein-Uhlenbeck process:

$$dr(t) = k(\theta - r(t))dt + \sigma dW^{\mathbb{Q}}(t),$$

where k, θ and σ are constants and $W^{\mathbb{Q}}(t)$ is a Brownian motion at time t under the risk-neutral measure. The mean reverting rate is denoted by θ. If a realisation of $r(t)$ is larger than θ, the drift term will become negative and the process will tend to θ from above, while if the realisation of $r(t)$ is smaller than θ, the reverse will happen, i.e., the drift term will become positive and the process will tend to θ from below. Parameter k is called the mean reverting speed. As its name suggests, it is the speed at which the rate reverts back to θ. The volatility is denoted by σ. Using Itô's lemma Oosterlee and Grzelak, 2020 for $t > 0$, the solution of the above SDE is given below:

$$r(t) = r(0)e^{-kt} + k\theta(1 - e^{-kt}) + \sigma \int_0^t e^{-ku} dW^{\mathbb{Q}}(u).$$

Note, for $s < t$ the short-rate in the Vasicek model is normally distributed with:

$$\begin{aligned} \mathbb{E}^{\mathbb{Q}}[r(t)|\mathcal{F}_s] &= r(s)e^{-k(t-s)} + k\theta(1 - e^{-k(t-s)}), \\ \mathrm{Var}^{\mathbb{Q}}[r(s) \mid \mathcal{F}_s] &= \frac{\sigma^2}{2k}\left(1 - e^{-2k(t-s)}\right). \end{aligned}$$

The conditional probability that the short-rate is negative at time $t > s > 0$ is equal to:

$$\mathbb{Q}(r(t) < 0|\mathcal{F}_s) = \Phi\left(\frac{r(s)e^{-k(t-s)} + k\theta(1 - e^{-k(t-s)})}{\sqrt{\frac{\sigma^2}{2k}\left(1 - e^{-2k(t-s)}\right)}}\right),$$

where $\Phi(\cdot)$ is the standard normal cumulative distribution function.

A drawback of this model is that the model implied initial term structure (at $t = 0$), i.e., the prices of the zero-coupon bonds $P(0,T)$ for $T > 0$, does not align with the observed market prices. This problem is addressed by the Hull-White model, an extension of the Vasicek model, which is discussed in the next section.

3.2.2. Hull-White Model

The dynamics of the instantaneous short-rate in the Hull-White model under the risk-neutral measure $\mathbb{Q}$ are given by:

$$dr(t) = (\theta(t) - ar(t))\,dt + \sigma dW^{\mathbb{Q}}(t) = a\left(\frac{\theta(t)}{a} - r(t)\right)dt + \sigma dW^{\mathbb{Q}}(t), \tag{3.1}$$

where $\theta(t)$ is a deterministic function calibrated such that the model implied initial term structure matches the market observed term structure. Then $\frac{\theta(t)}{a}$ is a time-dependent mean reverting rate, a is the mean reverting speed and σ is a constant volatility. Using Itô's lemma the short-rate in the Hull-White model is given by:

$$r(t) = r(0)e^{-at} + \int_0^t \theta(u)e^{-a(t-u)}du + \sigma \int_0^t e^{-a(t-u)} dW^{\mathbb{Q}}(u). \tag{3.2}$$

The Hull-White model belongs to the class of affine short-rate models Andersen and Piterbarg, 2010. For affine short-rate models there is a formula for zero-coupon bond prices, which can be obtained with Proposition 3.1. Since the dynamics of Equation (3.1) satisfy the conditions of Proposition 3.1, the price of a zero-coupon bond can be derived by solving two ODEs. These ODEs can be solved analytically to obtain the following formula for the term structure:

$$\begin{aligned} P(t,T) &= A(t,T)\exp(-B(t,T)r(t)), \\ \log A(t,T) &= \frac{\sigma^2}{2}\int_t^T B^2(u,T)du - \int_t^T \theta(u)B(u,T)du, \\ B(t,T) &= \frac{1}{a}(1-\exp(-a(T-t))). \end{aligned} \tag{3.3}$$

In order to fit to the initial term structure, an expression for $\theta(t)$ has to be obtained. By substituting Equation (3.3) into the formula for the instantaneous forward rate, given in Definition 2.2, the following formula is derived:

$$\begin{aligned} f(0,T) &= \frac{\partial}{\partial T}B(0,T)r(0) - \frac{\partial}{\partial T}\log(A(0,T)) \\ &= r(0)e^{-aT} - \frac{\sigma^2}{2a^2}(1-e^{-aT})^2 + e^{-aT}\int_0^T \theta(u)e^{au}du. \end{aligned}$$

This implies:

$$\theta(t) = \frac{\partial}{\partial t}f(0,t) + af(0,t) + \frac{\sigma^2}{2a}(1-e^{-2at}). \tag{3.4}$$

For details we refer to Sterling and Hári, 2007. Substituting Equation (3.4) into Equation (3.2) gives:

$$r(t) = r(0)e^{-at} + g(t) - g(0)e^{-at} + \sigma\int_0^t e^{-a(t-u)}dW^{\mathbb{Q}}(u), \tag{3.5}$$

where

$$g(t) = f(0,t) + \frac{\sigma^2}{2a^2}(1-e^{-at})^2. \tag{3.6}$$

Substituting Equation (3.5) into Equation (3.3) yields the formula for the zero-coupon bond prices:

$$P(t,T) = \frac{P(0,T)}{P(0,t)}\exp\left(B(t,T)f(0,t) - \frac{\sigma^2}{4a}B^2(t,T)(1-e^{-2at}) - B(t,T)r(t)\right). \tag{3.7}$$

We note that for $s < t$ the short-rate in the Hull-White model is, as well as in the Vasicek model, normally distributed with:

$$\begin{aligned} \mathbb{E}^{\mathbb{Q}}[r(t) \mid \mathcal{F}_s] &= r(s)e^{-a(t-s)} + g(t) - g(s)e^{-a(t-s)}, \\ \mathrm{Var}^{\mathbb{Q}}[r(s) \mid \mathcal{F}_s] &= \frac{\sigma^2}{2a}\left(1-e^{-2a(t-s)}\right). \end{aligned}$$

The conditional probability that the short-rate at time $t > s > 0$ is negative is equal to:

$$\mathbb{Q}\left(r(t) < 0 | \mathcal{F}_s\right) = \Phi\left(\frac{r(s)e^{-a(t-s)} + g(t) - g(s)e^{-a(t-s)}}{\sqrt{\frac{\sigma^2}{2a}\left(1-e^{-2a(t-s)}\right)}}\right).$$

Historical negative rates admitted by the Hull-White model were seen as a disadvantage of the model. However, nowadays in the low/negative rate environment this became an advantage of the model.

3.2.2.1. Zero mean process

Since the expression for the instantaneous forward rate $f(0,t)$ is a cumbersome term, due to the derivative in the definition, one prefers to remove this term in the zero-coupon bond price formula and work with the so-called zero mean process that has the following dynamics under the risk-neutral measure:

$$\begin{aligned} dx(t) &= -ax(t)dt + \sigma dW^{\mathbb{Q}}(t), \\ x(0) &= 0. \end{aligned}$$

With Itô's lemma, the solution for the above SDE is given by:

$$x(t) = x(0)e^{-at} + \sigma \int_0^t e^{-a(t-u)} dW^{\mathbb{Q}}(u).$$

Note that:

$$r(t) = x(t) + g(t),$$

with $g(t)$ as in (3.6). By substituting this into Equation (3.7), the formula for the zero-coupon bond price, without the $f(0,t)$ term, becomes:

$$P(t,T) = \frac{P(0,T)}{P(0,t)} \exp\left(-G(t,T) - B(t,T)x(t)\right),$$

where:

$$G(t,T) = \frac{\sigma^2}{2a} B(t,T)(1-e^{-at}) \left(\frac{B(t,T)}{2}(1+e^{-at}) + \frac{1-e^{-at}}{a} \right).$$

3.2.3. Hull-White model with piecewise constant volatility

In this section we consider an extension of the one-factor Hull-White model with piecewise constant volatility. Piecewise constant volatility gives the model more flexibility. A model with piecewise constant volatility can be calibrated to multiple calibration instruments, for example, to n caps/floors, with maturities $t_1 < ... < t_n$. This gives an extra degree of freedom in the calibration process, which is an advantage of piecewise constant volatility compared to the constant volatility. Taking the same volatility on each interval degenerates it to the constant one-factor Hull-White model.

We assume that the instantaneous short-rate is modelled by:

$$r(t) = x(t) + \bar{g}(t), \tag{3.8}$$

where $\bar{g}(t)$ is a deterministic function which has to be determined by a calibration to the initial term structure. Moreover, the dynamics of the zero mean process $x(t)$ under the risk-neutral measure are given by:

$$\begin{aligned} dx(t) &= -ax(t)dt + \sigma(t)dW^{\mathbb{Q}}(t), \\ x(0) &= 0, \end{aligned} \tag{3.9}$$

where $\sigma(t)$ is piecewise constant on the intervals between $0 = t_0 < t_1 < ... < t_n = T$.

Proposition 3.2. *Let us define the piecewise constant volatility function by $\sigma(t) = \sigma_j$ for any $t \in (t_{j-1}, t_j]$, $j \in \{1, 2, ..., n\}$. Then the time t price of a zero-coupon bond with maturity $T = t_n$ under the Hull-White model with piecewise constant volatility is given by:*

$$P(t,T) = \frac{P(0,T)}{P(0,t)} \exp\left(\frac{1}{2}(W(t,T) - W(0,T) + W(0,t)) - B(t,T)x(t) \right),$$

with

$$\begin{aligned} B(t,T) &= \frac{1}{a}\left(1 - e^{-a(T-t)}\right), \\ W(t,T) &= \overline{W}(t,t_j) + \sum_{k=j}^{n-1} \overline{W}(t_k, t_{k+1}), \end{aligned}$$

where $P(0,t)$ and $P(0,T)$ are the zero-coupon bond prices observed in the market and for every $(l,u) \subseteq (t_k, t_{k+1}]$:

$$\overline{W}(l,u) = \int_l^u \sigma_{k+1}^2 B^2(s,T)ds = \frac{\sigma_{k+1}^2}{2a^3}\left(e^{-2aT}(e^{au}-e^{al})(e^{au}+e^{al}+4e^{aT})+2a(u-l)\right).$$

Proof. For a proof, we refer to Hoorens, 2011. □

3.3. Pricing methods

In this section two different pricing methods to obtain caplet/floorlet prices are described. We begin with the Hull-White pricing kernel approach yielding analytical pricing formulae in Section 3.3.1. Thereafter, we look into the numerical MC simulation in Section 3.3.2. The two methods are applied to price both LIBOR caplets/floorlets and caplets/floorlets on compounded rates.

3.3.1. Hull-White pricing kernel

In this section we derive an analytic formula for caplet/floorlet prices using the kernel approach. The idea behind the kernel pricing is, first, to formulate the pricing problem as a problem of solving the corresponding PDE, see Theorem 2.2. Second, apply the so-called Green functions approach to solve this pricing PDE. In Section 2.4.3 we briefly sketched the idea behind the Green functions approach to solve differential equations. Note, that herewith the pricing formulae for both LIBOR caplets/floorlets and caplets/floorlets on compounded rates are derived. We denote $\hat{P}(t,T,x(t)) \equiv P(t,T)$, to be clear that the zero-coupon bond depends on process $x(t)$.

3.3.1.1. Hull-White pricing kernel for LIBOR rates

Consider a derivative with payoff $V(T,x(T))$ dependent on the value of the process $x(t)$ at time T, where $x(t)$ is given as in Equation (3.9) with deterministic yet time-dependent volatility $\sigma(t)$. According to Theorem 2.1, the value of this derivative at time $t < T$ is given by:

$$h(t,x(t)) = \mathbb{E}\left[e^{-\int_t^T r(u)du}V(T,x(T)) \mid \mathcal{F}_t\right]. \tag{3.10}$$

From the Feynman-Kac Theorem, it follows that (3.10) is a solution of the Kolmogorov backward diffusion equation:

$$\frac{\partial h}{\partial t} - ax\frac{\partial h}{\partial x} + \frac{1}{2}\sigma^2(t)\frac{\partial^2 h}{\partial x^2} - r(t)h = 0,$$

for $t \geq 0$ with the final condition $h(T,x) = V(T,x)$.

Turfus, 2019 derives the following Green function that solves the above Kolmogorov backward diffusion equation:

$$G(x,t;\xi,T) = \hat{P}(t,T,x)\varphi(\xi + I(t,T) - x\phi(t,T); \Sigma(t,T)),$$

where $\hat{P}(t,T,x)$ is the zero-coupon bond price under the Hull-white model and

$$\begin{aligned}
\varphi(x;\Sigma) &= \frac{1}{\sqrt{2\pi\Sigma}}\exp\left(-\frac{1}{2\Sigma}x^2\right),\\
\phi(t,T) &= \exp(-a(T-t)),\\
\Sigma(t,T) &= \int_t^T \phi^2(u,T)\sigma^2(u)du,\\
I(t,T) &= \int_t^T \phi(u,T)\Sigma(t,u)du.
\end{aligned}$$

For the details of the derivation of this pricing kernel, we refer to Appendix B.

This Green function is also called the pricing kernel. Note, that x represents the value of the process $x(t)$ at time t and ξ the value of $x(t)$ at time T. The price at time $t < T$ of a derivative with payoff $V(T,x(T))$ can be obtained by calculating the following integral:

$$h(t,x(t)) = \int_{\mathbb{R}} V(T,\xi)G(x,t;\xi,T)d\xi. \tag{3.11}$$

LIBOR caplet/floorlet prices Below we derive the pricing formula for the LIBOR caps/floors using the kernel approach. The caplet/floorlet payoff at time T_{i+1} with notional N and strike K on the LIBOR rate over $[T_i, T_{i+1}]$ can be written as:

$$V(T_{i+1}, x(T_i)) = N\tau \max\left(\omega\left[\frac{1}{\tau}\left(\frac{1}{\hat{P}(T_i, T_{i+1}, x(T_i))} - 1\right) - K\right], 0\right),$$

where ω equals 1 in case of a caplet and -1 in case of a floorlet.

In order to determine the present value of the caplet/floorlet, first the value of the caplet/floorlet at time T_i has to be determined:

$$V(T_i, x(T_i)) = \hat{P}(T_i, T_{i+1}, x(T_i))V(T_i, x(T_i)).$$

Second, the pricing kernel can be applied to the T_i-value to calculate the present value of the caplet/floorlet at time $t = 0$. Notice, for $t = 0$, also $x(t) = 0$. This approach then yields the following formulae for the today's present value of caplets/floorlets:

$$\begin{aligned} V^C(0,0) &= N(P(0,T_i)\Phi(-d_1) - (1+\tau K)P(0,T_{i+1})\Phi(-d_2)), \\ V^P(0,0) &= N((1+\tau K)P(0,T_{i+1})\Phi(d_2) - P(0,T_i)\Phi(d_1)), \end{aligned} \tag{3.12}$$

where

$$\begin{aligned} d_1 &= \frac{\log\left(\frac{P(0,T_{i+1})}{P(0,T_i)}(1+\tau K)\right) - \frac{1}{2}B^2(T_i,T_{i+1})\Sigma(0,T_i)}{B(T_i,T_{i+1})\sqrt{\Sigma(0,T_i)}}, \\ d_2 &= d_1 + B(T_i,T_{i+1})\sqrt{\Sigma(0,T_i)}. \end{aligned}$$

For the derivations, we refer to Appendix C.1. Notice, these pricing formulae are the same as the well known analytical formulae for caplets/floorlets which are described in the literature, see e.g. Sterling and Hári, 2007. This is expected since the same model is used but only a different approach.

3.3.1.2. Hull-White pricing kernel for compounded rates

For caplets/floorlets linked to the new RFR, the payoff no longer depends on the LIBOR rate but on a compounding rate. Although the rates are daily compounding, their usual approximation by a continuously compounded rate is used in practice. The interest over a period $[t, T]$ is calculated by:

$$\tilde{M}(t,T) = \exp\left(\int_t^T r(s)ds\right) - 1. \tag{3.13}$$

Therefore, the compounded interest (3.13) is path dependent. Subsequently, the payoff of a caplet/floorlet on compounded rates depends not only on the process $x(t)$ at the start of the caplet/floorlet, but also on the whole path of $x(t)$ until maturity. Following Turfus, 2020a we introduce a new variable $z(t)$:

$$z(t) = \int_0^t (\hat{g}(t) + x(s))\, ds,$$

where $\bar{g}(t) = \hat{g}(t) + f(0,t)$. Using $r(t)$ from Equation (3.8), we rewrite the interest over a period $[t, T]$ as:

$$\tilde{M}(t,T) = \frac{P(0,t)}{P(0,T)}\exp(z(T) - z(t)) - 1.$$

Let us now consider a derivative with payoff $\tilde{V}(T, x(T), z(T))$ that depends on the process $x(T)$ at maturity and the variable $z(T)$ at maturity. For such a derivative, the following pricing PDE holds:

$$\frac{\partial h}{\partial t} - ax\frac{\partial h}{\partial x} + (\hat{g}(t) + x)\frac{\partial h}{\partial z} + \frac{1}{2}\sigma^2(t)\frac{\partial^2 h}{\partial x^2} - r(t)h = 0,$$

for $t \geq 0$ and $h(T, x, z) = \tilde{V}(T, x, z)$.

Analogously to the previous section, this pricing PDE can be solved using the Green function approach. In Turfus, 2020b the Green function for the above PDE is derived in the following form:

$$\tilde{G}(x,z,t;\xi;\zeta,T) = \hat{P}(t,T,x)\varphi_2\Big[\xi + I(t,T) - x\phi(t,T), \zeta + K(t,T) - \mu(x,t,T) - z; \Sigma^+(t,T)\Big],$$

where $\varphi_2[\cdot,\cdot;\Sigma]$ is a bivariate Gaussian probability density function with a covariance Σ and:

$$\begin{aligned} K(t,T) &= \int_t^T I(t,u)du, \\ \Sigma^+(t,T) &= \begin{pmatrix} \Sigma(t,T) & I(t,T) \\ I(t,T) & 2K(t,T) \end{pmatrix}. \end{aligned}$$

Using this Green function the price at time $t < T$ of a derivative with payoff $\tilde{V}(x(T), z(T), T)$ can be obtained by calculating:

$$h(t,x(t),z(t)) = \int_{\mathbb{R}} \tilde{V}(T,\xi,\zeta)\tilde{G}(x,z,t;\xi,\zeta,T). \tag{3.14}$$

Caplet/floorlet prices on compounded rates Using the above result, the caps/floors on the compounded rates can be priced with the kernel approach. The caplet/floorlet payoff at time T_{i+1} on compounded rates over the period $[T_i, T_{i+1}]$ with notional N and strike K is defined as:

$$\tilde{V}_{CR}(T_{i+1}, x(\cdot), z(\cdot)) = N\tau \max\left(\omega\left[\frac{1}{\tau}M(T_i,T_{i+1}) - K\right], 0\right), \tag{3.15}$$

where ω is equals 1 in case of a caplet and -1 in case of a floorlet.

The calculation of today's present value of the caplet/floorlet on compounded rates is a two step approach. First, the pricing kernel needs to be applied to the payoff at time T_{i+1} to determine the time-T_i value of the caplet/floorlet. Second, the kernel has to be applied again, but then to the time-T_i value to obtain the present value. With this approach the present value (at time $t = 0$) of a caplet/floorlet on compounding rates is given by:

$$\begin{aligned} \tilde{V}^C_{CR}(0,0,0) &= N\Big(P(0,T_i)\Phi(-d_2) - \kappa P(0,T_{i+1})\Phi(-d_1)\Big), \\ \tilde{V}^P_{CR}(0,0,0) &= N\Big(\kappa P(0,T_{i+1})\Phi(d_1) - P(0,T_i)\Phi(d_2)\Big), \end{aligned} \tag{3.16}$$

where

$$\begin{aligned} d_2 &= \frac{\log\left(\frac{P(0,T_{i+1})}{P(0,T_i)}(1+\tau K)\right) - \frac{1}{2}\left(B^2(T_i,T_{i+1})\Sigma(0,T_i) + 2K(T_i,T_{i+1})\right)}{\sqrt{B^2(T_i,T_{i+1})\Sigma(0,T_i) + 2K(T_i,T_{i+1})}}, \\ d_1 &= d_2 + \sqrt{B^2(T_i,T_{i+1})\Sigma(0,T_i) + 2K(T_i,T_{i+1})}, \end{aligned}$$

and $\Phi(\cdot)$ is a Gaussian cumulative distribution function. For details of the derivation, we refer to Appendix C.2.

3.3.2. Monte Carlo simulation

The last approach we describe is pricing caps/floors using MC simulations. For a short introduction to MC methods we refer to Section 2.4.1 and references therein. With the MC approach, process $x(t)$ needs to be simulated. Therefore, in this section we explain how to determine the value of caplets/floorlets when process $x(t)$ is simulated directly from the distribution. First, we discuss LIBOR caps/floors and then consider caps/floors on compounded rates.

3.3.2.1. Monte Carlo simulation for LIBOR rates

Under the one-factor Hull-White model the short-rate can be expressed as in Section 3.2.2.1. The price of a LIBOR caplet/floorlet over the period $[T_i, T_{i+1}]$ is equal to:

$$V(t,x(\cdot)) = \mathbb{E}^{\mathbb{Q}}\left[\exp\left(-\int_t^{T_{i+1}} r(s)ds\right)\max\left(\omega\left[\frac{1}{P(T_i,T_{i+1})} - (1+\tau K)\right], 0\right)\middle|\mathcal{F}_t\right],$$

where the conditional expectation is under the risk-neutral measure and ω equals 1 in case of a caplet and -1 in case of a floorlet. To calculate this expression using the MC estimator, one would need to simulate the process $x(t)$ at time T_i to compute $P(T_i, T_{i+1})$ and simulate the whole path of process $x(t)$ to compute the money-market numeraire $\exp\left(-\int_t^{T_{i+1}} r(s)ds\right)$.

As explained in Section 2.2.2, it might be more convenient to price such a caplet/floorlet under the T-forward measure. Therefore, first the value of the caplet/floorlet at time T_i is considered under the T_{i+1}-forward measure, where the martingale property is used:

$$\begin{aligned}\frac{V(T_i, x(T_i))}{P(T_i, T_{i+1})} &= \mathbb{E}^{\mathbb{Q}^{T_{i+1}}}\left[\frac{V(T_{i+1}, x(T_i))}{P(T_{i+1}, T_{i+1})}\middle|\mathcal{F}_{T_i}\right] \\ \Longrightarrow V(T_i, x(T_i)) &= P(T_i, T_{i+1})\max\left(\omega\left[\frac{1}{P(T_i, T_{i+1})} - (1+\tau K)\right], 0\right).\end{aligned}$$

Second, the general T-forward measure is used to obtain the t-value of the caplet/floorlet:

$$\frac{V(t, x(T_i))}{P(t,T)} = \mathbb{E}^{\mathbb{Q}^T}\left[\frac{V(T_i, x(T_i))}{P(T_i, T)}\middle|\mathcal{F}_t\right],$$

which implies:

$$\begin{aligned}V(t, x(T_i)) &= P(t,T)\mathbb{E}^{\mathbb{Q}^T}\left[\frac{V(T_i, x(T_i))}{P(T_i, T)}\middle|\mathcal{F}_t\right] \\ &= P(t,T)\mathbb{E}^{\mathbb{Q}^T}\left[P(T_i, T_{i+1})\frac{V(T_{i+1}, x(T_i))}{P(T_i, T)}\middle|\mathcal{F}_t\right] \\ &= P(t,T)\mathbb{E}^{\mathbb{Q}^T}\left[\frac{P(T_i, T_{i+1})}{P(T_i, T)}\max\left(\omega\left[\frac{1}{P(T_i, T_{i+1})} - (1+\tau K)\right], 0\right)\middle|\mathcal{F}_t\right]\end{aligned}$$

As a result, under the T-forward measure, process $x(t)$ only needs to be simulated at time T_i in order to compute $P(T_i, T_{i+1})$ and $P(T_i, T)$. This result follows because zero-coupon bonds are used to discount the payoff instead of the money-market account.

Since we change to pricing under the T-forward measure, we also need the dynamics of $x(t)$ under the T-forward measure. By applying Itô's lemma on Equation (3.3), the dynamics of the zero-coupon bond price in the Hull-White model are given by:

$$dP(t,T) = r(t)P(t,T)dt + \sigma(t)B(t,T)P(t,T)dW^{\mathbb{Q}}(t).$$

The Radon-Nikodym of $\mathbb{Q}^T$ with respect to $\mathbb{Q}$ given by:

$$\eta = \frac{M(t_0)/M(T)}{P(t_0,T)/P(T,T)},$$

is a martingale under $\mathbb{Q}$, where $t_0 = 0$ is today's date. The SDE of this Radon-Nikodym derivative is given by:

$$d\eta(t) = -\eta(t)\sigma(t)B(t,T)dW^{\mathbb{Q}}(t).$$

Solving this SDE gives:

$$\eta(t) = \exp\left(-\frac{1}{2}\int_0^T \sigma^2(u)B^2(u,T)du + \int_0^T \sigma(u)B(u,T)dW^{\mathbb{Q}}(u)\right).$$

According to Girvanov's Theorem 2.6:

$$dW^{\mathbb{Q}^T}(t) = \sigma(t)B(t,T)dt + dW^{\mathbb{Q}}(t),$$

is a Brownian motion under $\mathbb{Q}^T$. With this expression of the Brownian motion, the dynamics of $x(t)$ under the T-forward measure are given by:

$$\begin{aligned}dx(t) &= \left[-\sigma(t)^2B(t,T) - ax(t)\right]dt + \sigma(t)dW^{\mathbb{Q}^T}(t), \\ x(0) &= 0.\end{aligned}$$

Using Itô's lemma, process $x(t)$ is presented by:

$$x(t) = x(s)e^{-a(t-s)} - \int_s^t e^{-a(t-u)}\sigma^2(u)B(u,T)du + \int_s^t e^{-a(t-u)}\sigma(u)dW^{\mathbb{Q}^T}(u).$$

Therefore, process $x(t)$ can be simulated directly from the distribution for any $t > s$ under the T-forward measure with:

$$x(t) = \mathbb{E}^{\mathbb{Q}^T}[x(t)|x(s)] + \sqrt{\mathrm{Var}^{\mathbb{Q}^T}[x(t)|x(s)]}\mathcal{N}(0,1),$$

where $\mathcal{N}(0,1)$ is a standard normal random variable.

Conditional expectation and variance under the *T*-forward measure As mentioned above, the conditional expectation and variance are needed to simulate process $x(t)$ directly from the distribution. This expectation and variance at time t conditional on the information at time s are given by:

$$\begin{aligned}\mathbb{E}^{\mathbb{Q}^T}[x(t)|x(s)] &= x(s)e^{-a(t-s)} - \int_s^t e^{-a(t-u)}\sigma^2(u)B(u,T)du,\\ \mathrm{Var}^{\mathbb{Q}^T}[x(t)|x(s)] &= \int_s^t e^{-2a(t-u)}\sigma^2(u)du.\end{aligned}$$

Note, that the variance is independent of $x(s)$.

Since we consider a case of the piecewise constant volatility, we simplify the above expressions on the constant intervals, with volatility σ, yielding:

$$\begin{aligned}\int_l^u e^{-a(t-s)}B(s,T)ds &= \frac{\sigma^2}{2a}\left(e^{-a(T+t)}(e^{al}-e^{au})(e^{al}-e^{aT}+e^{au})\right),\\ \int_l^u e^{-2a(t-s)}\sigma^2 ds &= \frac{\sigma^2}{2a}\left(e^{-2a(t-u)}-e^{-2a(t-l)}\right).\end{aligned}$$

3.3.2.2. Monte Carlo simulation for compounded rates

For the LIBOR caplets/floorlets a single zero-coupon bond price $P(T_i, T_{i+1})$ determines the LIBOR rate. In contrast, for the caplets/floorlets on compounded rates a sequence of daily zero-coupon bonds along the path should be used to calculate the compounded rate. The value of the compounded rate can be presented in terms of daily bond prices since the value of the overnight rate is simple compounded and can be calculated by:

$$\frac{1}{\tau_j}\left(\frac{1}{P(t_j, t_{j+1})} - 1\right),$$

where the overnight fixing is for day t_j and τ_j is the year fraction corresponding to $[t_j, t_{j+1}]$. The daily compounded rate is determined as in Definition 2.2, which can be simplified by taking the following product:

$$CR(T_i, T_{i+1}) = \frac{1}{\tau}\left(\prod_{j=1}^{n}\frac{1}{P(t_j\, t_{j+1})} - 1\right),$$

where the compounded rate is over the period $[T_i, T_{i+1}]$ with fixing dates $T_i = t_1 < \ldots < t_n = T_{i+1}$ and τ is the year fraction from T_i to T_{i+1}. Notice, the zero-coupon bond $P(t_j, t_{j+1})$ depends on the simulation of process $x(t)$ at time t_j. Therefore, to compute this daily compounded rate, process $x(t)$ has to be simulated on each date within the tenor of the caplet. Based on these realisations of $x(t)$ the daily bond prices $P(t_j, t_{j+1})$ are computed.

3.4. Numerical results

In this section we compare different approaches to the cap/floor pricing under the Hull-White model. A comparison between the pricing kernel and the MC simulation for caps/floors on compounded rates is presented in Section 3.4.1. Thereafter, a convergence test for the MC approach for compounded rates is shown in Section 3.4.2. Lastly, the values of the LIBOR caplets and the caplets on compounded rates are compared in Section 3.4.3. Therein we also comment on a relation between their prices.

3.4.1. Pricing kernel vs Monte Carlo

In this section we compare prices of the caplets on compounded rates obtained by different methods: the Hull-White pricing kernel, see Section 3.3.1.2, and the MC simulation, see Section 3.3.2.2. To do so, we fix a realistic piecewise constant volatility shown in Table 3.1. Since there does not exists a liquid market for options on compounded rates, we consider a proxy market generated from $3M$ LIBOR caplets and the market implied United States Dollar Secured Overnight Financing Rate (USD SOFR) curve as of 23-11-2020. The calibration instruments that are used to calibrate the volatilities are $3M$ LIBOR caplets with maturities $2Y, 5Y, 7Y, 10Y$ and $15Y$. For more details about this proxy market and how the volatilities are calibrated, we refer to Chapter 5.

For the comparison of the two pricing methods, a set of caplets is priced with a tenor of $1Y$ on a grid of maturities $[2Y, 5Y, 7Y, 10Y, 15Y]$ and strikes $[-10\%, -2\%, 0\%, 0.5\%, 1\%, 2\%, 10\%]$. For completeness, the extreme cases of a strike of -10% and 10% are included in this comparison. We consider caplets with a tenor of $1Y$ as those are expected to be the most commonly traded ones in the market. Also to calculate caplets on compounded rates we use the market implied USD SOFR curve as of 23-11-2020.

$t \in$	$[0, 2)$	$[2, 5)$	$[5, 7)$	$[7, 10)$	$[10, 15)$
σ	0.5503%	0.7768%	0.9814%	0.7433%	1.0071%

Table 3.1: Piecewise constant volatility with mean reversion speed $a = 0.03$ and t is in years.

Table 3.3 summarises the values of the caplets on the aforementioned grid of maturities and strikes. We observe that the difference between the values obtained by the pricing kernel and by the MC simulation are in line with the corresponding standard errors. Hence, the analytical formula derived from the kernel approach is correct. Furthermore, the prices behave as expected. More specifically, for any fixed maturity the price behaves monotonically in strike dimension. In particular, the price decreases when the strike increases. Note, for a high strike of 10% the caplets are deep Out of the Money (OTM) and, thus, their values are expected to be close to zero. This is in line with the results of Table 3.3. Furthermore, for a low strike of -10% the caplets are deep It the Money (ITM) and, thus, their values are expected to be close to the values of the corresponding swaplets. Table 3.4 illustrates that this holds for the extreme low strike of -10%.

Further to the above, we present computation times of the calculations in Table 3.2. First, notice that, as we expected, the computation times are independent of the maturity and strike. For the MC estimator, this is the case since we sample directly from the distribution and do not apply a time discretisation between the reference date and the start of the caplet. In other words, one jump is made in the simulation from the reference date to the start date of the caplet. Furthermore, it is not a surprise that the computation times of the MC simulation are much higher than those of the pricing kernel for compounded rates. For the MC estimator, a daily realisation of process $x(t)$ is needed, which causes these high computational times.

Strike	**Maturity 1Y**		**Maturity 2Y**		**Maturity 5Y**		**Maturity 10Y**		**Maturity 15Y**	
	Kernel	**MC**	**Kernel**	**MC**	**Kernel**	**MC**	**Kernel**	**MC**	**Kernel**	**MC**
-10%	0.209	887	0.359	753	0.295	753	0.410	767	0,350	774
-2%	0.279	758	0.264	734	0.306	750	0.360	778	0.330	769
0%	0.270	726	0.271	742	0.320	746	0.437	782	0.355	767
0.5%	0.237	745	0.280	752	0.360	757	0,330	762	0.358	773
1%	0.304	801	0.310	734	0.320	753	0.336	766	0.363	771
2%	0.295	752	0.290	739	0.280	758	0.335	766	0.478	766
10%	0.340	747	0.246	743	0.344	757	0.350	779	0.376	787

Table 3.2: Computation time in seconds for caplet prices on compounded rates obtained with the Hull-White pricing kernel for compounded rates and the MC simulation for compounded rates. For the MC simulation 10.000.000 paths are used. The caplets have a tenor of $1Y$ and are on the aforementioned grid of maturities and strikes. The computations are done on a computer with processor: Intel(R) Xeon(R) Gold 6132 CPU @ 2.60GHz (2 processors) and 256 GB RAM.

Strike	Kernel	Monte Carlo	Standard error	Difference
-10%	1005	1005	$1 \cdot 10^{-2}$	$4 \cdot 10^{-3}$
-2%	206	206	$1 \cdot 10^{-2}$	$6 \cdot 10^{-3}$
0%	16	16	$6 \cdot 10^{-3}$	$3 \cdot 10^{-2}$
0.5%	1	1	$2 \cdot 10^{-3}$	$7 \cdot 10^{-3}$
1%	$1 \cdot 10^{-2}$	$1 \cdot 10^{-2}$	$2 \cdot 10^{-4}$	$1 \cdot 10^{-4}$
2%	$3 \cdot 10^{-9}$	0	0	$3 \cdot 10^{-9}$
10%	$9 \cdot 10^{-200}$	0	0	$9 \cdot 10^{-200}$

(a) Results for caplets with a maturity of $1Y$.

Strike	Kernel	Monte Carlo	Standard error	Difference
-10%	1003	1003	$2 \cdot 10^{-2}$	$-2 \cdot 10^{-2}$
-2%	207	207	$2 \cdot 10^{-2}$	$1 \cdot 10^{-2}$
0%	29	29	$1 \cdot 10^{-2}$	$-4 \cdot 10^{-3}$
0.5%	9	9	$7 \cdot 20^{-3}$	$1 \cdot 10^{-2}$
1%	2	2	$3 \cdot 10^{-3}$	$2 \cdot 10^{-3}$
2%	$2 \cdot 10^{-2}$	$2 \cdot 10^{-2}$	$3 \cdot 10^{-4}$	$9 \cdot 10^{-5}$
10%	$3 \cdot 10^{-52}$	0	0	$3 \cdot 10^{-52}$

(b) Results for caplets with a maturity of $2Y$.

Strike	Kernel	Monte Carlo	Standard error	Difference
-10%	1044	1044	$4 \cdot 10^{-2}$	$-3 \cdot 10^{-2}$
-2%	255	255	$4 \cdot 10-2$	$2 \cdot 10^{-2}$
0%	86	86	$3 \cdot 10^{-2}$	$2 \cdot 10^{-2}$
0.5%	57	57	$3 \cdot 10^{-2}$	$-2 \cdot 10^{-2}$
1%	35	35	$2 \cdot 10^{-2}$	$-3 \cdot 10^{-2}$
2%	10	10	$1 \cdot 10^{-2}$	$3 \cdot 10^{-3}$
10%	$2 \cdot 10^{-10}$	0	0	$2 \cdot 10^{-10}$

(c) Results for caplets with a maturity of $5Y$.

Strike	Kernel	Monte Carlo	Standard error	Difference
-10%	1057	1057	$6 \cdot 10^{-2}$	$-7 \cdot 10^{-3}$
-2%	311	311	$6 \cdot 10^{-2}$	$3 \cdot 10^{-2}$
0%	152	152	$5 \cdot 10^{-2}$	$-2 \cdot 10^{-2}$
0.5%	120	120	$4 \cdot 10^{-2}$	$-2 \cdot 10^{-2}$
1%	92	92	$4 \cdot 10^{-2}$	$1 \cdot 10^{-2}$
2%	50	50	$3 \cdot 10^{-2}$	$3 \cdot 10^{-2}$
10%	$2 \cdot 10^{-3}$	$2 \cdot 10^{-3}$	$1 \cdot 10^{-4}$	$-7 \cdot 10^{-5}$

(d) Results for caplets with a maturity of $10Y$.

Strike	Kernel	Monte Carlo	Standard error	Difference
-10%	993	992	$8 \cdot 10^{-2}$	$8 \cdot 10^{-2}$
-2%	304	304	$7 \cdot 10^{-2}$	$6 \cdot 10^{-2}$
0%	165	165	$6 \cdot 10^{-2}$	$2 \cdot 10^{-1}$
0.5%	136	136	$5 \cdot 10^{-2}$	$1 \cdot 10^{-1}$
1%	111	111	$5 \cdot 10^{-2}$	$2 \cdot 10^{-1}$
2%	70	70	$4 \cdot 10^{-2}$	$5 \cdot 10^{-2}$
10%	$9 \cdot 10^{-2}$	$9 \cdot 10^{-2}$	$1 \cdot 10^{-3}$	$1 \cdot 10^{-3}$

(e) Results for caplets with a maturity of $15Y$.

Table 3.3: Values of caplets on the aforementioned grid of strikes and maturities with a tenor of 1Y and a notional of 10.000. The values of the caplet are computed with the pricing kernel for compounded rates and the MC simulation for compounded rates. For the MC simulation 10.000.000 paths are used. Furthermore, this table presents the standard error which is made due to the MC simulation and the difference between the values obtained with the pricing kernel and the MC simulation for compounded rates.

Maturity	Caplet	Swaplet
$2Y$	1005	1005
$5Y$	1003	1003
$7Y$	1044	1044
$10Y$	1057	1057
$15Y$	993	993

Table 3.4: Values of caplets and swaplets with a tenor of $1Y$ for a strike of -10% and a notional of 10.000.

3.4.2. Convergence Monte Carlo method

SDE MC estimation, in general, involves two types of errors: a discretisation error and a standard error. The discretisation error results from an application of some discretisation scheme. However, in our setting we sample exactly from the distribution and, thus, our MC estimator does not have a discretisation error. As mentioned in Section 2.4.1, the standard error is given by:

$$\epsilon_{\tilde{N}} = \frac{\tilde{v}_{\tilde{N}}}{\sqrt{\tilde{N}}},$$

where $\bar{v}_{\tilde{N}}^2$ is the sample variance. Therefore, when the number of MC paths increases with a factor 10, the standard error should decrease with a factor $\sqrt{10} \approx 3.16$. This straightforward result is shown in Figure 3.1 and Table 3.5. Figure 3.1 illustrates standard errors for different numbers of paths and three caplets with different maturities. Table 3.5 shows the corresponding values of caplets on compounded rates with a MC simulation and the Hull-White pricing kernel for various number of MC paths. We indeed observe that if the numbers of MC paths increases with a factor 10, the standard error decreases with a factor of $\sqrt{10}$. Furthermore, the difference between the values obtained with the MC simulation and the pricing kernel also decreases when the number of MC paths increase. Hence, we observe a convergence of the MC simulation to the pricing kernel if the number of MC paths increases.

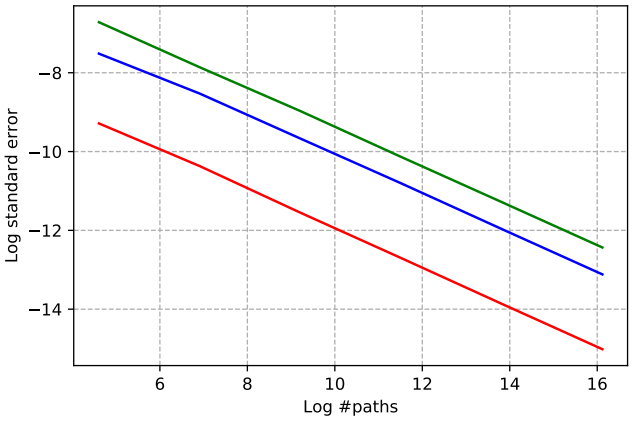

Figure 3.1: A log-log plot of the standard error made by the MC simulation against number of MC paths. This is shown for caplets with a tenor of $1Y$ and maturity of $2Y$ (red), $5Y$ (blue) and $10Y$ (green).

3.4.3. LIBOR vs Compounded rates

In this section, the values of LIBOR caplets and the values of caplets on compounded rates are compared. To start, we compare the pricing formulae for the LIBOR caplets and the caplets on compounded rates. For LIBOR caplets over the period $[T_i, T_{i+1}]$ formula (3.12) is considered and compared to formula (3.16) for caplets on compounded rates over the period $[T_i, T_{i+1}]$. It is easy to spot that if $K(T_i, T_{i+1})$ in Equation (3.16) is set equal to zero, it collapses to Equation (3.12). Therefore, we investigate the impact of $2K(T_i, T_{i+1})$ on the LIBOR caplet formula and seek for a relation between $2K(T_i, T_{i+1})$ and $B^2(T_i, T_{i+1})\Sigma(0, T_i)$, see Equation (3.17) and (3.18). For the sake of simplicity we assume a constant volatility.

First, we would like to mention that $\Sigma(0, T_i)$ is the accumulated variance from the reference date until the start of a caplet and $K(T_i, T_{i+1})$ is the accumulated variance of the integrated short-rate over the period $[T_i, T_{i+1}]$. One can think of $B^2(T_i, T_{i+1})\Sigma(0, T_i)$ as the variance of a LIBOR rate and $B^2(T_i, T_{i+1})\Sigma(0, T_i)$ $+2K(T_i, T_{i+1})$ as the variance of a compounded rate.

Second, we analytically compare the formulae of $2K(T_i, T_{i+1})$ and $B^2(T_i, T_{i+1})\Sigma(0, T_i)$ to find a relation. Let us assume $a \geq 0$, $0 \leq t \leq T$ and define $\Delta = T_{i+1} - T_i$. The following then holds:

$$2K(T_i, T_{i+1}) = \sigma^2 \int_t^T B^2(T_i, u)du \leq \frac{\sigma^2}{a^2}\Delta, \tag{3.17}$$

$$B^2(T_i, T_{i+1})\Sigma(0, T_i) = B(T_i, T_{i+1})\frac{\sigma^2}{2a}(1 - e^{-2aT_i}) = \frac{\sigma^2}{2a^2}(1 - e^{-a\Delta})(1 - e^{-2aT_i}). \tag{3.18}$$

From these two equations, one can conclude:

- the upper bound of $2K(T_i, T_{i+1})$ is dependent on the caplet tenor, Δ, and is independent of the caplet start time T_i;
- $B^2(T_i, T_{i+1})\Sigma(0, T_i)$ depends on the caplet tenor, Δ, and grows monotonically with the caplet start time T_i;

#Paths	Monte Carlo	Standard error	Difference
100	2,05	$9,27 \cdot 10^{-1}$	$-1,26 \cdot 10^{-1}$
1.000	1,89	$3,14 \cdot 10^{-1}$	$3,43 \cdot 10^{-2}$
10.000	1,96	$9,63 \cdot 10^{-2}$	$-3,10 \cdot 10^{-2}$
100.000	1,94	$3,05 \cdot 10^{-2}$	$-1,14 \cdot 10^{-2}$
1.000.000	1,92	$9,53 \cdot 10^{-3}$	$4,41 \cdot 10^{-3}$
10.000.000	1,92	$3,01 \cdot 10^{-3}$	$2,01 \cdot 10^{-3}$

(a) Caplets with a maturity of $2Y$. The value obtained with the kernel is $1,93$.

#Paths	Monte Carlo	Standard error	Difference
100	27,57	5,45	7,02
1.000	34,37	1,98	2,23
10.000	34,16	$6,32 \cdot 10^{-1}$	$4,33 \cdot 10^{-1}$
100.000	34,93	$2,03 \cdot 10^{-1}$	$-3,37 \cdot 10^{-1}$
1.000.000	34,52	$6,36 \cdot 10^{-2}$	$7,41 \cdot 10^{-2}$
10.000.000	34,62	$2,01 \cdot 10^{-2}$	$-2,52 \cdot 10^{-2}$

(b) Caplets with a maturity of $5Y$. The value obtained with the kernel is $34,59$.

#Paths	Monte Carlo	Standard error	Difference
100	103,25	12,1	-10,9
1.000	88,81	3,86	3,52
10.000	94,67	1,27	-2,34
100.000	91,99	$3,97 \cdot 10^{-1}$	$3,38 \cdot 10^{-1}$
1.000.000	92,45	$1,26 \cdot 10^{-1}$	$-1,17 \cdot 10^{-1}$
10.000.000	92,32	$3,98 \cdot 10^{-2}$	$1,33 \cdot 10^{-2}$

(c) Caplets with a maturity of $10Y$. The value obtained with the kernel is $92,33$.

Table 3.5: Value of caplets on compounded rates with a strike of 1% and a notional of 10.000 for various numbers of MC paths. The caplets have a tenor of $1Y$ and a maturity of $2Y$, $5Y$ and $10Y$. Furthermore, the value of the caplets obtained with the pricing kernel for compounded rates are shown, the standard error due to the MC simulation is presented and the difference between the values obtained with the pricing kernel and the MC simulation for compounded rates are given.

Since $B^2(T_i, T_{i+1})\Sigma(0, T_i)$ is bounded from below by zero, the difference between $B^2(T_i, T_{i+1})\Sigma(0, T_i)$ and $2K(T_i, T_{i+1})$ is always bounded by zero and $\frac{\sigma^2}{a^2}\Delta$.

To continue, Figure 3.2 illustrates the value of $2K(T_i, T_{i+1})$ and $B^2(T_i, T_{i+1})\Sigma(0, T_i)$ for two different tenors and various maturities. First, notice that $2K(T_i, T_{i+1})$ is constant for the different maturities and only differs for the two tenors. Recall, this is the special case of constant volatility. Second, observe that $B^2(T_i, T_{i+1})\Sigma(0, T_i)$ grows with the maturity, while this is not the case for $2K(T_i, T_{i+1})$. More specifically, for a tenor of $1Y$, the difference between $2K(T_i, T_{i+1})$ and $B^2(T_i, T_{i+1})\Sigma(0, T_i)$ at the $1Y$ maturity is of an order $\frac{1}{2}$ and at the $4Y$ maturity of an order 1. Furthermore, it is clear that the impact of $2K(T_i, T_{i+1})$ decreases when the maturity increases. This is also in line with Figure 3.3 and the conclusion from Equations (3.17) and (3.18).

Table 3.6 shows the values of both LIBOR caplets and the corresponding caplets on compounded rates for two different tenors and various maturities. As in line with the above points, the differences are larger for caplets with short maturities than for caplets with long maturities. With the put-call parity, it is easy to observe that the same holds for floorlets. However, note that this comparison assumes a constant volatility. When piecewise constant volatility is considered, the comparison does not hold anymore. An example is shown in Table 3.7. In particular, for a maturity of $5Y$ the difference between a LIBOR caplet and caplet on compounded rates is larger than for a maturity of $1Y$.

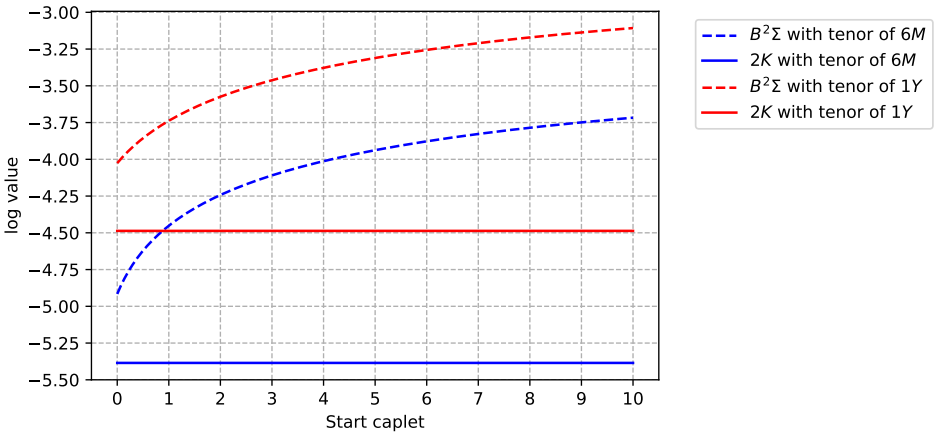

Figure 3.2: The log values of $B^2(T_i, T_{i+1})\Sigma(0, T_i)$ and $2K(T_i, T_{i+1})$ for two different tenors. In blue we have $B^2(T_i, T_{i+1})\Sigma(0, T_i)$ and $2K(T_i, T_{i+1})$ with a tenor of 6 months and in red we have $B^2(T_i, T_{i+1})\Sigma(0, T_i)$ and $2K(T_i, T_{i+1})$ with a tenor of 1 year. The horizontal axis denotes the start time of the caplet in years.

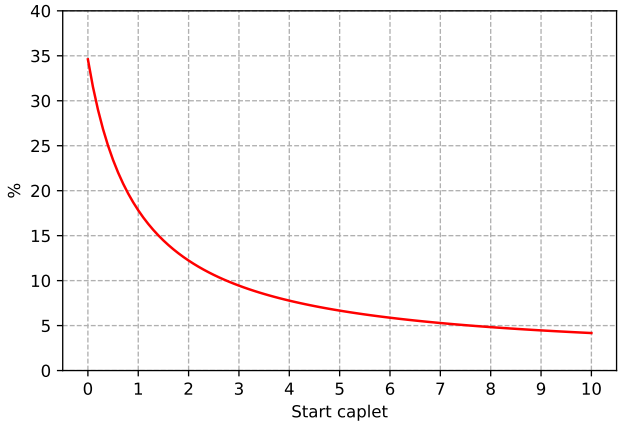

Figure 3.3: $2K(T_i, T_{i+1})$ as a percentage of $B^2(T_i, T_{i+1})\Sigma(0, T_i)$, where we consider a tenor of 1Y and the horizontal axis denotes the start time of the caplet in years.

3.5. Conclusion

Based on the results from Section 3.4 a conclusion is given below. For the Hull-White model, two approaches have been considered to price caplets/floorlets on compounded rates: the pricing kernel approach and the MC simulation. The results showed that the differences between the two approaches are in line with the MC error. Moreover, as expected, the computation time with the pricing kernel approach was smaller than with the MC simulation. Therefore, we use the analytical pricing formula obtained with the pricing kernel to price caplets/floorlets on compounded rate in the comparative study in Chapter 5.

Further, the convergence of the MC simulation has been investigated. As in line with the theory, the standard error increases with a factor 2 when the MC paths increases with a factor 4. Moreover, the MC estimation converged to the value obtained with the analytic pricing kernel.

Last, the LIBOR caplets/floorlets have been compared to the caplets/floorlets on compounded rates. First, the difference in the analytical pricing formula has been observed and results in an extra convexity adjustment term for the compounded rate. Further, in case of a constant volatility, this convexity adjustment has the most impact for caplets/floorlets with a shorter maturity than for caplets/floorlets with a longer maturity. However, this does not hold in the case of non-constant volatility.

Maturity	LIBOR caplet	Caplet on compounded rate	Difference (bps)
$2Y$	7,63	8,66	1,03
$5Y$	30,20	31,00	0,81
$10Y$	57,36	57,93	0,57

(a) Tenor of 6M.

Maturity	LIBOR caplet	Caplet on compounded rate	Difference (bps)
$2Y$	9,04	13,27	4,23
$5Y$	54,44	57,76	3,32
$10Y$	111,27	113,61	2,33

(b) Tenor of 1Y

Table 3.6: Caplet values calculated with the pricing kernel used for LIBOR rates and the pricing kernel for compounded rates for various maturities and two tenors. In the right column the difference between the two caplets is presented in Basis Points (bps). The caplets have a strike of 1%, a notional of 10.000 and a constant volatility of 1% is used.

Maturity	LIBOR caplet	Caplet on compounded rate	Difference (bps)
$2Y$	1,24	1,53	0,30
$5Y$	18,53	19,21	0,69
$10Y$	46,73	47,13	0,40

(a) Tenor of 6M.

Maturity	LIBOR caplet	Caplet on compounded rate	Difference (bps)
$2Y$	0,95	1,93	0,97
$5Y$	31,75	34,59	2,84
$10Y$	90,70	92,33	1,63

(b) Tenor of 1Y

Table 3.7: Caplet values calculated with the pricing kernel used for LIBOR rates and the pricing kernel for compounded rates for various maturities and two tenors. In the right column the difference between the two caplets is presented in bps. The caplets have a strike of 1%, a notional of 10.000 and the piecewise volatility from Table 3.1 is used.

4

Black-Karasinski model

This chapter introduces the Black-Karasinski model in Section 4.1. As in Chapter 3 on the Hull-White model, various methods to price caps/floors under the Black-Karasinski model are investigated in Section 4.2. For every method, both LIBOR caps/floors and caps/floors on compounded rates are considered. Thereafter, a comparison of the various pricing methods is given in Section 4.3. The chapter is concluded in Section 4.4.

4.1. Short-rate model

The Black-Karasinski model is a log-normal short-rate model. Within this model the instantaneous short-rate process is assumed to be modelled as an exponential of an Ornstein-Uhlenbeck process with time-dependent parameters, for further details see e.g. Brigo and Mercurio, 2007. The dynamics of the short-rate under the risk-neutral measure are given by:

$$\begin{aligned} d\ln(r(t)) &= [\theta(t) - a(t)\ln(r(t))]\,dt + \sigma(t)dW^{\mathbb{Q}}(t), \\ r(0) &= r_0. \end{aligned}$$

The volatility and mean reversion parameter are denoted by $\sigma(t)$ and $a(t)$, respectively. As in the Hull-White model, $\theta(t)$ is a deterministic function calibrated such that the model implied initial term structure matches the market observed term structure. For the rest of this thesis, we assume the mean reversion parameter to be constant, i.e., $a(t) = a$.

Using Itô's lemma, the short-rate under the Black-Karasinski model is given by:

$$r(t) = \exp\left(\ln(r(0))e^{-at} + \int_0^t e^{-a(t-u)}\theta(u)du + \int_0^t e^{-a(t-u)}\sigma(t)dW^{\mathbb{Q}}(t)\right).$$

Hence, the short-rate is log-normally distributed with the following conditional expectation and variance, for $s < t$:

$$\begin{aligned} \mathbb{E}\left[r(t)|\mathcal{F}s\right] &= \exp\left(\ln(r(s))e^{-a(t-s)} + \int_s^t e^{-a(t-u)}\theta(u)du\right), \\ Var\left[r(t)|\mathcal{F}s\right] &= \int_s^t e^{-2a(t-u)}\sigma^2(u)du. \end{aligned}$$

For log-normally distributed short-rates, the expected value of the money-market account is infinite for every maturity, see Proposition 4.1 and Andersen and Piterbarg, 2010 for a more general discussion. This is one of the drawbacks of modelling the short-rate with a log-normal model.

In contrast to the Hull-White model, the Black-Karasinski model does not have an analytic formula for the zero-coupon bond prices. This makes the calibration to the market observed term structure harder than for the Hull-White model. In order to calibrate to the initial term structure, trees can be used. The construction of a trionomial tree and the calibration to the initial term structure is described in Section 4.2.2.

Proposition 4.1. *Assume the short-rate to be modelled by the Black-Karasinski model, then the expectation of the money-market account is infinite, for every maturity T, i.e.,*

$$\mathbb{E}\left[\exp\left(\int_t^T r(s)ds\right)\right] = \infty.$$

Proof. For a proof, we refer to Brigo and Mercurio, 2007. □

4.2. Pricing methods

This section describes three pricing methods for the caps/floors. We begin with the pricing kernel for the Black-Karasinski model in Section 4.2.1. Thereafter, we discuss the trinomial trees and the MC simulation for the caps/floors pricing in Section 4.2.2 and Section 4.2.3, respectively.

4.2.1. Black-Karasinski pricing kernel

Similar to the Hull-White model, there exists a pricing kernel for the Black-Karasinski model provided in Turfus, 2021. However, contrary to the Hull-White case, there does not exist a closed form formula for the cap/floor prices. Using the pricing kernel for the Black-Karasinski model, an approximation for caplet/floorlet prices can be obtained. In this section, we present the approximate pricing formulae for both LIBOR caplets/floorlets and caplets/floorlets on compounded rates derived using the pricing kernel approach.

4.2.1.1. Black-Karasinski pricing kernel for LIBOR rates

First, we introduce the pricing PDE in the Black-Karasinski model. Thereafter, the formulae for the present value of the caplets/floorlets are provided.

To proceed further, we represent the short-rate as:

$$r(t) = \tilde{r}(t)\exp\left(x(t) - \frac{1}{2}\Sigma(0,t)\right), \tag{4.1}$$

where $\tilde{r}(t)$ is a deterministic function to be calibrated to the initial term structure, $x(t)$ is the zero mean process defined by Equation (3.9) and $\Sigma(0,t)$ is defined as in Section 3.3.1.1.

Similar to the Hull-White model, the pricing PDE for the Black-Karasinski model is given by:

$$\frac{\partial h}{\partial t} - ax\frac{\partial h}{\partial x} + \frac{1}{2}\sigma^2(t)\frac{\partial^2 h}{\partial x^2} - r(t)h = 0, \tag{4.2}$$

for $t \geq 0$ with $h(T,x) = V(T,x)$ for a derivative with the payoff $V(T,x)$. Then, according to Feynman-Kac Theorem 2.2, the solution of the PDE gives the value function of the corresponding derivative.

Following Turfus, 2021, Chapter 5, this pricing PDE can be solved with a Green function. This results in the following approximation of the pricing formulae for the present value $(t = 0)$ of LIBOR caplets/floorlets:

$$\begin{aligned}
V^C(0,0) \;=\; & \left(D(0,T_i) - \kappa D(0,T_{i+1})\right)\Phi(-d_1(x^*,0,T_i)) \\
& - D(0,T_i)\int_0^{T_i}\bar{r}(u)\left(\Phi(-d_2(x^*,0,T_i,u)) - \Phi(-d_1(x^*,0,T_i))\right)du \\
& + \kappa D(0,T_{i+1})\int_0^{T_{i+1}}\bar{r}(u)\left(\Phi(-d_2(x^*,0,T_i,u)) - \Phi(-d_1(x^*,0,T_i))\right)du \\
& - \kappa D(0,T_{i+1})\int_{T_i}^{T_{i+1}}\bar{r}(v)\int_0^{v}\bar{r}(u)e^{\phi(u,v)\Sigma(0,u)}\left(\Phi(-d_2^*(x^*,0,T_i,u,v))\right. \\
& \left. - \Phi(-d_2(x^*,0,T_i,v))\right)dudv + \kappa D(0,T_{i+1})\int_{T_i}^{T_{i+1}}\bar{r}(v)\int_0^{v}\bar{r}(u)\Big(\Phi(-d_1^*(x^*,0,T_i,u,v)) \\
& - \Phi(-d_2(x^*,0,T_i,v)) + \Phi(-d_2(x^*,0,T_i,u)) - \Phi(-d_1(x^*,0,T_i))\Big)dudv + \mathcal{O}(\epsilon^3),
\end{aligned}$$

$$
\begin{aligned}
V^P(0,0) \;=\;& (\kappa D(0,T_{i+1}) - D(0,T_i))\,\Phi(d_1(x^*,0,T_i)) \\
&+D(0,T_i)\int_0^{T_i}\bar{r}(u)\,(\Phi(d_2(x^*,0,T_i,u)) - \Phi(d_1(x^*,0,T_i)))\,du \\
&-\kappa D(0,T_{i+1})\int_0^{T_{i+1}}\bar{r}(u)\,(\Phi(d_2(x^*,0,T_i,u)) - \Phi(d_1(x^*,0,T_i)))\,du \\
&+\kappa D(0,T_{i+1})\int_{T_i}^{T_{i+1}}\bar{r}(v)\int_0^{v}\bar{r}(u)e^{\phi(u,v)\Sigma(0,u)}\left(\Phi(d_2^*(x^*,0,T_i,u,v)) - \Phi(d_2(x^*,0,T_i,v))\right)dudv \\
&-\kappa D(0,T_{i+1})\int_{T_i}^{T_{i+1}}\bar{r}(v)\int_0^{v}\bar{r}(u)\Big(\Phi(d_1^*(x^*,0,T_i,u,v)) - \Phi(d_2(x^*,0,T_i,v)) \\
&+\Phi(d_2(x^*,0,T_i,u)) - \Phi(d_1(x^*,0,T_i))\Big)dudv + \mathcal{O}(\epsilon^3),
\end{aligned}
$$

where

$$
\begin{aligned}
d_1(\xi,t,T_i) &:= \frac{\xi}{\sqrt{\Sigma(t,T_i)}}, \\
d_2(\xi,t,T_i,w) &:= d_1(\xi - \phi(T_i\wedge w, T_i\vee w)\Sigma(t,T_i\wedge w),t,T_i), \\
d_1^*(\xi,t,T_i,u,v) &:= d_1(\xi - \phi(T_i,v)\Sigma(u\wedge T_i,T_i),t,T_i), \\
d_2^*(\xi,t,T_i,u,v) &:= d_2(\xi - \phi(T_i,v)\Sigma(u\wedge T_i,T_i),t,T_i,u).
\end{aligned}
$$

The binary operators $\wedge$ and $\vee$ denote the minimum and maximum, respectively. Further, x^* is defined in (D.7). For details, we refer to Appendix D.1.

4.2.1.2. Black-Karasinski pricing kernel for compounded rates

In this section, the Black-Karasinski pricing kernel is extended to compounded rates. Similar to Section 3.3.1.2, the compounded interest can be modelled as in (3.13), where the short-rate for the Black-Karasinski model is defined by Equation (4.1). Recall, the payoff of the caplet/floorlet on compounded rates is not only dependent on the value of $x(t)$ at maturity, but also on the whole path of the process $x(t)$ from t to T. Therefore, a new variable is introduced:

$$
z(t) := \int_0^t \tilde{r}(s)e^{x(s)-\frac{1}{2}\Sigma(0,s)} - \bar{r}(s)ds. \tag{4.3}
$$

Let us consider a derivative which t-value depends on $x(t)$ and $z(t)$, i.e., $\tilde{V}(t,x(t),z(t))$. The corresponding pricing PDE is then given by:

$$
\frac{\partial h}{\partial t} - ax\frac{\partial h}{\partial x} + \left(\tilde{r}(t)e^{\hat{\theta}(x,t,t)} - \bar{r}(t)\right)\frac{\partial h}{\partial z} + \frac{1}{2}\sigma^2(t)\frac{\partial^2 h}{\partial x^2} - \tilde{r}(t)e^{\theta(x,t,t)}h = 0, \tag{4.4}
$$

for $t \geq 0$ and where $\hat{\theta}(x,t,T)$ is defined as in (D.4) and $h(T,x,z) = \tilde{V}(T,x,z)$. Following Turfus, 2021, Chapter 13, an approximation for caplets/floorlets on compounded rates can be derived with the kernel approach, yielding:

$$
V_{CR}^C(0,0) \approx V^C(0,0) + \Delta V_{CR}^C(0,0),
$$

where

$$
\begin{aligned}
V^C(0,0) &= (D(0,T_i) - \kappa D(0,T_{i+1}))\Phi(-d_1(x^*,0,T_i)) \\
&\quad -D(0,T_i)\int_0^{T_i} \bar{r}(t_1)(\Phi(-d_2(x^*,0,T_i,t_1)) - \Phi(-d_1(x^*,0,T_1)))dt_1 \\
&\quad +\kappa D(0,T_{i+1})\int_0^{T_{i+1}} \bar{r}(t_1)(\Phi(-d_2(x^*,0,T_i,t_1)) - \Phi(-d_1(x^*,0,T_1)))dt_1 \\
&\quad -\kappa D(0,T_{i+1})\int_{T_i}^{T_{i+1}} \bar{r}(t_2)\int_0^{t_2} \bar{r}(t_1)e^{\phi(t_1,t_2)\Sigma(0,t_1)}(\Phi(-d_2^*(x*,0,T_i,t_1,t_2)) \\
&\quad -\Phi(-d_2(x^*,0,T_i,t_1)))dt_1dt_2 \\
&\quad +\kappa D(0,T_{i+1})\int_{T_i}^{T_{i+1}} \bar{r}(t_2)\int_0^{t_2} \bar{r}(t_1)(\Phi(-d_1^*(x^*,0,T_i,t_1,t_2)) - \Phi(-d_2(x^*,0,T_i,t_2)) \\
&\quad +\Phi(-d_2(x^*,0,T_i,t_1)) - \Phi(-d1(x^*,0,T_i)))dt_1dt_2,
\end{aligned}
$$

with x^* as defined in (D.7) and

$$
\begin{aligned}
d_1(\xi,t,T_i) &:= \frac{\xi + \hat{K}(T_i,T_{i+1})}{\sqrt{\Sigma(t,T_i) + 2\hat{K}(T_i,T_{i+1}}}, \\
d_2(\xi,t,T_i,w) &:= d_1(\xi - \phi(T_i \wedge w, T_i \vee w)\Sigma(t,T_i \wedge w) - 2\hat{K}(T_i,T_{i+1})), \\
\hat{K}(T_i,T_{i+1}) &:= \int_{T_i}^{T_{i+1}} \bar{r}(t_2)\int_{T_i}^{t_2} \bar{r}(t_1)e^{\Delta x*(T_i,t_1,t_2)}(e^{\phi(t_1,t_2)\Sigma(T_i,t_1)} - 1)dt_1dt_2, \\
\Delta x^*(T_i,t_1,t_2) &:= \phi(T_i,t_1)\phi(T_1,t_2)\Sigma(0,T_1).
\end{aligned}
$$

The formula for $\Delta V_{CR}^C(0,0)$ is given by:

$$
\begin{aligned}
\Delta V_{CR}^C(0,0) &= \frac{D(0,T_i)}{\hat{K}(T_i,T_{i+1})}\int_{T_i}^{T_{i+1}} \bar{r}(t_2)\int_{T_i}^{t_2} \bar{r}(t_1)e^{\Delta x*(T_i,t_1,t_2)}(e^{\phi(t_1,t_2)\Sigma(T_i,t_1)} - 1)\cdot \\
&\quad (\varphi(-d_2(x^* - \Delta x^*(T_i,t_1,t_2),0,T_1)) - \varphi(-d_2(x*,0,T_i)))dt_2dt_2.
\end{aligned}
$$

For details, we refer to Appendix D.2.

4.2.2. Trinomial tree

In this section, caplets/floorlets are priced with the tree method. A short introduction to option pricing with trees has been given in Section 2.4.2. In Section 4.2.2.1, trinomial trees are constructed to price LIBOR caplet/floorlets. Thereafter, the trinomial trees are expanded to pricing of the caplets/floorlets on compounded rates in Section 4.2.2.2.

4.2.2.1. Trionomial tree for LIBOR rates

To construct the trinomial tree, we follow Brigo and Mercurio, 2007. Let $x(t)$ be the zero mean process as defined in (3.9). We define a deterministic function:

$$\alpha(t) = \ln(r_0)e^{-at} + \int_0^t e^{-a(t-u)}\theta(u)du.$$

Then, the short-rate can be written as:

$$r(t) = \exp\left(x(t) + \alpha(t)\right). \tag{4.5}$$

Two steps have to be taken in order to build a trinomial tree for the short-rate. First, a trinomial tree for the zero mean process $x(t)$ has to to be constructed. Second, the nodes of the tree for the zero mean process have to be displaced. More precisely, for each time step t_i, the nodes of the tree have to be displaced by the corresponding $\alpha(t_i)$.

Construction of tree for the zero mean process To construct a trinomial tree for the process $x(t)$ we fix a time grid from 0 to T, $0 = t_0 < t_1 < ... < t_n = T$. Note, the time grid does not necessary have to be equidistant. The distance between the neighbouring points in the time grid is denoted by $\Delta t_i = t_{i+1} - t_i$. Let us denote the nodes of the tree by (i,j) for i ranging from 0 to n and j from $\underline{j}$ to $\bar{j}$. The value of process $x(t)$ at the node (i,j) is denoted by $x_{i,j}$ and is calculated by $j\Delta x_i$. Notice, Δx_i is the vertical discretisation at time t_i of the tree and still has to be determined.

From node (i,j) at time t_i process $x(t)$ can move to three possible nodes at time t_{i+1}, namely to nodes $\{(i+1, k+l)\}_{l=1,0,-1}$ with respectively the probabilities p_u, p_m and p_d. The k-th node at time t_{i+1} is called the central node. In the below, the level of k and the value of Δx_i are determined. Therefore, we make use of the following conditional expectation and variance:

$$\mathbb{E}\left[x(t_{i+1})|x(t_i) = x_{i,j}\right] = x_{i,j}e^{-a\Delta t_i} =: E_{i,j}, \tag{4.6}$$

$$Var\left[x(t_{i+1})|x(t_i) = x_{i,j}\right] = \int_{t_i}^{t_{i+1}} e^{-2a(t_{i+1}-u)}\sigma^2(u)du =: V_i^2. \tag{4.7}$$

The next step is to determine the probabilities p_u, p_m and p_d such that they match the conditional expectation and variance given by (4.6) and (4.7), respectively. Since p_u, p_m and p_d are probabilities, they are all positive numbers that sum up to one. Further, notice that $\{x_{i+1,k+l}\}_{l=1,0,1} = \{x_{i+1,k} + l \cdot \Delta x_{i+1}\}_{l=1,0,1}$. Then, the matching conditions can be written as the following set of equation:

$$\begin{cases} p_u(x_{i+1,k} + \Delta x_{i+1}) + p_m x_{i+1,k} + p_d(x_{i+1,k} - \Delta x_{i+1}) &= E_{i,j}, \\ p_u(x_{i+1,k} + \Delta x_{i+1})^2 + p_m x_{i+1,k}^2 + p_d(x_{i+1,k} - \Delta x_{i+1})^2 &= V_i^2 + E_{i,j}^2. \end{cases}$$

This can be simplified to:

$$\begin{cases} x_{i+1,k} + (p_u - p_d)\Delta x_{i+1} &= E_{i,j}, \\ x_{i+1,k}^2 + 2x_{i+1,k}\Delta x_{i+1}(p_u - p_d) + \Delta x_{i+1}^2(p_u + p_m) &= V_i^2 + E_{i,j}^2. \end{cases}$$

Set $\eta_{i,j} = E_{i,j} - x_{i+1,k}$ to get:

$$\begin{cases} (p_u - p_d)\Delta x_{i+1} &= \eta_{i,j}, \\ \Delta x_{i+1}^2(p_u + p_d) &= V_i^2 + \eta_{i,j}^2. \end{cases}$$

Reckoning that $p_u + p_m + p_d = 1$, the above equations are solved to:

$$\begin{aligned} p_u &= \frac{V_i^2}{2\Delta x_{i+1}^2} + \frac{\eta_{i,j}^2}{2\Delta x_{i+1}^2} + \frac{\eta_{i,j}}{2\Delta x_{i+1}}, \\ p_m &= 1 - \frac{V_i^2}{\Delta x_{i+1}^2} - \frac{\eta_{i,j}^2}{\Delta x_{i+1}^2}, \\ p_d &= \frac{V_i^2}{2\Delta x_{i+1}^2} + \frac{\eta_{i,j}^2}{2\Delta x_{i+1}^2} - \frac{\eta_{i,j}}{2\Delta x_{i+1}}. \end{aligned}$$

It remains to make sure that p_u, p_m and p_d are all positive. This is done by the choice of $\Delta x_{i+1} = \sqrt{3V_i^2}$ and the choice of the level of k such that $x_{i+1,k}$ is as close as possible to $E_{i,j}$ by:

$$k = \text{round}\left(\frac{E_{i,j}}{\Delta x_{i+1}}\right),$$

where round(x) is the closest integer to x. The probabilities can then be written as:

$$\begin{aligned} p_u &= \frac{1}{6} + \frac{\eta_{i,j}^2}{6V_i^2} + \frac{\eta_{i,j}}{2\sqrt{3}V_i}, \\ p_m &= \frac{2}{3} - \frac{\eta_{i,j}^2}{3V_i^2}, \\ p_d &= \frac{1}{6} + \frac{\eta_{i,j}^2}{6V_i^2} - \frac{\eta_{i,j}}{2\sqrt{3}V_i}. \end{aligned}$$

Now it can be easily seen that p_u and p_d are positive for every value of $\eta_{i,j}$. Meanwhile, p_m is positive if $|\eta_{i,j}| \leq \sqrt{2}V_i$. The aforementioned choice of k implies that $|\eta_{i,j}| \leq \frac{\sqrt{3}}{2}V_i$ and, thus, p_m is positive, as well. The value of Δx_{i+1}, the level of k and the probabilities define the geometry of the tree for process $x(t)$.

Displacement of the tree nodes The tree for the zero mean process $x(t)$ described above can be used to build a tree for the short-rate process. Formula (4.5) is used to displace all the tree nodes from $x(t)$ to $r(t)$. In order to displace all the nodes with this formula, a deterministic function $\alpha(t)$ is needed. In turn, $\alpha(t)$ is determined recursively by a calibration to the initial term structure. Contrarily to the Hull-White model case, this has to be done numerically since there exists no analytic expression for the zero-coupon bond prices in the Black-Karasinski model.

Let us denote the displacement at time t_i by α_i. This displacement is the same for all states at time t_i. To determine these displacements the present value of an instrument paying 1 if node (i,j) is reached and zero otherwise is used, denoted by $Q_{i,j}$[1]. First, set $\alpha_0 = \log(-\log(P(0,t_1))/\Delta t_1)$ to get the correct discount factor at time t_1. Then $Q_{i+1,j}$ for $j = \underline{j}_{i+1}, \dots, \bar{j}_{i+1}$ are recursively defined as:

$$Q_{i+1,j} = \sum_h Q_{i,h} q(h,j) \exp\left(-\exp(\alpha_i + h\Delta x_i)\Delta t_i\right),$$

where the sum is calculated over all states at time t_i and $q(h,j)$ denotes the probability of going from the node (i,h) to the node $(i+1,j)$. Notice, the sum over all $Q_{i,j}$ at time t_i should match the market observed term structure. Then, α_i can be obtained by solving:

$$\psi(\alpha_i) := P(0,t_{i+1}) - \sum_{j=\underline{j}_i}^{\bar{j}_i} Q_{i,j} \exp\left(-\exp(\alpha_i + j\Delta x_i)\Delta t_i\right) = 0.$$

This root-finding problem has to be solved numerically, for example, one can use the Newton-Raphson method, Oosterlee and Grzelak, 2020. Note, that the Newton-Raphson method is a gradient method and, thus, requires the derivative of $\psi(\alpha_i)$:

$$\frac{d}{d\alpha_i}\psi(\alpha_i) = \sum_{j=\underline{j}_i}^{\bar{j}_i} Q_{i,j} \exp\left(-\exp(\alpha_i + j\Delta x_i)\Delta t_i\right) \exp(\alpha_i + j\Delta x_i)\Delta t_i.$$

The final step to build the tree for the short-rate process from the tree of the zero mean process $x(t)$, is to take the exponential function of $\alpha_i + x_{i,j}$ for every node in the tree such that $r_{i,j} = \exp(\alpha_i + x_{i,j})$, see Equation (4.5).

4.2.2.2. Trees for compounded rates

In order to price caplets/floorlets on compounded rates, the tree for the short-rate needs to be expanded to a tree for the compounded short-rate. This is because the compounded rate can be seen as an expression involving an average, see for example (3.13) as a continuously compounded rate. A daily compounded rate over the period $[S = t_1, \dots, t_n = T]$ can then be modelled by:

$$M_{daily}(S,T) = \exp\left(\sum_{i=1}^{n} \tau_i r(t_i)\right) - 1,$$

where τ_i is the year fraction from t_i to t_{i+1} and $r(t_i)$ is the short-rate at time t_i. Consider the tree in Figure 4.1. For node E it is clear how to determine the value of the compounded rate in this point. However, there are multiple paths to reach node G and each paths will give a different value of the compounded rate. The number of possible compounded rates at each node will explode with the increase of the number of time steps in the tree. Therefore, we follow Klassen, 2001 for an efficient

[1] Similar as Arrow-Debreu prices, see Andersen and Piterbarg, 2010.

implementation of a tree for Asian options. The caps/floors on the compounded rate can be seen as Asian options where the compounded rate is similar to an average of the underlying stock of the Asian option. The idea by Klassen, 2001 is not to keep track of all the possible paths to reach one node and, thus, all the possible compounded rates at each node. Instead, the idea is to consider a representative set of compounded rate values at each node. This approach consists of three steps:

1. Determine the set of representative compounded rates for each node;
2. Calculate the payoff of the derivative at every leaf (or every node which represents a payment date) of the tree for each compounded rate in the representative set;
3. Backward step to obtain the present value of the derivative.

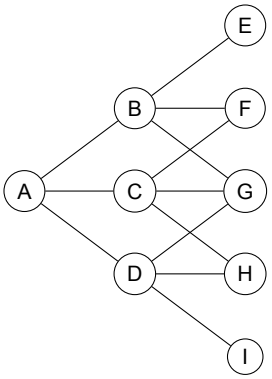

Figure 4.1: A trinomial tree.

First, we explain how the representative set of compounded rate values at each node can be chosen. For each node (i,j) the minimum and maximum values of the compounded rate, which correspond to the paths in Figure 4.2, have to be calculated. Let us denote these minimum and maximum values of the compounded rate at the node (i,j) by $A_{min}(i,j)$ and $A_{max}(i,j)$, respectively. The representative values between $A_{min}(i,j)$ and $A_{max}(i,j)$ are then set to be:

$$A_k(i,j) = A_{min}(i,j)e^{k\Delta t_i}, \text{ for } k = 1,2,\dots,k_{max}, \tag{4.8}$$

where k_{max} is the smallest integer such that $A_k(i,j) \geq A_{max}(i,j)$.

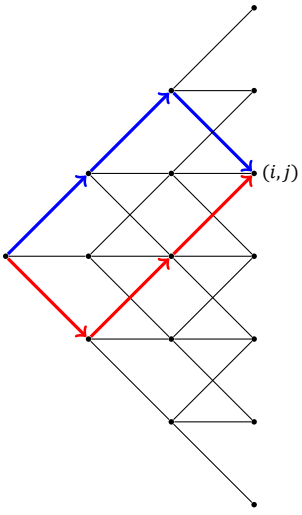

Figure 4.2: The paths corresponding to the maximum and minimum value of the compounded rate at node (i,j) in blue and red respectively.

When the representative values for each node are determined, the payoff for the representative values at each leaf can be calculated. For a caplet/floorlet, the payoff for every representative value $A_k(i,j)$ at leaf node (i,j) is given by:

$$N\tau \max\left(\omega\left[\frac{1}{\tau}\left(\exp\left(A_k(i,j)\right)-1\right)-K,\right]0\right),$$

where ω is equal to 1 in case of a caplet and equal to -1 in case of a floorlet.

Given the payoff at each leaf and each corresponding representative value of the average, the recursive backward run is performed to calculate the present value of the derivative. For a given time step i consider representative value $A_k(i,j)$ from node (i,j). In the backward step, the value of the derivative corresponding to $A_k(i,j)$ is determined. For $A_k(i,j)$ there are three different values for the average in the next time step $i+1$, namely, $\{A_l\}_{l=up,mid,down}$ corresponding to the nodes $\{(i+1, j+l)\}_{l=-1,0,1}$ respectively. To obtain the value $\tilde{V}_{CR}(i,j,A_k)$ corresponding to representative value $A_k(i,j)$, the values $\{\tilde{V}_{CR}(i+1,j+1,A_l)\}_{l=up,mid,down}$ corresponding to the representative values $\{A_l\}_{l=up,mid,down}$ are needed. If the values $\{A_l\}_{l=up,mid,down}$ are not available in the representative sets of the nodes $\{(i+1,j+l)\}_{l=-1,0,1}$ respectively, an interpolate between the neighbouring values of $\{A_l\}_{l=up,mid,down}$ in the representative sets can be used to obtain $\{\tilde{V}_{CR}(i+1,j+1,A_l)\}_{l=up,mid,down}$. With these three values, the value corresponding to $A_k(i,j)$ can be derived with the following formula:

$$\tilde{V}_{CR}(i,j,A_k) = e^{-r\Delta t_i}\left[p_u\tilde{V}_{CR}(i+1,j+1,A_{up}) + p_m\tilde{V}_{CR}(i+1,j+1,A_{mid}) + p_d\tilde{V}_{CR}(i+1,j+1,A_{down})\right].$$

This is also illustrated in Figure 4.3. This procedure is done for all values in the representative set of the nodes of time step i. Thereafter, the same step is carried out for all the nodes at time step $i-1$, and so on.

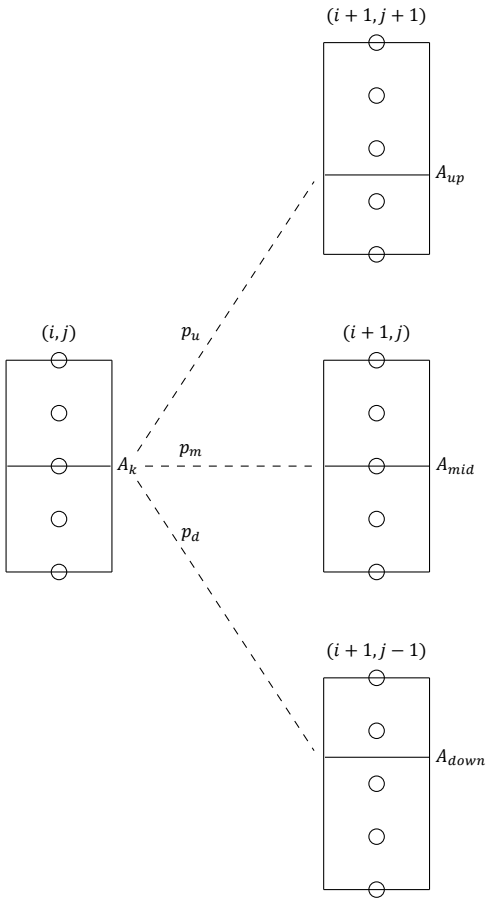

Figure 4.3: The backward step to calculate the value corresponding to A_k.

4.2.3. Monte Carlo simulation

This section is dedicated to a MC approach to price caplets/floorlets on compounded rates. For the Hull-White model, the zero-coupon bond prices can be used to price both LIBOR caplets/floorlets and caplets/floorlets on compounded rates. In contrast to the Hull-White model, there is no analytic expression for the zero-coupon bond in the Black-Karasinski model. This makes it computationally harder to use the MC simulation with zero-coupon bonds as one would need to calculate the bond price numerically. However, to simulate the daily compounded rate, the short-rate can be used as their approximation. Notice that this approach is only applicable for caplets/floorlets on daily compounded rates and not for LIBOR caplets/floorlets. The short-rate at time t is the interest rate for a infinitesimally short period of time from time t. Approximating bond prices with a longer tenor, for example in the case of LIBOR, by the instantaneous short-rate would lead to too big errors. Therefore, the MC simulation using the short-rate directly is only shown below for caplets/floorlets on daily compounded rates.

4.2.3.1. Pricing of caplets and floorlets on compounded rate with Monte Carlo

As explained above, a MC simulation can be used to approximate the short-rate. In that case the time t-value of a caplet/floorlet on the compounded rate between $[T_i, T_{i+1}]$ under the risk-neutral measure is given by:

$$V_{CR}^{C}(t, x(\cdot)) = \mathbb{E}^{\mathbb{Q}}\left[\exp\left(-\int_t^{T_{i+1}} r(s)ds\right) N\tau \max\left(\omega\left(\frac{1}{\tau}\left[\exp\left(\int_{T_i}^{T_{i+1}} r(s)ds\right) - 1\right] - K\right), 0\right)\middle|\mathcal{F}_t\right],$$

where $r(s)$ denotes the short-rate and ω is equal to 1 in case of a caplet and equal to -1 in case of a floorlet. Recall from Section 4.2.2, the short-rate can be written as $r(t) = \exp(x(t) + \alpha(t))$. Therefore, paths of the process $x(t)$ are simulated using MC and then $\alpha(t)$ is added to obtain the short-rate paths. Note, that the deterministic function $\alpha(t)$ needs to be calibrated to the initial term structure. This, for example, can be done using the trinomial trees.

For the MC simulation under the Hull-White model, caplets/floorlets were priced under the T-terminal measure and, thus, the process $x(t)$ was simulated under the T-terminal measure, see Section 3.3.2. As mentioned before, for the Hull-White model it is convenient to price caplets/floorlets under the terminal measure since there exists an analytic formula for the zero-coupon bond prices. Then, the discount factor can be calculated with only one realisation of process $x(t)$. In contrast to the Hull-White model, there does not exists an analytic solution for zero-coupon bond prices. Therefore, the zero-coupon bond price needs to be calculated numerically in order to use for discounting under the T-forward measure. For the Black-Karasinski model both under the risk-neutral measure with the money-market account as numeraire as under the T-forward measure, the discount factor has to be calculated numerically. Hence, for the Black-Karasinski model, we price the caplets/floorlets under the risk-neutral measure with the money-market account as numeraire.

4.3. Results

This section is dedicated to the results obtained with various pricing methods for the Black-Karasinski model described above. Based on the advantages and disadvantages of the different pricing methods given in Section 4.3.1, the same numerical test as for the Hull-White model could not be done for the Black-Karasinski model. However, a convergence test of the tree for compounded rates is discussed in Section 4.3.2. Moreover, in this section we comment on the computation times. Therefore, we note that the computations are done on a computer with processor: Intel(R) Xeon(R) Gold 6132 CPU @ 2.60GHz (2 processors) and 256 GB RAM.

4.3.1. Advantages and disadvantages of the methods

In this section, we discuss the advantages and the disadvantages of the different pricing methods for caplets/floorlets on compounded rates: Black-Karasinski pricing kernel, see Section 4.2.1, trees, see Section 4.2.2, and MC simulation, see Section 4.2.3.

4.3.1.1. Black-Karasinski pricing kernel

An advantage of the Black-Karasinski pricing kernel relative to the other two methods, is the existence of an approximate semi-analytical pricing formula for a low rate environment, see Section 4.2.1.2. However, the semi-analytic formula is complex and computationally challenging. For example, to get the

value of x^*, see Equation (D.7), a numerical optimisation is needed over the zero-coupon bond value as a target. In turn, the zero-coupon bond formula is, as already known, only semi-analytic and contains two-dimensional integrals, that have to be computed numerically and involve some embedded integrals. This all makes it computationally expensive to find x^*.

In order to speed up the computation we pre-calculated some of the integrals on a fixed grid. If a value of the integral is needed which is not on the grid, a linear interpolation is used. Nevertheless, this did not speed up the computation enough to use it in practice. Even after a day, the computation to get a value for x^* was not yet completed. Therefore, we do not gain anything in computation time in comparison to a MC simulation, see Section 4.3.1.3. Due to these complexities, we do not consider the Black-Karasinski pricing kernel for other tests.

4.3.1.2. Trees

The main advantage of trees, in general, is their computational speed in comparison to MC simulations. A disadvantage of the tree method is that they become more complex for multi-dimensional asset options. For example, the tree method is less useful for pricing basket options because it is difficult to construct a multi-dimensional tree.

For the special case of derivatives on compounded rates, a disadvantage of the tree method is the computation time. For pricing such derivatives with the tree method, it is clear that the computation time depends on the number of time steps in the discretisation. However, it might be less clear, the computation time also depends on the volatility. The volatility has an impact on the minimum and maximum value of the compounded rate at a node of the tree. The value of this minimum and maximum subsequently have an impact on the number of values in the representative set of the node. An increase of the size of the representative sets, increases the computational time. Recall, these representative sets represent the possible compounded rates at the corresponding node. Instead of considering every possible compounded rate at each node of the tree, this representative set of the compounded rate is considered at each note.

For caplets/floorlets on compounded rates the tree method is not useful in practice due to enormous computation time. The caplets/floorlets with a tenor of $1Y$ are expected to be most commonly traded in the market. The length of the tenor has an impact on the computation time. For a derivative on daily compounded rates, a daily discretisation within the tenor of the derivative is needed. Therefore, the longer the tenor, the longer the computation time. In our case, we estimate the computation time to obtain the price of a caplet on daily compounded rates with tenor of $1Y$ to be in order of months. Therefore, we consider two solutions for this computational challenge: consider a smaller representative set or use a coarser grid than a daily grid. Note, the high computation times arise due to the backward step in order to price a derivative and not due to the construction of the tree itself. Moreover, we would like to note, in contrast to caplets on compounded rates, the computation time of LIBOR caplets with trees is in order of seconds and is useful in practice.

The convergence of the compounded tree when using a coarser grid than a daily grid, is discussed in Section 4.3.2. For a smaller representative set the following formulae, instead of (4.8), are considered:

$$\begin{aligned} A_k(i,j) &= A_{min}(i,j)e^{2k\Delta t_i}, \text{for } k = 1, 2, \dots, k_{max}, \\ A_k(i,j) &= A_{min}(i,j)e^{3k\Delta t_i}, \text{for } k = 1, 2, \dots, k_{max}, \\ A_k(i,j) &= A_{min}(i,j)e^{4k\Delta t_i}, \text{for } k = 1, 2, \dots, k_{max}. \end{aligned}$$

The results of using these representative sets are presented in Table 4.1. The values of an At the Money (ATM) caplet are calculated for three different levels of the interest rate curves. The value corresponding to $k = 1$ is the value of the caplet on a weekly compounded rate. We observe a convergence of the caplet price with respect of the size of the representative set. However, the difference between the values for $k = 1$ and $k \neq 1$ are still essential. Therefore, this is not a solution which can be used to speed up the computation time.

4.3.1.3. Monte Carlo simulation

An advantage of MC simulations is their flexibility in comparison to other numerical pricing approaches. MC simulations can be used for different types of payoffs. On the other hand, MC simulations are in general considered to be slow. However, in the case of Black-Karasinski for compounded rates, it can be that MC will be the most time-efficient one compared to the other two methods.

k	1	2	3	4
Value 5% flat curve	15,93	15,39	15,39	12,95
Value 3% flat curve	3,18	2,03	0,17	0,16
Value 1% flat curve	4,03	2,96	0,00	0,00

Table 4.1: The value of an ATM caplet on weekly compounded rates with a maturity of $1Y$, tenor of $6M$ and notional of 10.000 for three different levels of interest rate curves and various representative sets of the compounded rate.

A disadvantage is the standard error of the MC estimator. This standard error decreases when the number of MC paths increases. In turn, an increase in the number of MC paths also results in an increase of computation time, see Table 4.2. However, the computational time for this MC simulation is significantly less in relation to the computation time with trees.

#Paths	Computation time
100	2.85
1.000	2.61
10.000	3.10
100.000	5.97
1.000.000	91.6

Table 4.2: The computation time, in seconds, of a caplet on compounded rates with a tenor of $1Y$ and a maturity of $2Y$ computed with a MC simulation for various number of MC paths.

Another disadvantage of the MC simulation for caplets under the Black-Karasinski model, is the absence of an analytical formula for zero-coupon bonds. Hence, it is more convenient to price under the risk-neutral measure with the money-market account as numeraire than under the T-forward measure. However, this has as a consequence that process $x(t)$ has to be simulated on a dense grid from the reference date until the maturity in order to compute value of the money-market account needed to discount the payoff. As shown in Table 4.3, this increases the computation time when the maturity increases.

Maturity	Computation time
$2Y$	1.53
$5Y$	3.07
$7Y$	4.09
$10Y$	5.58
$15Y$	8.32

Table 4.3: The computation time, in minutes, of a caplet on compounded rates with a tenor of $1Y$ computed with a MC simulation.

As mentioned before in Section 4.1, the expectation of the money-market account is equal to infinity in the Black-Karasinski model. This, in particular, has an impact on the MC simulation. For some of the paths of the MC simulation an explosion of the money-market account is observed. Namely, on single realisations, the value of the money-market account is so big that it is out of value range for standard double floats. Table 4.4 displays numbers of paths with the explosion of the money-market account for various piecewise constant volatilities. Notice, the number of explosions depends on the volatility. The number of paths with an explosion is small in comparison to the total number of paths. Therefore, we use an approximation for the paths where we observed an explosion. The applied approximation is described below. Notice, for the piecewise constant volatility corresponding to σ_1, the number of explosions are of a higher order than for the other volatilities. This high number of explosions is caused by the high volatility corresponding to σ_1.

The t_0-value of a caplet on a compounded rate over the period $[t, T]$ is given by:

$$V_{CR}^{C}(t_0, x(\cdot)) = N\mathbb{E}^{\mathbb{Q}}\left[\exp\left(-\int_{t_0}^{T} r(s)ds\right)\max\left(\exp\left(\int_{t}^{T} r(s)ds\right) - (1+\tau K), 0\right)\middle|\mathcal{F}_{t_0}\right].$$

Since the money-market account, denoted in red, explodes, $(1+\tau K)$ can be neglected. By neglecting

Maturity	$1Y$	$2Y$	$3Y$	$4Y$	$5Y$	$6Y$	$7Y$	$8Y$	$9Y$	$10Y$	$11Y$	$12Y$	$13Y$	$14Y$	$15Y$
σ_1	0	0	0	0	0	5	26	95	363	995	1921	2661	3954	5314	6904
σ_2	0	0	0	0	0	0	0	0	0	0	0	2	2	3	7
σ_3	0	0	0	0	0	0	0	0	0	0	0	0	0	0	0
σ_4	0	0	0	0	0	0	0	0	0	0	0	0	0	0	0

Table 4.4: Number of paths where an explosion is observed with corresponding piecewise constant volatility $\sigma_1 = [105.2\%, 199.0\%, 187.6\%, 337.8\%, 337.8\%]$, $\sigma_2 = [124.1\%, 42.24\%, 72.73\%, 89.32\%, 123.8\%]$, $\sigma_3 = [112.0\%, 7.374\%, 39.62\%, 59.42\%, 75.52\%]$ and $\sigma_4 = [102.1\%, 19.56\%, 5.112\%, 48.48\%, 58.36\%]$ for $t \in [[0,2),[2,5),[5,7),[7,10),[10,15)]$. The paths are used to compute the price of a caplet on compounded rates with a MC simulation. In total 1.000.000 paths are used.

$(1+\tau K)$, the following is obtained:

$$V_{CR}^{C}(t_0, x(\cdot)) \approx N\mathbb{E}^{\mathbb{Q}}\left[\exp\left(-\int_{t_0}^{T} r(s)ds\right)\max\left(\exp\left(\int_{t}^{T} r(s)ds\right), 0\right)\middle|\mathcal{F}_{t_0}\right].$$

The max function can be removed as well since the value of the money-market account is definitely greater than zero, which gives the following:

$$V_{CR}^{C}(t_0, x(\cdot)) \approx N\mathbb{E}^{\mathbb{Q}}\left[\exp\left(-\int_{t_0}^{T} r(s)ds\right)\exp\left(\int_{t}^{T} r(s)ds\right)|\mathcal{F}_{t_0}\right] = N\mathbb{E}^{\mathbb{Q}}\left[\exp\left(-\int_{t_0}^{t} r(s)ds\right)\middle|\mathcal{F}_{t_0}\right].$$

4.3.2. Tree for compounded grids

As discussed above, the computation time for the daily compounded tree is too high to use in practice. Therefore, we cannot do the same comparison for caplets under the Black-Karasinski model as for caplets under the Hull-White model. However, to gain confidence in the implementation and the accuracy of the MC simulation, we investigate whether the tree converges to the MC value. Therefore, a coarser grid than a daily compounded grid is considered. Then, we perform a numerical test to investigate the convergence of the prices when the coarser grid becomes finer.

For this convergence test, the value of an ATM caplet with a tenor of $3M$ and a maturity of $9M$ is calculated. Note, the choice of this test caplet is motivated by computational time reasons. The prices are calculated under three different interest rate curves with corresponding realistic[2] constant volatility presented in Table 4.5.

Curve	Volatility
1% flat	17.84%
3% flat	5.162%
5% flat	18.12%

Table 4.5: The constant volatility used for the convergence test of the compounded tree. For each interest rate curve, a different constant volatility is used.

Figure 4.4 illustrates the value of the caplet price for the various compounded grids. The horizontal axis defines the compounded grid. For example, 2 means a bi-daily compounded grid and 4 means a four-daily compounded grid. Further to this, the value obtained with the MC simulation is shown. Note, for the MC simulation a daily compounded rate is used. As the figure shows, the value from the compounded tree converges to the MC value for all curves. Additionally, observe for the 1% flat curve that the value of the compounded tree does not converge monotonically to the MC value. This is a known phenomena for trees, for details see e.g. Albrecher et al., 2013.

Further to the above, Table 4.6 shows the computation times of the compounded tree. As expected, the finer the compounded grid, the higher the computation time. Moreover, as mentioned before, the computation time depends on the volatility, the higher the volatility, the higher the computation time. Notice, the computation time for the caplet on the bi-daily compounded grid for the 1% flat curve is approximately 18 days.

[2]The used volatility was fitted to a proxy market, see Chapter 5 for the details.

Compounded grid	1% flat curve	3% flat curve	5% flat curve
14	0.73	0.085	0.023
10	6.97	0.74	0.136
7	39.47	3.76	0.63
4	692.63	61.59	8.72
2	25972.43	2229.44	291.55

Table 4.6: The computation time, in minutes, to compute a caplet on compounded rates with a tenor of $6M$ and maturity of $9Y$ with the tree method for three different interest rate curves and various compounded grids.

Last, to gain extra confidence in the implementation and accuracy of the MC simulation, we implemented the MC simulation from Section 4.2.3 for the Hull-White model and compared it with the analytic pricing formula from Section 3.3.1.2. With this test, the difference between the two methods was in line with the standard error.

4.4. Conclusion

Based on the results discussed in Section 4.3, a conclusion is given below for the Black-Karasinski model. For the Black-Karasinski model three approaches have been considered to price caplets/floorlets: the pricing kernel approach, the trinomial trees and the MC simulation. Due to computational complexities, the Black-Karasinski pricing kernel has not been considered further in the result section. With this approach not much was gained in terms of computation time in comparison to the MC simulation.

Further, due to the high computation times of the calculation with the compounded trinomial tree, we could not make the same comparison as for the Hull-White model. In order to gain confidence in the implementation and the accuracy of the MC simulation for the Black-Karasinski model, the convergence of the compounded tree has been investigated in Section 4.3.2. There we saw the convergence of the compounded tree to the value of the MC simulation. Moreover, we implemented this MC simulation for the Hull-White model and compared it with the analytic pricing formula from Section 3.3.1.2. With this test, the difference between the two methods was in line with the standard error. Therefore, we gained confidence in the correctness of the MC implementation. As a result, the MC simulation is used in the comparative study, see Chapter 5, to calculate the price of caplets/floorlets on compounded rates. In case the price of a LIBOR caplet has to be calculated, the tree method is used.

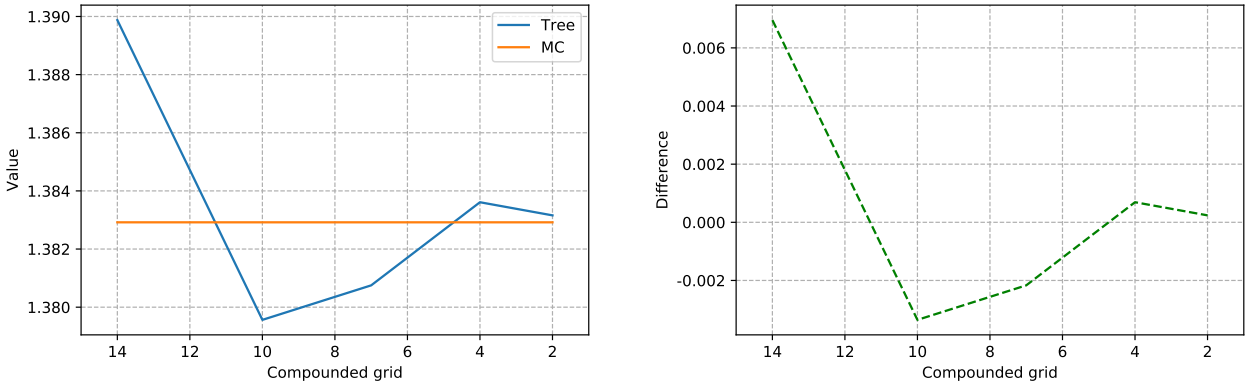

(a) Flat 1% curve.

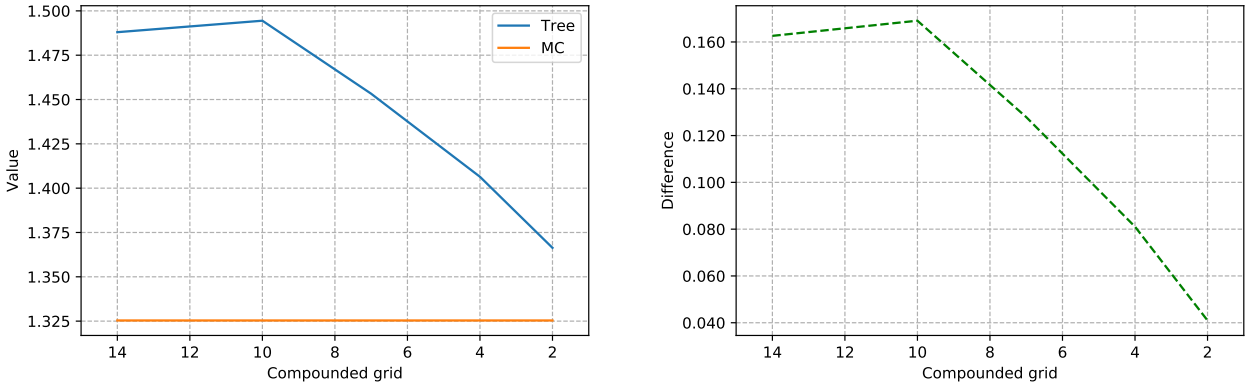

(b) Flat 3% curve.

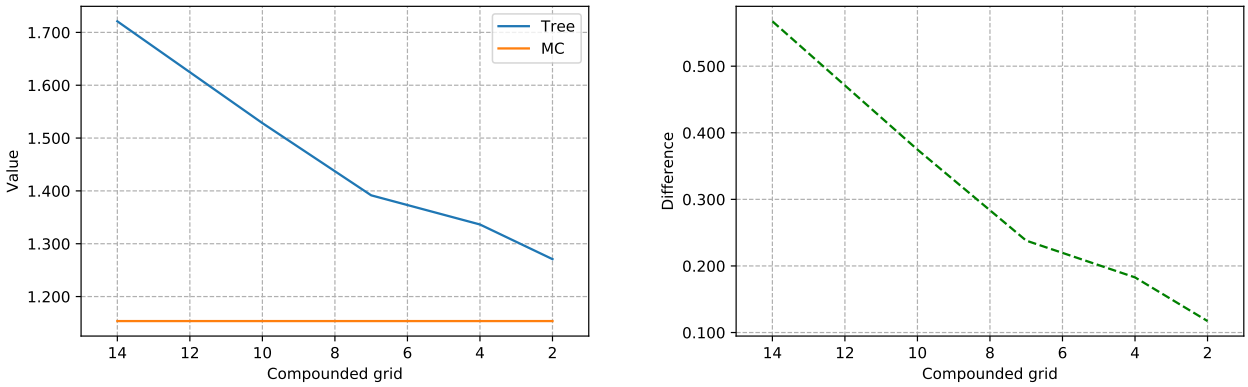

(c) Flat 5% curve.

Figure 4.4: The value of ATM caplets on compounded rates with a tenor of $3M$ and a maturity of $9M$ for three different interest rate curves. In orange the value of the MC simulation using a daily compounded rate and 100.000.000 paths is illustrated. In blue the convergence of the compounded tree is illustrated where the compounded grid is denoted on the horizontal axis in days. Moreover, the difference between the value of the caplets on compounded rates obtained with the two methods is presented.

5

Comparative study

This chapter is dedicated to a comparison between the Hull-White and Black-Karasinski models. The Hull-White model can be used as an interpolation model, see Section 5.1 for a short introduction. This leads to potential model risk. Therefore, we do a comparative study to infer the model risk measured by differences in Bachelier implied volatilities. In this comparative study, we choose the pricing kernel approach for pricing caps/floors on compounded rates under the Hull-White model, based on the discussion in Section 3.5. Further, we use a MC simulation for pricing caps/floors on compounded rates under the Black-Karasinski model based on Section 4.4. The model calibration is described in Section 5.2, the testing strategy for this comparative study is outlined in Section 5.3 and the results are discussed in Section 5.4.

5.1. Introduction

The market quotes cap/floor implied volatilities on a grid of strikes and maturities, for example Bachelier implied volatilities. In order to price caps/floors, which are not on this grid, an interpolation is needed to obtain the corresponding implied volatility to be plugged into the Bachelier formula. In the case of swaptions, the Stochastic Alpha, Beta, Rho (SABR) model is often used as interpolation model for the swaption volatilities, for details see e.g. Iwashita, 2014. Similar, in the context of this thesis, the Hull-White model can be used as an interpolation model for cap/floor volatilities.

Every model brings certain risks due to, for example, model assumptions and data and calibration errors. Therefore, when the Hull-White model is used as an interpolation model, it can lead to potential model risk. To this end, we perform a comparative study to infer the model risk. For this comparative study, we compare the caplet prices obtained using the Hull-White and Black-Karasinski models and measure their difference in terms of Bachelier implied volatilities. This inversion to Bachelier implied volatilities is only done for comparison purposes. It is a metric often used by practitioners, e.g. traders and risk managers, in such contexts. In order to make this comparison, both models have to be calibrated, see Section 5.2.

5.2. Model calibration

In order to compare models one would usually calibrate them to market data, where they are assumed to be applied. However, at the moment there exists no liquid market for caps/floors on compounded rates linked to the new RFR[1]. Therefore, we use a proxy market. We take $3M$ USD LIBOR volatilities, represented in terms of normal volatilities, as an approximation for SOFR volatilities, and the USD SOFR curve for forwarding and discounting. The market data is taken as of 23-11-2020. Then, one of the models is heuristically calibrated to this proxy market and the second model is calibrated to the first model. More details about this heuristic calibration are given in Section 5.2.2.1.

To be more precise, to be able to compare two models, we first heuristically calibrate the Black-Karasinski model to a proxy market to find potentially realistic values for the caplets on the compounded

[1] Recall, this is the new Risk-Free Rate.

rates. Then, we calibrate the Hull-White model to these realistic values. The proxy market and quasi-calibration of the Black-Karasinski model are described in Section 5.2.2. Both the Hull-White model and the Black-Karasinski model are fitted on a grid of maturities and strikes. For each strike we consider, the models are separately calibrated to the market. This results in an individually calibrated model for each strike.

Before we continue with a particular case of the calibration of the Black-Karasinski model, the general problem of calibration is given below in section 5.2.1. Within this section a global fitting method and the stripping method are described.

5.2.1. Calibration methods

This section describes the problem of model calibration. The general problem of the calibration is to find model parameters such that the model prices are as close as possible to the market prices. In our case we calibrate to cap/floor prices. Two calibration methods are described below. The first method is a global fitting methodology, see Section 5.2.1.1. Thereafter, the stripping method is discussed in Section 5.2.1.2.

5.2.1.1. Global fitting method

With the global fitting method the differences between the model and market prices for a set of calibration instruments has to be minimised. Consider a set of n calibration instruments, for example caplets, with different maturities. Denote by $\mathcal{P}^i_{market}$ and $\mathcal{P}^i_{model}$ the market and model price of calibration instrument i, respectively. With the global fitting method, the total difference for all $i = 1, ...n$ between $\mathcal{P}^i_{market}$ and $\mathcal{P}^i_{model}$ has to be minimised. By taking a piecewise constant volatility with $m \leq n$ intervals, we have m degrees of freedom in the piecewise constant volatility. When $m < n$, a perfect fit to all calibration instruments can not be achieved. However, we seek for the solution where, for example, a weighted quadratic distance between the market and model price is minimised. Then, the global fitting is as follows:

$$\min_{\sigma} \sum_{i=1}^{n} w_i \left(\mathcal{P}^i_{model} - \mathcal{P}^i_{market}\right)^2.$$

The sum is over all calibration instruments, the minimisation is over the model volatility, denoted by σ, and w_i is the weight corresponding to calibration instrument i. For more information about a global fitting, we refer to White and Iwashita, 2014. A multi-dimensional optimisation is needed for the global fitting and, thus, the global fitting is complex and rather tedious. For instance, the global fitting may end up in a local minimum which is not desirable. Therefore, we consider a stripping method, see Section 5.2.1.2, which is a series of one-dimensional optimisations.

5.2.1.2. Stripping method

Recall, in our particular case, we fix a strike and then calibrate the model for that specific strike. We seek for a piecewise constant volatility with m degrees of freedom. With the stripping method, we strip over non-overlapping caplets and fit these caplets to the market. This leads to a sequence of one-dimensional problems. To obtain m degrees of freedom in the piecewise constant volatility, m caps are needed in ascending order of maturity. With stripping, one aims to obtain an exact fit to the market data.

For the following steps of the stripping method, we follow White and Iwashita, 2014. First, put the caps in ascending order of maturity. Second, find the price difference for the caps. Third, partition the caplets such that they are assigned to the relevant price difference. Fourth, for each caplet partition, assign a common volatility for the price difference with a one-dimension root finding method.

5.2.2. Calibration Black-Karasinski model

This section explains how to obtain the Black-Karasinski model with realistic parameters for prices of caplets/floorlets on compounded rates. We fix the mean reversion speed $a = 0.03$ and then a quasi-calibration is used to calibrate to a proxy market. For the sake of readability, we refer below to this proxy market and quasi-calibration as simply market and calibration.

As we already have observed, on the level of model prices, the values of LIBOR caplets and caplets on compounded rates do not differ much, see Section 3.4.3. Note, market prices between the LIBOR

caplets and caplets linked to the new RFR might differ more. Due to the lack of data, we use LIBOR caps/floors market data. Then, we calibrate the Black-Karasinski model to the market prices of LIBOR caplets. For this calibration, the stripping method is used, described in Section 5.2.1.2. The LIBOR caplet prices for the Black-Karasinski model are computed using trinomial trees introduced in Chapter 4. The tree method is used in this case because for LIBOR caplets this is a fast approach. Since for the trees it is not straightforward to use a gradient method as optimisation in the stripping method, we use a bisection to solve the optimisation/root-finding problem. The volatilities obtained herewith are then used to calculate the prices of caplets on compounded rates under the Black-Karasinski model. We consider these volatilities and corresponding prices for caplets on compounded rates as realistic values for the Black-Karasinski model and use them for our further analysis. Later, Section 5.2.3 explains how the Hull-White model can be calibrated to the prices obtained by the Black-Karasinski model.

As mentioned before, the market consists of $3M$ LIBOR volatilities represented in terms of normal volatilities and the market implied USD SOFR curve is used for discounting and forwarding. Since the volatilities are presented as normal volatilities, we use the Bachelier model to calculate the $3M$ LIBOR caplets. We fix the Black-Karasinski piecewise constant volatility grid on the following maturities $[2Y, 5Y, 7Y, 10Y, 15Y]$ and on each interval one caplet is used to calibrate the corresponding volatility using stripping. For the sake of simplicity, we calibrate to the market data with only one caplet. Since we fit the model per strike, we consider the stripping method for calibration, see Section 5.2.1.2, and seek for an exact match. As calibration instruments $3M$ LIBOR caplets are used with maturities corresponding to the Black-Karasinski volatility grid. Furthermore, the USD SOFR curve is used and the calibration is done on the following grid of strikes $[0.5\%, 1\%, 1.5\%, 2\%]$.

The results of the Black-Karasinski volatilities for a strike of 1% are shown in Table 5.1. For the other strikes, the stripping is not so straightforward. For a strike of 0.5% the market price could not be reached, not even for unreasonably high volatilities. This is caused by the following. Nowadays, normal volatilities are used to calculate the market prices. For example, with a pure log-normal model, it is not possible to obtain prices observed in the current low/negative rate environment. Therefore, on the one hand, we calculated the market prices with the Bachelier model, which is a normal model, and, thus, does not have an upper bound for the caplet prices. On the other hand, the Black-Karasinski model is a log-normal model and assumes a positive underlying. For a positive underlying, there is a model independent upper bound which is given by the discounted forward rate corresponding to the caplet. For the low strike of 0.5%, the market price of the caplet with maturity $15Y$ is higher than the upper bound of the Black-Karasinski model. Therefore, we are not able to match the market price for this maturity. This is also illustrated by Table 5.2. Even when a higher volatility is used, the difference between the market and model price is not less than 2 bps. Remark, the volatility in the row of $2Y$ corresponds to the piecewise constant volatility from $0Y$ tot $2Y$, the volatility in the row of $5Y$ corresponds to the piecewise constant volatility from $2Y$ tot $5Y$, etc.

$t \in$	$[0,2)$	$[2,5)$	$[5,7)$	$[7,10)$	$[10,15)$
σ	124.1%	42.24%	72.73%	89.32%	123.8%

Table 5.1: The piecewise constant volatility for the Black-Karasinski model with a strike of 1%.

Maturity	BK vol	Market price	Model price	Diff prices
2Y	105.2%	0,23	0,23	$-1,83 \cdot 10^{-7}$
5Y	199.0%	13,79	13,79	$-3,13 \cdot 10^{-6}$
7Y	187.6%	21,92	21,92	$4,64 \cdot 10^{-6}$
10Y	337.8%	29,44	29,44	$-2,98 \cdot 10^{-6}$
15Y	337.8%	30,43	28,38	-2,06

Table 5.2: The piecewise constant volatility, with corresponding market and model prices with a notional of 10.000, for the Black-Karasinski model with a strike of 0.5%.

For the strikes of 1.5% and 2% a volatility squeeze is observed. This means that at some stage of stripping, given already some fitted volatility, a new volatility for a later maturity cannot be attained. Even for volatilities close to zero, the model price is too high for the market price. For example, we are able to calibrate to the first caplet with a maturity of $2Y$. However, even if a volatility close to zero is

used between $2Y$ and $5Y$, the value of the caplet with a maturity of $5Y$ is higher than its market price. Therefore, we are not able to calibrate to the second caplet with a maturity of $5Y$. This is called a volatility squeeze. Note, this can be an indication that the model is not the most suitable model for the data.

In practice, a global fitting along the whole strike, instead of stripping, can be used to avoid a volatility squeeze. However, this leads to a multi-dimensional optimisation which might end up in a local minimum. Since we use the tree method to price LIBOR caplets, we do not have an analytic pricing formula. Hence, it is not straightforward to use a gradient method for the global calibration. As a consequence, there will be a high computation time to perform the global optimisation. Therefore, we seek for a balance in computation time and accuracy. A solution used in practice, instead of using a global fitting, is to relax the requirement of matching the volatility exactly. The simplest approach is to set the volatility to an arbitrarily low value for the interval where a volatility squeeze is observed. Often in practice, one is then able to calibrate to the subsequent caplet. This is the first approach we consider.

The aim is to set the volatility to an arbitrarily low value for the interval where a volatility squeeze is observed. Then, we investigate how well the calibrated model fits to the market data. For the strike of 1%, Black-Karasinski volatilities in a range of $[40\%, 130\%]$ are obtained. Therefore, we suspect that setting the volatility to 1%, for the interval where a volatility squeeze is observed, is low enough to continue the calibration for the other maturities. However, to investigate the impact of the size of that low volatility value, we also set the volatility to 0.5% and 5% for the interval where a volatility squeeze is observed. The results for strike 1.5% and 2% are shown in Table 5.3. Firstly, notice that for the strike of 1.5% there is still a volatility squeeze between $5Y$ and $7Y$ when the volatility between $2Y$ and $5Y$ is set to a low value. For the strike of 2% this is also the case. Moreover, for this strike a volatility squeeze between $7Y$ and $10Y$ is observed. As a consequence, the market prices and model prices do not match for these caplets. Secondly, the volatility is set to $0.5\%, 1\%$ or 5% when a volatility squeeze is observed. However, for all three of these values the impact of the model price is of the same order. Therefore, the value of 1% was indeed low enough and better results would not be obtained if the value of the volatility is reduced even more. With this calibration, the model cannot be fitted appropriately to the market. Note, this is expected since we calibrate a log-normal model to prices from a low rate environment. In this case, such a high volatility is already needed to fit to the first maturity, that it is not possible to obtain an exact fit for longer maturities.

It can be concluded that for both strikes the volatility calibrated to the first caplet is too high in order to also calibrate to the second, third, and for strike 2% even the fourth, caplet. As mentioned before, a global fitting method could be used to avoid a volatility squeeze. However, as a compromise between computation time and accuracy, a heuristic fitting is proposed. Therefore, the requirement to match the volatility exactly up to $2Y$ is relaxed by setting the volatility up to $2Y$ to a lower value. After relaxing this requirement, the volatility for the later maturities might have an exact fit. We do this in a heuristic way described below. This approach is considered instead of a global fit, in order to still be able to make use of stripping, i.e., one-dimensional optimisation instead of a multi-dimensional optimisation.

5.2.2.1. Heuristic approach

This section describes how one can still make use of stripping, i.e., one-dimensional optimisation, but avoid volatility squeezing using a heuristic approach. We want to calibrate a log-normal model to prices from a low rate environment. Here, we want to avoid a volatility squeeze on a significant part of the piecewise constant volatility grid, see Table 5.3. Therefore, we compromise on an exact fit for shorter maturities, e.g., by lowering the model volatility such that a slightly lower price is obtained for these maturities. This is done with the purpose of having a better fit for the longer maturity. With this approach, the goal is to have a better overall fit for all prices compared to the plain stripping method.

Suppose one wants to calibrate to caplets with maturity $T_1, T_2, \dots, T_n$. If a volatility squeeze for the caplet with maturity T_i is observed, take the following steps:

Step 1: Lower the volatility, obtained with the plain stripping method, belonging to maturity T_{i-1} by setting it to $1 - \frac{n}{8}$ times the original volatility with $n = 1$ initially.

Step 2: If the volatility squeeze for maturity T_i is still observed, go back to **step 1** and take $n = 2n$. If no volatility squeeze for maturity T_i is observed, go to the **step 3**.

Step 3: Increase the volatility belonging to maturity T_{i-1} by setting it to $1 - 1/(\frac{8}{n} + m)$ times the original volatility, where $m = 1$ initially and n is the highest number from step 1 where no volatility squeeze for

Maturity	BK vol	Market price	Model price	Diff prices
$2Y$	140.0%	0,28	0,28	$-1,16 \cdot 10^{-7}$
$5Y$	5%	4,59	6,29	-1,70
$7Y$	5%	9,60	11,30	-1,70
$10Y$	46.26%	15,88	15,88	$2,89 \cdot 10^{-6}$
$15Y$	74.87%	17,91	17,91	$-5,81 \cdot 10^{-6}$

(a) Strike 1.5% in case of volatility squeeze set volatility to 5%.

Maturity	BK vol	Market price	Model price	Diff prices
$2Y$	140.0%	0,28	0,28	$-1,16 \cdot 10^{-7}$
$5Y$	1%	4,59	6,24	-1,65
$7Y$	1%	9,60	11,31	-1,70
$10Y$	46.41%	15,88	15,88	$-4,93 \cdot 10^{-6}$
$15Y$	74.90%	17,91	17,91	$-2,79 \cdot 10^{-6}$

(b) Strike 1.5% in case of volatility squeeze set volatility to 1%.

Maturity	BK vol	Market price	Model price	Diff prices
$2Y$	140.0%	0,28	0,28	$-1,16 \cdot 10^{-7}$
$5Y$	0.5%	4,59	6,24	-1,65
$7Y$	0.5%	9,60	11,31	-1,70
$10Y$	46.41%	15,89	15,88	$7,93 \cdot 10^{-7}$
$15Y$	74.91%	17,91	17,91	$7,94 \cdot 10^{-7}$

(c) Strike 1.5% in case of volatility squeeze set volatility to 0.5%.

Maturity	BK vol	Market price	Model price	Diff prices
$2Y$	153.2%	0,30	0,30	$-1,73 \cdot 10^{-7}$
$5Y$	5%	3,26	6,42	-3,17
$7Y$	5%	6,40	10,42	-4,03
$10Y$	5%	11,47	13,19	-1,72
$15Y$	53.05%	13,46	13,46	$5,43 \cdot 10^{-6}$

(d) Strike 2% in case of volatility squeeze set volatility to 5%.

Maturity	BK vol	Market price	Model price	Diff prices
$2Y$	153.2%	0,30	0,30	$-1,73 \cdot 10^{-7}$
$5Y$	1%	3,26	6,43	-3,17
$7Y$	1%	6,40	10,43	-4,03
$10Y$	1%	11,47	13,21	-1,74
$15Y$	53.17%	13,46	13,46	$3,59 \cdot 10^{-7}$

(e) Strike 2% in case of volatility squeeze set volatility to 1%.

Maturity	BK vol	Market price	Model price	Diff prices
$2Y$	153.2%	0,30	0,30	$-1,73 \cdot 10^{-7}$
$5Y$	0.5%	3,26	6,43	-3,17
$7Y$	0.5%	6,40	10,43	-4,03
$10Y$	0.5%	11,47	13,21	-1,74
$15Y$	53.18%	13,46	13,46	$-2,79 \cdot 10^{-6}$

(f) Strike 2% in case of volatility squeeze set volatility to 0.5%.

Table 5.3: Values of the calibrated volatility for strike 1.5% and 2% and the corresponding market price and Black-Karasinski model price. When we observe a volatility squeeze we set the volatility to $0.5\%, 1\%$ or 5%.

maturity T_i is observed.
Step 4: If no volatility squeeze for maturity T_i is observed, go back to **step 3** and increase m by 1. If a volatility squeeze for maturity T_i is observed, take n as in **step 3** and $m = m - 1$ and continue with the calibration for the other maturities.

This heuristic approach is illustrated for a strike of 1.5%. With the plain stripping method, a volatility squeeze for maturity $5Y$ is observed. Hence, we want to lower the volatility for maturity $2Y$.
Step 1: The originally fitted volatility for maturity $2Y$ is 140%. Reduce this volatility by multiplying the original value by $1 - \frac{1}{8}$, which gives a volatility of 122.5%.
Step 2: With this volatility, a volatility squeeze for maturity $5Y$ is observed as shown in Table 5.4a. Therefore, go back to *step 1*.
Step 1: Take $140\% \cdot (1 - \frac{1}{4}) = 105\%$ as volatility for maturity $2Y$.
Step 2: As shown in Table 5.4b there is no volatility squeeze observed anymore for maturity $5Y$. Therefore, go to *step 3*.
Step 3: Then, take $140\% \cdot (1 - 1/(\frac{8}{2} + 1)) = 112\%$ as volatility for maturity $2Y$.
Step 4: As shown in Table 5.4c there is no volatility squeeze observed for maturity $5Y$. Therefore, go back to *step 3* and take $m = 2$.
Step 3: Take $140\% \cdot (1 - 1/(\frac{8}{2} + 2)) = 116,6\%$ as volatility for maturity $2Y$.
Step 4: As shown in Table 5.4d there is a volatility squeeze observed for maturity $5Y$. To this end, take 112% as volatility for maturity $2Y$ and continue the calibration for the other maturities.

The Black-Karasinski volatilities for strike 1.5% and 2% fitted in this heuristic manner are shown in Table 5.5. As expected, there is a difference for a maturity of $2Y$, since we heuristically relaxed the requirement of a perfect match of the piecewise constant volatility for that interval. However, for the other maturities there is a match up to a small error. With this heuristic approach, the total error for strike 1.5% and 2% is of 0,21 and 0,27 bps, respectively. While applying the plain stripping method results in a total difference of 3.35 and 8,94 bps between the model and market prices for respectively

Maturity	BK vol	Market price	Model price	Diff prices
$2Y$	122.5%	0,28	0,13	0,15
$5Y$	1%	4,59	5,13	-0,54

(a) Volatility up to 2Y is set to $(1 - \frac{1}{8}) \cdot$ original volatility.

Maturity	BK vol	Market price	Model price	Diff prices
$2Y$	105.0%	0,28	0,05	0,23
$5Y$	26.37%	4,59	4,59	$-2,2 \cdot 10^{-7}$
$7Y$	41.70%	9,60	9,60	$2,46 \cdot 10^{-6}$
$10Y$	59.84%	15,88	15,88	$-2,5 \cdot 10^{-6}$
$15Y$	75.51%	17,91	17,91	$-4,3 \cdot 10^{-6}$

(b) Volatility up to 2Y is set to $(1 - \frac{1}{4}) \cdot$ original volatility.

Maturity	BK vol	Market price	Model price	Diff prices
$2Y$	112.0%	0,28	0,07	0,21
$5Y$	7.374%	4,59	4,59	$1,26 \cdot 10^{-6}$
$7Y$	39.62%	9,60	9,60	$2,56 \cdot 10^{-6}$
$10Y$	59.42%	15,88	15,88	$3,03 \cdot 10^{-6}$
$15Y$	75,52%	17,91	17,91	$3,74 \cdot 10^{-6}$

(c) Volatility up to 2Y is set to $(1 - \frac{1}{5}) \cdot$ original volatility.

Maturity	BK vol	Market price	Model price	Diff prices
$2Y$	116.6%	0,28	0,09	0,19
$5Y$	1%	4,59	4,75	-0,16

(d) Volatility up to 2Y is set to $(1 - \frac{1}{6}) \cdot$ original volatility.

Table 5.4: Values of the calibrated volatility where we use the heuristic approach described in Section 5.2.2.1.

strike 1.5% and 2%, see Table 5.3b and 5.3e. With this heuristic approach a better overall fit with the market is obtained than with the plain stripping method. Table 5.6 presents the calibrated volatilities per strike for the Black-Karasinski model, which will be used in the remainder of this thesis.

Maturity	BK vol	Market price	Model price	Diff prices
$2Y$	112.0%	0,28	0,07	-0,21
$5Y$	7.374%	4,59	4,59	$-1,26 \cdot 10^{-6}$
$7Y$	39.62%	9,60	9,60	$-2,56 \cdot 10^{-6}$
$10Y$	59.42%	15,88	15,88	$-3,03 \cdot 10^{-6}$
$15Y$	75.52%	17,91	17,91	$-3,74 \cdot 10^{-6}$

(a) For a strike of 1.5%.

Maturity	BK vol	Market price	Model price	Diff prices
$2Y$	102.1%	0,30	0,03	0,27
$5Y$	19.56%	3,26	3,26	$-1,14 \cdot 10^{-6}$
$7Y$	5.112%	6,40	6,40	$3,29 \cdot 10^{-9}$
$10Y$	48.48%	11,47	11,47	$-2,62 \cdot 10^{-6}$
$15Y$	58.36%	13,46	13,46	$3,32 \cdot 10^{-6}$

(b) For a strike of 2%.

Table 5.5: Black-Karasinski volatilities for strikes 1.5% and 2%. The model prices are obtained from the Black-Karasinski model. The prices are of LIBOR caplet with a tenor of $3M$ and a notional of 10.000.

5.2.3. Calibration Hull-White model

In this section, the calibration of the Hull-White model to the Black-Karasinski model is described. The Black-Karasinski volatilities obtained with the approach from the previous section are shown in Table 5.6. Table 5.7 displays the Black-Karasinski cap prices on compounded rates obtained with these volatilities under the Black-Karasinski model. Note, these caps assume the $1Y$ tenor for their

$t \in$	$[0,2)$	$[2,5)$	$[5,7)$	$[7,10)$	$[10,15)$
σ_1	105.2%	199.0%	187.6%	337.8%	337.8%
σ_2	124.1%	42.24%	72.73%	89.32%	123.8%
σ_3	112.0%	7.374%	39.62%	59.42%	75.52%
σ_4	102.1%	19.56%	5.112%	48.48%	58.36%

Table 5.6: The piecewise constant volatilties σ_1, σ_2, σ_3 and σ_4 for the Black-Karasinski model corresponding to strikes $0.5\%, 1\%, 1.5\%$ and 2%, respectively.

caplets. For the Hull-White model we also fix the mean reversion speed $a = 0.03$ and fix a volatility grid $[2Y, 5Y, 7Y, 10Y, 15Y]$. Since for the Hull-White model there exists a fast analytic pricing formula for caplets on compounded rates, we calibrate to caps with maturities corresponding to the volatility grid. For this calibration the stripping method with a bisection for root-finding is used. Since there exists an analytic pricing formula, a gradient method like Newton-Raphson could also be used. However, it was decided to use the bisection for the calibration since this is a more robust method. The results of this calibration are presented in Table 5.8.

Maturity	$K = 0.5\%$	$K = 1\%$	$K = 1.5\%$	$K = 2\%$
$2Y$	0,64	0,52	0,16	0,04
$5Y$	80,21	43,19	25,16	15,84
$7Y$	229,79	137,86	85,75	57,08
$10Y$	540,15	360,35	239,24	163,88
$15Y$	767,52	819,02	577,30	414,40

Table 5.7: Cap prices on compounded rates obtained with the volatilities presented in Table 5.6 and the Black-Karasinski model. The caps consists of consecutive caplets with a tenor of $1Y$ and notional of 10.000.

$t \in$	$[0,2)$	$[2,5)$	$[5,7)$	$[7,10)$	$[10,15)$
σ_1	0.235%	0.697%	0.951%	0.649%	0.593%
σ_2	0.426%	0.656%	0.814%	0.742%	0.788%
σ_3	0.523%	0.702%	0.675%	0.773%	0.733%
σ_4	0.591%	0.779%	0.605%	0.760%	0.745%

Table 5.8: The piecewise constant volatilties $\sigma_1, \sigma_2, \sigma_3$ and σ_4 for the Hull-White model corresponding to strikes 0.5%, 1%, 1.5% and 2%, respectively.

5.3. Testing strategy

In order to make a comparison between the Hull-White and Black-Karasinski model, both models need to be calibrated. This sections first gives a recap of the calibration steps and then describes the testing strategy of the model comparison.

First, the Black-Karsinski model is calibrated to prices of $3M$ LIBOR caplets on a grid of maturities $[2Y, 5Y, 7Y, 10Y, 15Y]$ and strikes $[0.5\%, 1\%, 1.5\%, 2\%]$. The mean reversion speed is set to $a = 0.03$ and a separate calibration is done for each strike. The stripping method is used for strikes 0.5% and 1%, see Section 5.2.1.2. For the other two strikes, the calibration is done with the heuristic approach described in Section 5.2.2.1. Second, the calibrated Black-Karasinski model is used to price caps on compounded rates, with the same maturities and strikes as mentioned above. Third, for each strike, a piecewise constant Hull-White volatility is calibrated to prices of caps on compounded rates, generated by the Black-Karasinski model. This generates a grid of cap prices on which the Hull-White and Black-Karasinski model are calibrated.

With the calibrated Hull-White and Black-Karasinski model the prices of individual caplets with a tenor of $1Y$ can be calculated. The models are not explicitly calibrated to these caplets. Therefore, these can be seen as interpolated values for these caplets. The tenor of $1Y$ is chosen since it is expected to be the most commonly traded one in the market. Thereafter, the prices of these individual caplets are inverted to derive Bachelier implied volatilities which allows a uniform comparison. Note,

the inversion to Bachelier implied volatilities is only done for comparison purposes. The comparison of the difference in Bachelier implied volatilities can give an insight into the model risk for caplets on compounded rates. The results of this comparison are given Section 5.4.

5.4. Results

In this section, a comparison between the Hull-White model and the Black-Karasinski model is made. This comparison is for pricing caplets on compounded rates. The Bachelier implied volatilities are used to make a uniform model comparison. These Bachelier implied forward volatilities are obtained from caplets with a tenor of $1Y$ and are also referred to as forward volatilities. Table E.1 presents the Bachelier implied volatilities obtained from the Hull-White and Black-Karasinski models. Moreover, the Bachelier implied volatilities are illustrated in Figure 5.1. The orange lines in the figure display the difference between the Bachelier volatilities implied by the Black-Karasinski model and the Hull-White model. Since we price caplets that are not on the calibrated grid, we expect to find a difference in the Bachelier implied volatilities.

First, as shown in the figure below, we observe a difference in Bachelier implied volatilities for all strikes. The differences are significant and only up to one order less than the volatility. For example, for strike 0.5% and maturity $8Y$, the implied volatilities are 58 and 62 bps for the Black-Karasinski and Hull-White models, respectively. This results in a difference of 4 bps. This means that, as expected, there is a difference in interpolation between the two models.

Second, for a strike of 0.5% we observe differences in the implied volatility between -3 and 4 bps. As Figure 5.1b shows, the difference in the implied volatility for a strike of 1% is between -4 and 1.5 bps. Moreover, for a strike of 1.5% we observe a difference in the implied volatility between -3 and 1 bps and for a strike of 2% we observe a difference in the implied volatility between -1 and 35 bps.

Last, for a strike of 2% the difference in implied volatility for the first caplet is up to 30 bps, while for the longer maturities the difference is in a range of -1 and 1 bps, see Figure 5.1d. Moreover, Table E.1d shows that the difference in price for a maturity of $1Y$ is only of order 10^{-8} bps. This can be explained by a low Vega for short maturities. Vega measures the sensitivity of the option price with respect to the change in the volatility of the underlying asset. Due to a low Vega for short maturities, a large volatility is needed for a small change in the price. This can result in a large difference in implied volatility, for a small maturity, even though the difference in price is small.

5.5. Conclusion

This chapter was dedicated to a comparison between the Hull-White and Black-Karasinski models for pricing caplets on compounded rates. In order to do a model comparison, both models have to be calibrated to market data. However, at the moment there exists no liquid market for caps/floors on compounded rates linked to the new RFR. Therefore, we took the LIBOR caps market as a proxy market. Then, for each strike, the Black-Karasinski model was separately calibrated to this market and the prices of caps on compounded rates were calculated on a grid of maturities. Thereafter, the Hull-White model was calibrated to these cap values.

For the calibration of the Black-Karasinski model to the market, the stripping method was used. For two strikes, a volatility squeeze was observed. A global fitting method instead of the stripping method could avoid this. However, as a balance in computation time and accuracy, we proposed a heuristic fitting approach instead of a global fitting method. With this heuristic fitting approach a better total fit to the market was obtained than with the plain stripping method.

When the models were calibrated on a grid of strikes and maturities, individual caplets could be priced with both the calibrated Hull-White and Black-Karasinski models. To make a uniform comparison these caplet prices were inverted to Bachelier implied volatilities. These implied volatilities were compared and could give an insight of the model risk for caplets on compounded rates. As expected we observed differences in the implied volatilities. These differences were in a range of -4 and 4 bps which is one order less than the implied volatities themselves. There was one exception on this range for strike 2% and maturity $1Y$, but this could be explained by a low Vega for short maturities.

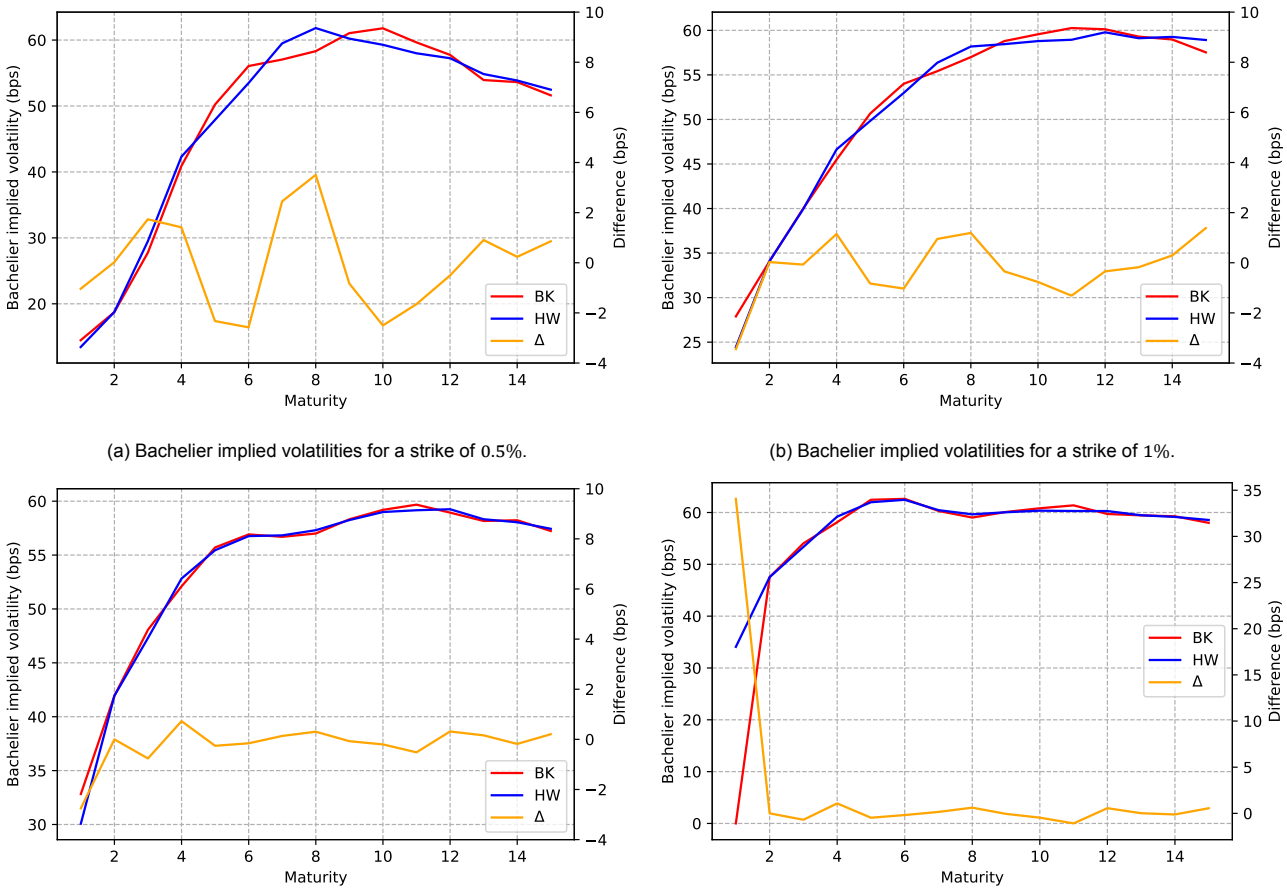

(a) Bachelier implied volatilities for a strike of 0.5%.

(b) Bachelier implied volatilities for a strike of 1%.

(c) Bachelier implied volatilities for a strike of 1.5%.

(d) Bachelier implied volatilities for a strike of 2%.

Figure 5.1: The Bachelier implied volatitities for the Hull-White model (blue) and Black-Karasinski model (red) for the different strikes. In orange the differences between the implied volatilities obtained with the Black-Karasinski and Hull-White models are illustrated. All values are expressed in bps.

6

Conclusion and future recommendations

This chapter concludes the thesis and provides recommendations for further research.

6.1. Conclusion

As a result of the IBOR reform, the IBOR rates will cease to exist and be replaced by the new RFR rates. This new RFR is an in-arrears backward-looking rate and therefore only known at the end of the accrual period. Standard models like the Black and Bachelier models cannot be applied directly anymore in order to price derivatives linked to this new RFR. Hence, this thesis is dedicated to option pricing on backward-looking rates. The first main research objective was how to price options on backward-looking rates efficiently under various models.

In this thesis two models have been considered. The first model was the one-factor Hull-White model. This is a normally distributed short-rate model which captures mean reversion. Within the Hull-White model two pricing approaches have been considered. First, the pricing kernel approach was used to price caplets/floorlets. For the LIBOR caplets/floorlets the same analytical formula was obtained as already known in the literature. Moreover, for caplets/floorlets on compounded rates also an analytical formula was obtained. To verify the correctness of this formula we implemented a MC simulation. The prices obtained with the kernel approach and the MC simulation were in line with the standard error of the MC simulation. Furthermore, the computation times of the kernel approach and the MC simulation were compared. As expected, the computation time of the MC simulation was significantly higher. This is caused by the daily simulation which is needed for a daily compounded rate. Lastly, LIBOR caplets/floorlets were compared to caplets/floorlets on compounded rates. The difference between the pricing formulae of these two caplets/floorlets is a convexity adjustment which is added for the compounded rate. We observed, that for a constant volatility case, the convexity adjustment had more impact on caplets/floorlets with a shorter maturity than caplets/floorlets with a longer maturity. However, this does not have to hold in case of non-constant volatility.

The second model we considered was the Black-Karasinski model. This is a log-normally distributed short-rate model which also captures mean reversion. For the Black-Karasinski model we considered three different pricing approaches: the pricing kernel approach, the trinomial tree method and a MC simulation. With the Black-Karasinski pricing kernel a semi-analytic pricing formula for caplets/floorlets is obtained. However, we observed complexities and challenges in both the derivation and computation time. As a consequence, this approach was not used further for the numerical tests. The second approach was the trinomial tree method. For caplets/floorlets on compounded rates the tree method was computationally hard due to the backward step and the size of the representative sets of the compounded rates. Our estimation predicts the computation time to calculate the price of a caplet/floorlet with a tenor of $1Y$ and maturity of $1Y$ to be in the order of months. Subsequently, we considered two solutions to speed up the computation. The first option was to consider smaller representative sets for the compounded rate. Despite the convergence with respect to the size of the representative sets, which we observed, the differences between the prices for the various representative sets were essential. The second option to speed up the computation was to consider a coarser compounded grid than a daily compounded grid. Therefore, we investigated the convergence of the compounded tree when

the coarser grid becomes finer. A convergence of the compounded tree was observed. Moreover, the value converged to the value obtained with a MC simulation. Despite the observed convergence, the difference between the value with a daily compounded grid and a coarser grid was still essential. The last method considered for the Black-Karasinski model was a MC simulation. For log-normal models, like the Black-Karasinski model, the expectation of the money-market account is equal to infinity. This is what we call an explosion of the money-market account. This had in particular an impact on the MC simulation. On single realisations of the money-market account such an explosion was observed. The number of MC paths that is equal to infinity, and thus explode, depends on both the interest rate curve and the volatility. For the MC paths where an explosion of the money-market account was observed, an approximation of the caplet/floorlet value was used. Further, the computation time for caplets on compounded rates with the MC simulation was in the order of minutes while the computation time for both the kernel approach as the trinomial tree method were significantly higher.

Based on the high computation time for the compounded tree, not the same numerical test has been performed for the Black-Karasinski model as for the Hull-White model. However, with the convergence test of the compounded tree, we gained confidence in the implementation and accuracy of the MC simulation. As a result, the MC simulation was further used in the comparative study.

The second main research objective was to perform a model comparison between the Hull-White and Black-Karasinski models to infer the model risk. Prices of vanilla options are in general quoted on a grid of maturities and strikes. Therefore, option prices for other maturities and strikes have to be inferred from the quoted instruments. It is market practice to use a model for this. For example, SABR is used to parametrise the swaption volatility smile and Black/Bachelier is used to strip LIBOR caplet/floorlet volatilities. For the caps/floors linked to the new RFR, either the Hull-White model or Black-Karasinski model can be used. In the current low/negative rate environment, the Hull-White model might be a bit more realistic. Using a model to interpolate the quoted volatilities can lead to potential model risk. To this end, a comparative study has been performed to investigate the model risk arising from applications of the Hull-White and Black-Karasinski models. For this model comparison, caplets/floorlets on compounded rates had to be priced. For the Hull-White model the analytic formula obtained with the pricing kernel approach has been used, based on the discussion in Chapter 3. Furthermore, for the Black-Karasinski model the numerical MC has been used, based on the discussion in Chapter 4.

In order to perform a model comparison, both models have to be calibrated to market data. Since at the moment there exists no liquid market for caps/floors on the new RFR, a proxy market was used. First, a quasi-calibration was used to calibrate the Black-Karasinski model to the proxy market. With the calibrated Black-Karasinski model, cap prices on compounded rates were calculated on a grid of maturities. Then, the Hull-White model was calibrated to these cap prices obtained by the Black-Karasinski model. For each considered strike, a separate calibration was performed which resulted in an individual model for each strike. The stripping method was used for the calibration, where we sought for an exact match with the market. For some of the strikes, there were challenges to calibrate the Black-Karasinski model to the proxy market. The Black-Karasinski model assumes a positive underlying short-rate. For a positive underlying there is a model independent upper bound. For one strike we observed that the market price was higher than the upper bound. For another strike, we observed a volatility squeeze. A global fitting instead of a stripping method can be used to avoid a volatility squeeze. However, this leads to a complex multi-dimensional optimisation problem instead of a series of one-dimensional optimisation problems. To obtain a balance in computation time and accuracy, we used a heuristic approach to calibrate the Black-Karasinski model in case of a volatility squeeze. This heuristic approach was valid since we made use of proxy market data. Moreover, we compromised on the fit for some short maturities, in order to improve the fit for longer maturities. This was done with the purpose of reducing the overall calibration error.

After the calibration, both the Hull-White and Black-Karasinski models were calibrated on a grid of maturities for the considered strikes. For the comparative study, the individual caplets with a tenor of $1Y$ were calculated with the calibrated models. Then, to make a uniform comparison, the caplet prices were inverted to Bachelier implied volatilities. Since these caplets are not on the calibrated grid, we expected a difference in the Bachelier implied volatilities obtained from the Hull-White and Black-Karasinski models. With this comparative study, we observed differences of Bachelier implied volatilities in a range of -4 to 4 bps for maturities greater than $1Y$. This was of one order less than the value of the Bachelier implied volatilities. The Bachelier implied volatilities can give an insight of the model risk for caplets on compounded rates.

6.2. Future research

This section gives recommendations for further research.

To begin with, this thesis considers the Black-Karasinski model which can only model positive short-rates. In the current negative/low rate environment, this is a drawback of the model. Therefore, for future research, a shifted Black-Karasinski model can be considered. A shifted Black-Karasinski model would be able to model these negative/low rates. Moreover, a shifted Black-Karasinski model might solve the challenges observed by the model calibration, i.e., the volatility squeeze due to the high volatility for the first interval of piecewise constant volatility and the market price which was higher than the upper bound of the model. The proxy market for the calibration was taken from a low rate environment. With a shifted Black-Karasinski model, we could shift to this low rate environment and obtain a better fit. For example, smaller volatility would be needed to fit to the first interval of the piecewise constant volatility, which could avoid the volatility squeeze for the other intervals. Moreover, the upper bound of the Black-Karasinski model could also be shifted with a shifted Black-Karasinski model.

Furthermore, we would recommend to investigate the use of the COS method to price caplets/floorlets on compounded rates. The COS method is a pricing approach based on Fourier cosine series. Generally, it can be used to approximate the probability density function. Then using the Feynman-Kac theorem, the price of derivatives can be obtained. Note, that the COS method can be used when the characteristic function is available. Since the Black-Karasinski model is a log-normally distributed model, the characteristic function is not known in closed form. Therefore, the COS method cannot be applied to a log-normal characteristic function. However, to recover the density function for a log-normal model, the COS method can be applied to a transformed form of a normal model, where the characteristic function is known. Notice that a two-dimensional COS method is needed in case of caplets/floorlets on compounded rates.

Lastly, variance reduction techniques can be applied to the MC simulation under the Black-Karasinski model. This potentially has to improve the computation time as less MC paths could be used while keeping the same accuracy. Examples of variance reduction techniques are control variate, antithetic variate, stratified sampling and importance sampling. For more information about the variance reduction techniques, we refer to Glasserman, 2004.

A

Derivation for OIS swaps

This appendix gives the derivation of the forward rate corresponding to an OIS swap. Moreover, the value of an OIS leg is derived.

Consider a notional of N and payment dates $\mathcal{T}_m \backslash T_0$, the floating coupon payments of an OIS leg are given by:

$$C_i^{OIS} = \tau_i N R_i^{OIS},$$

with

$$R_i^{OIS} = \frac{1}{\tau_i}\left(\prod_{j=1}^{n_i}(1+\tau_{ij}e_{ij}) - 1\right),$$

where the product includes all overnight fixings of the i-th coupon, e_{ij} is the j-th overnight rate fixing of the i-th coupon and τ_{ij} is the year fraction between the $(j-1)$-th and j-th fixing of the i-th coupon. Notice, R_i^{OIS} is a stochastic variable and known at the end of the coupon. In order to obtain the forward rate at time t, the expectation of this rate has to be considered. By definition:

$$e_{ij} = \frac{1}{\tau_{ij}}\left(\frac{1}{P(T_{begin}^{ij}, T_{end}^{ij})} - 1\right),$$

where T_{begin}^{ij} and T_{end}^{ij} are the start and end date of the j-th fixing of the coupon i, respectively. To make the notation a bit easier, we get rid of the index i corresponding to the coupon. The start and end date of the coupon are denoted by respectively T_{begin} and T_{end} and the start and end date of the j-th fixing of the coupon are denoted by respectively T_{begin}^{j} and T_{end}^{j}. The forward rate, under the T_{end}-forward measure, is then calculated by:

$$\begin{aligned}
F_{OIS}(t, T_{begin}, T_{end}) &= \mathbb{E}^{\mathbb{Q}^{T_{end}}}\left[\frac{1}{\tau}\left(\prod_{j=1}^{n}(1+\tau_j e_j) - 1\right)\middle|\mathcal{F}_t\right] \\
&= \mathbb{E}^{\mathbb{Q}^{T_{end}}}\left[\frac{1}{\tau}\left(\prod_{j=1}^{n}\left[1+\tau_j\frac{1}{\tau_j}\left(\frac{1}{P(T_{begin}^{j}, T_{end}^{j})} - 1\right)\right] - 1\right)\middle|\mathcal{F}_t\right] \\
&= \mathbb{E}^{\mathbb{Q}^{T_{end}}}\left[\frac{1}{\tau}\left(\prod_{j=1}^{n}\frac{1}{P(T_{begin}^{j}, T_{end}^{j})} - 1\right)\middle|\mathcal{F}_t\right] \\
&\overset{*}{=} \mathbb{E}^{\mathbb{Q}^{T_{end}}}\left[\frac{1}{\tau}\left(\frac{1}{P(T_{begin}, T_{end})} - 1\right)\middle|\mathcal{F}_t\right] \\
&= \frac{1}{\tau}\left(\frac{P(t, T_{begin})}{P(t, T_{end})} - 1\right).
\end{aligned}$$

Due to no arbitrage, for $S < T < V$ it holds that:

$$P(S,T)P(T,V) = P(S,V).$$

Notice, at the $\overset{*}{=}$-step we make use of this no arbitrage rule.

In order to calculate the expected value of a floating coupon, we also use the T_{end}-forward measure. We assume here that the pay date is the same as the end date. We consider two types of OIS coupons, coupons that start in the future, i.e., $t < T_i$, and running coupons. For a coupon that starts in the future the following holds:

$$\begin{aligned}
\mathbb{E}^{\mathbb{Q}^{T_{end}}}\left[P(t,T_{end})N\tau R^{OIS}|\mathcal{F}_t\right] &= P(t,T_{end})N\tau\mathbb{E}^{\mathbb{Q}^{T_{end}}}\left[\frac{1}{\tau}\left(\prod_{j=1}^{n}(1+\tau_j F_{OIS}(T^j_{begin},T^j_{begin},T^j_{end}))-1\right)\middle|\mathcal{F}_t\right]\\
&= P(t,T_{end})N\tau\mathbb{E}^{\mathbb{Q}^{T_{end}}}\left[\frac{1}{\tau}\left(\prod_{j=1}^{n}\frac{1}{P(T^j_{begin},T^j_{end})}-1\right)\middle|\mathcal{F}_t\right]\\
&= P(t,T_{end})N\tau\mathbb{E}^{\mathbb{Q}^{T_{end}}}\left[\frac{1}{\tau}\left(\frac{1}{P(T_{begin},T_{end})}-1\right)\middle|\mathcal{F}_t\right]\\
&= P(t,T_{end})N\tau\mathbb{E}^{\mathbb{Q}^{T_{end}}}\left[F_{OIS}(T_{begin},T_{begin},T_{end})|\mathcal{F}_t\right]\\
&= P(t,T_{end})N\tau F_{OIS}(t,T_{begin},T_{end})\\
&= P(t,T_{end})N\tau\left[\frac{1}{\tau}\left(\prod_{j=1}^{n}(1+\tau_j F_{OIS}(t,T^j_{begin},T^j_{end}))-1\right)\right].
\end{aligned}$$

Notice, this last step above is not required. It is more consistent to the payoff of the OIS coupon to multiply over all fixing dates. However, computationally this is much more expensive than directly calculating the forward over the whole period.

For a running coupon, the expectation of the OIS leg is given by:

$$\begin{aligned}
\mathbb{E}^{\mathbb{Q}^{T_{end}}}\left[P(t,T_{end})N\tau R^{OIS}|\mathcal{F}_t\right] &= P(t,T_{end})N\tau\mathbb{E}^{\mathbb{Q}^{T_{end}}}\left[\frac{1}{\tau}\left(\prod_{j=1}^{m}(1+\tau_j e_j)\cdot\right.\right.\\
&\qquad\left.\left.\prod_{j=m+1}^{n}(1+\tau_j F_{OIS}(T^j_{begin},T^j_{begin},T^j_{end}))-1\right)\middle|\mathcal{F}_t\right]\\
&= P(t,T_{end})N\mathbb{E}^{\mathbb{Q}^{T_{end}}}\left[\prod_{j=1}^{m}(1+\tau_j e_j)\frac{1}{P(T^{m+1}_{begin},T_{end})}-1\middle|\mathcal{F}_t\right]\\
&= P(t,T_{end})N\left(\prod_{j=1}^{m}(1+\tau_j e_j)\bar{\tau}F_{OIS}(t,T^{m+1}_{begin},T_{end})\right)\\
&= P(t,T_{end})N\left(\prod_{j=1}^{m}(1+\tau_j e_j)\prod_{j=m+1}^{n}(1+\tau_j F_{IOS}(t,T^j_{begin},T^j_{end})\right)
\end{aligned}$$

where m corresponds to the day of the last available historical overnight fixing rate of the running coupon and $\bar{\tau}$ is the year fraction from T^{m+1}_{begin} to T_{end}. Again notice, the last step above is not required.

B

Derivation Hull-White pricing kernel

This appendix provides an idea to obtain the Hull-White pricing kernel from Section 3.3.1. For detail and the full proof, we refer to Turfus, 2019. The short-rate in the Hull-White model can be written as:

$$r(t) = x(t) + \bar{g}(t),$$

where $x(t)$ is the zero mean process defined in (3.9) and $\bar{g}(t)$ is a deterministic function. Further, define the following for later use:

$$\begin{aligned}
\phi(t,T) &= e^{-a(T-t)}, \\
\Sigma(t,T) &= \int_t^T \phi^2(u,T)\sigma^2(u)du, \\
I(t,T) &= \int_t^T \phi(u,T)\Sigma(t,u)du, \\
B(t,T) &= \int_t^T \phi(t,u)du.
\end{aligned}$$

Consider the pricing PDE:

$$\frac{\partial h}{\partial t} - ax\frac{\partial h}{\partial x} + \frac{1}{2}\sigma^2(t)\frac{\partial^2 h}{\partial x^2} - (x + g(t))h = 0, \tag{B.1}$$

for $t \geq 0$ with the final condition $h(T,x) = V(T,x)$. Then according to the Feynman-Kac Theorem 2.2, the solution of the pricing PDE gives the value function of the corresponding derivative. This appendix provides the idea to obtain the Green function which solves this pricing PDE.

First, the following change of variables is applied to the pricing PDE:

$$\begin{aligned}
y &\equiv x\phi(t,T), \\
s &\equiv \Sigma(t,T), \\
p(y,s) &\equiv h(x,t),
\end{aligned}$$

which gives:

$$\frac{\partial p}{\partial s} - \frac{1}{2}\frac{\partial^2 p}{\partial y^2} + (A(s)y + R(s))\,p = 0,$$

for $0 < s < s_M$ where $s_M = \Sigma(0,T)$ and

$$\begin{aligned}
A(s) &\equiv \frac{1}{\sigma^2(t)\phi^3(t,T)}, \\
R(s) &\equiv \frac{g(t)}{\sigma^2(t)\phi^2(t,T)}.
\end{aligned}$$

In symbolic operator notation, this can be written as:

$$\left(\frac{\partial}{\partial s} - \mathcal{L}_0 - \mathcal{V}(s)\right) p(y,s) = 0,$$

where

$$\begin{aligned} \mathcal{L}_0 &= \frac{1}{2}\frac{\partial^2}{\partial y^2}, \\ \mathcal{V}(s) &= -\left(A(s)y + R(s)\right)\cdot. \end{aligned}$$

The Green function $G^*(y,s,\eta)$ for the above pricing PDE satisfies the following initial condition:

$$G^*(y,0;\eta) = \delta(\eta - y),$$

where $\delta(\cdot)$ is the Dirac delta function.

To obtain the Green function of (B.1), Turfus, 2019 uses Definition B.1 and Theorem B.1. We do not go into details of this definition and theorem. However, the idea is to treat $\mathcal{V}(s)$ as a perturbation on $\mathcal{L}_0$. Then, the Green function of (B.1) can be expressed as a product of the Green function of $\mathcal{L}_0$ and a rest-term corresponding to the perturbation $\mathcal{V}(s)$. The green function of:

$$\frac{\partial}{\partial s} = \mathcal{L}_0,$$

is well known, see for example Craig, 2018, and given by:

$$G_0^*(y,s;\eta) = \varphi\left(\frac{\eta - y}{\sqrt{s}}\right).$$

Further, to derive the Green function corresponding to (B.1), the following one-parameter family of operators is considered:

$$U(s) = \mathcal{E}_0^s(\mathcal{L}_0 + \mathcal{V}(\cdot)),$$

which satisfy the following initial value problem:

$$\begin{aligned} \frac{\partial U}{\partial s} &= \left(\mathcal{L}_0 + \mathcal{V}(s)\right) U \\ U(0) &= I. \end{aligned}$$

Moreover, the commutator function is used:

$$ad_{\mathcal{L}_0}(\mathcal{V}(u)) = \mathcal{L}_0\mathcal{V}(u) - \mathcal{V}(u)\mathcal{L}_0.$$

To derive this commutator, consider an arbitrary function $b(y)$ which is twice differentiable with respect to y. Then, we want to calculate:

$$ad_{\mathcal{L}_0}(\mathcal{V}(u))b(y) = \mathcal{L}_0\mathcal{V}(u)b(y) - \mathcal{V}(u)\mathcal{L}_0 b(y).$$

For clarity, we break down the right-hand side into two parts.

$$\begin{aligned} \mathcal{L}_0\mathcal{V}(u)b(y) &= \frac{1}{2}\frac{\partial^2}{\partial y^2}\left[-\left(A(u)y + R(u)\right)\right] b(y) \\ &= -\frac{\partial}{\partial y}\left[A(u)b(y) + \left(A(u)y + R(u)\right)\frac{\partial}{\partial y}b(y)\right] \\ &= -\frac{1}{2}\left[A(u)\frac{\partial}{\partial y}b(y) + A(u)\frac{\partial}{\partial y}b(y) + \left(A(u)y + R(u)\right)\frac{\partial^2}{\partial y^2}b(y)\right]. \end{aligned}$$

$$\mathcal{V}(u)\mathcal{L}_0 b(y) = -\left(A(u)y + R(u)\right)\cdot\frac{1}{2}\frac{\partial^2}{\partial y^2}b(y).$$

Combining this yields:

$$\begin{aligned} ad_{\mathcal{L}_0}(\mathcal{V}(u))b(y) &= -\frac{1}{2}\left[A(u)\frac{\partial}{\partial y}b(y) + A(u)\frac{\partial}{\partial y}b(y) + (A(u)y + R(u))\frac{\partial^2}{\partial y^2}b(y)\right] + \frac{1}{2}(A(u)y + R(u))\frac{\partial^2}{\partial y^2}b(y) \\ &= -A(u)\frac{\partial}{\partial y}b(y). \end{aligned}$$

This implies:

$$ad_{\mathcal{L}_0}(\mathcal{V}(u)) = -A(u)\frac{\partial}{\partial y}.$$

To end, the Green function corresponding to (B.1), derived with this approach, is given by:

$$G(x,t;\xi,T) = \hat{P}(t,T,x)\varphi(\xi + I(t,T) - x\phi(t,T); \Sigma(t,T)),$$

where $\hat{P}(t,T,x)$ is the zero-coupon bond price under the Hull-white model and

$$\varphi(x;\Sigma) = \frac{1}{\sqrt{2\pi\Sigma}}\exp\left(-\frac{1}{2\Sigma}x^2\right).$$

For details of the derivation, we refer to Turfus, 2019.

Definition B.1. *The quantity defined for a time-dependent linear operator $\mathcal{L}(t)$ by:*

$$\mathcal{E}_a^b(\mathcal{L}(\cdot)) = I + \sum_{n=1}^{\infty}\int_{a\le s_1\le\ldots\le s_n\le b}\mathcal{L}(s_n)\ldots\mathcal{L}(s_1)ds_1\ldots ds_n,$$

generalises the exponential of the integral of a function to the case of a time-dependent linear operator.

Note, in the case where the operator $\mathcal{L}(s)$ is replaced by the real-value function $k : [a,b] \to \mathbb{R}$, the following holds:

$$\mathcal{E}_a^b(k(\cdot)) = e^{\int_a^b k(u)du}.$$

More generally, the same holds when:

$$\int_0^t\int_0^{t_2}(\mathcal{L}(t_2)\mathcal{L}(t_1) - \mathcal{L}(t_1)\mathcal{L}(t_2))\,dt_1dt_2 = 0.$$

Theorem B.1. *Suppose that the initial boundary value problem:*

$$\begin{aligned} \left(\frac{\partial}{\partial s} - \mathcal{L}_0(s) - \mathcal{V}(s)\right)p(\mathbf{y},s) &= 0, \\ p(\mathbf{y},0) &= h(\mathbf{y}), \\ p(\mathbf{y},s) \to 0 \text{ as } ||\mathbb{y}|| \to \infty,\ s &> 0, \end{aligned}$$

is known to have a unique solution $p : \mathbb{R}^n \times [0,s_M] \to \mathbb{R}$ for linear operators $\mathcal{L}_0(s)$, $\mathcal{V}(s)$ depending continuously on the parameters s and some L^1 function $h : \mathbb{R}^n \to \mathbb{R}$. Denote by X the vector space generated by operation on p of multinomials of the form:

$$\mathcal{M}(s_1,\ldots s_n) = \prod_{i=1}^{n} M_i(s_i),$$

with $s_i \in [0,s_M]$, $M_i \equiv \mathcal{L}_0$ or $\mathcal{V}$ and $n \ge 0$, and by X_M the corresponding space resulting when the domain of $h(\cdot)$ is restricted to $[-M,M]$. Suppose further that, for any $M > 0$, $\mathcal{L}_0(s)$ and $\mathcal{V}(s)$ are uniformly bounded over X_M for $s \in [0,s_M]$ under some suitable norm. Then:

1. *There exists a linear operator $U(s)$ acting on X which satisfies the initial value problem:*

$$\begin{aligned} \frac{\partial U(s)}{\partial s} &= (\mathcal{L}_0(s) + \mathcal{V}(s))\, U(s), \\ U(0) &= I. \end{aligned}$$

2. *This operator can be expressed as:*

$$U(s) = Q(s)U_0(s),$$

where

$$\begin{aligned} U_0(s) &= \mathcal{E}_0^s(\mathcal{L}_0(\cdot)), \\ Q(s) &= \mathcal{E}_0^s(\mathcal{W}(\cdot, s)), \\ \mathcal{W}(u, s) &= \mathcal{E}_u^s\left(ad_{\mathcal{L}_0(\cdot)}\right)(\mathcal{V}(u)). \end{aligned}$$

Proof. For a proof of this theorem, we refer to Turfus, 2019. □

C

Derivation of caplet and floorlet prices with the Hull-White pricing kernel

In this appendix we derive the pricing formulae for both a LIBOR caplet and a caplet on compounded rates using the Hull-White pricing kernel. Before we start, we write the zero-coupon bond formula using the following notation:

$$\begin{aligned}
\phi(t,T) &= \exp(-a(T-t)), \\
\Sigma(t,T) &= \int_t^T \phi^2(u,T)\sigma^2(u)du, \\
I(t,T) &= \int_t^T \phi(u,T)\Sigma(t,u), \\
\nu(x,t,T) &= B(t,T)(x+I(0,t)) + \frac{1}{2}B^2(t,T)\Sigma(0,t),
\end{aligned}$$

which gives us:

$$\hat{P}(t,T,x(t)) = \frac{P(0,T)}{P(0,t)}\exp(-\nu(x(t),t,T)).$$

Moreover, with a calibration to the initial term structure we obtain $\hat{g}(t) = I(0,t)$. For details, we refer to Turfus, 2019. This notation makes it easier later in the derivation. Note that $P(t,T) \equiv \hat{P}(t,T,x(t))$.

C.1. Caplet price with pricing kernel

The payoff of a LIBOR caplet at time T_{i+1} depending on the LIBOR between $[T_i, T_{i+1}]$ with notional N and strike K is given by:

$$V^C(T_{i+1}, x(T_i)) = \tau N \max(L(T_i, T_{i+1}) - K, 0),$$

where τ is the year fraction between T_i and T_{i+1}.

With the pricing kernel from Equation (3.11) the present value of a LIBOR caplet is derived. In order to arrive to that formula, first the value of the caplet at time T_i has to be determined. Equation (C.1) gives this value where κ is equal to $(1+\tau K)$:

$$V^C(T_i, x(T_i)) = \hat{P}(T_i, T_{i+1}, x(T_i))N \max\left(\frac{1}{\hat{P}(T_i, T_{i+1}, x(T_i)} - \kappa, 0\right). \tag{C.1}$$

In order to derive the present value of a LIBOR caplet, the price at time T_i of the caplet is considered as the payoff of the caplet at time T_i. Then, the pricing kernel is applied to the payoff at time T_i:

$$V^C(T_0, x(T_0)) = \int_{\mathbb{R}} N\hat{P}(T_i, T_{i+1}, \xi) \max\left(\frac{1}{\hat{P}(T_i, T_{i+1}, \xi)} - \kappa, 0\right) \hat{P}(T_0, T_i, x(T_0)) \cdot \frac{1}{\sqrt{2\pi\Sigma(T_0, T_i)}} \exp\left(\frac{1}{2\Sigma(T_0, T_i)} \left[\xi + I(T_0, T_i) - x(T_0)\phi(T_0, T_i)\right]^2\right) d\xi.$$

Note that $x(T_0) = 0$ and we set $T_0 = 0$. In order to get rid of the max function we need the following:

$$\frac{1}{\hat{P}(T_i, T_{i+1}, \xi)} - \kappa \geq 0,$$

$$\frac{P(0, T_i)}{P(0, T_{i+1})} \exp\left(-B(T_i, T_{i+1})(\xi + I(0, T_i)) - \frac{1}{2}B^2(T_i, T_{i+1})\Sigma(0, T_i)\right) - \kappa \geq 0,$$

$$\xi \leq -\frac{\log\left(\frac{P(0,T_{i+1})}{P(0,T_i)}\kappa\right) + B(T_i, T_{i+1})I(0, T_i) + \frac{1}{2}B^2(T_i, T_{i+1})\Sigma(0, T_i)}{B(T_i, T_{i+1})}.$$

Substitute $m = \frac{1}{\sqrt{\Sigma(0,T_i)}}(\xi + I(0, T_i))$, this gives:

$$m \leq -\frac{\log\left(\frac{P(0,T_i)}{P(0,T_{i+1})})\kappa\right) + \frac{1}{2}B^2(T_i, T_{i+1})\Sigma(0, T_i)}{B(T_i, T_{i+1})\sqrt{\Sigma(0, T_i)}} =: d_1.$$

With this substitution the following formula for the LIBOR caplet price is obtained:

$$\begin{aligned} V^C(0,0) &= \int_{d_1}^{\infty} N\left(\frac{1}{\hat{P}(T_i, T_{i+1}, \Sigma(0, T_i)m - I(0, T_i))} - \kappa\right) \hat{P}(T_i, T_{i+1}, \Sigma(0, T_i)m - I(0, T_i)) \cdot \\ &\quad P(0, T_i)\frac{1}{\sqrt{2\pi}} \exp\left(\frac{1}{2}m^2\right) dm \\ &= NP(0, T_i)\Phi(-d_1) \\ &\quad - \int_{d_1}^{\infty} N\kappa\hat{P}(T_i, T_{i+1}, \Sigma(0, T_i)m - I(0, T_i))P(0, T_i))\frac{1}{\sqrt{2\pi}} \exp\left(\frac{1}{2}m^2\right) dm \\ &= NP(0, T_i)\Phi(-d_1) - \int_{d_1}^{\infty} N\kappa\frac{P(0, T_{i+1})}{P(0, T_i)}P(0, T_i) \cdot \\ &\quad \frac{1}{\sqrt{2\pi}} \exp\left(-B(T_i, T_{i+1})m - \frac{1}{2}B^2(T_i, T_{i+1})\Sigma(0, T_i)\right) \exp\left(\frac{1}{2}m^2\right) dm. \end{aligned}$$

Substituting $h = m - B(T_i, T_{i+1})\sqrt{\Sigma(0, T_i)}$ gives:

$$\begin{aligned} V^C(0,0) &= NP(0, T_i)\Phi(-d_1) \\ &\quad - \int_{d_2}^{\infty} N\kappa P(0, T_{i+1})\frac{1}{\sqrt{2\pi}} \exp\left(\frac{1}{2}h^2\right) dh \\ &= NP(T_0, T_i)\Phi(-d_1) - N\kappa P(T_0, T_{i+1})\Phi(-d_2), \end{aligned}$$

where $d_2 = d_1 - B(T_i, T_{i+1})\sqrt{\Sigma(0, T_i)}$.

With this derivation we obtain the present value of a LIBOR caplet given by:

$$V^C(0,0) = N(P(0, T_i)\Phi(-d_1) - (1 + \tau K)P(0, T_{i+1})\Phi(-d_2)),$$

where

$$\begin{aligned} d_1 &= \frac{\log\left(\frac{P(0,T_{i+1})}{P(0,T_i)}(1 + \tau K)\right) - \frac{1}{2}B^2(T_i, T_{i+1})\Sigma(0, T_i)}{B(T_i, T_{i+1})\sqrt{\Sigma(0, T_i)}}, \\ d_2 &= d_1 + B(T_i, T_{i+1})\sqrt{\Sigma(0, T_i)}. \end{aligned}$$

For the present value of a floorlet, the exact same steps as above can be followed, but then one should start with a payoff of:

$$V^P(T_{i+1}, x(T_i)) = \tau N \max(K - L(T_i, T_{i+1}), 0).$$

C.2. Caplet price with compounded pricing kernel

The payoff of a caplet at time T_{i+1} on compounded rates over the period $[T_i, T_{i+1}]$ with notional N and strike K is given by:

$$V_{CR}^C(T_{i+1}, x(\cdot)) \quad = \quad N\tau \max\left(\frac{1}{\tau}(M(T_i, T_{i+1}) - 1) - K, 0\right),$$

where τ is the year fraction between T_i and T_{i+1} and $M(T_i, T_{i+1})$ can be modelled by:

$$M(T_i, T_{i+1}) = \frac{P(0, T_i)}{P(0, T_{i+1})} \exp\left(z(T_{i+1}) - z(T_i)\right) - 1,$$

where

$$z(t) = \int_0^t (\hat{g}(t) + x(s))\, ds.$$

Note, the caplet on compounded rates now also depends on $z(\cdot)$. Hence, we use the notation $\tilde{V}_{CR}^C(t, x(\cdot), z(\cdot))$ for the t-value of a caplet on compounded rates.

With the compounded pricing kernel from Equation (3.14) the present value of a caplet on compounded rates can be derived. In order to derive that formula, first the pricing kernel has to be applied to get the value of the caplet at time T_i. In the derivation below, κ is equal to $(1 + \tau K)$.

$$\begin{aligned}
\tilde{V}_{CR}^C(T_i, x(T_i), z(T_i)) \quad = \quad & \int\int_{\mathbb{R}^2} N \max\left(\frac{P(0, T_i)}{P(0, T_{i+1})} \exp\left(\zeta - z(T_i)\right) - \kappa, 0\right) \hat{P}(T_i, T_{i+1}, x(T_i)) \cdot \\
& \frac{1}{2\pi\sqrt{\Sigma(T_i, T_{i+1})}\sqrt{2K(T_i, T_{i+1})}} \exp\Bigg(-\frac{1}{2\left(1 - \frac{I^2(T_i, T_{i+1})}{2K(T_i, T_{i+1})\Sigma(T_i, T_{i+1})}\right)} \\
& \Bigg[\frac{1}{\Sigma(T_i, T_{i+1})}(\xi + I(T_i, T_{i+1}) - x\phi(T_i, T_{i+1}))^2 \\
& + \frac{1}{2K(T_i, T_{i+1})}(\zeta + K(T_i, T_{i+1}) - \nu(x(T_i), T_i, T_{i+1}) - z(T_i))^2 \\
& - \frac{2I(T_i, T_{i+1})}{2K(T_i, T_{i+1})\Sigma(T_i, T_{i+1})}(\xi + I(T_i, T_{i+1}) - x\phi(T_i, T_{i+1})) \cdot \\
& (\zeta + K(T_i, T_{i+1}) - \nu(T_i, T_{i+1}, x(T_i)) - z(T_i))\Bigg]\Bigg) d\xi d\zeta.
\end{aligned}$$

In order to get rid of the max function, the following is needed:

$$\begin{aligned}
\frac{P(0, T_i)}{P(0, T_{i+1})} \exp\left(\zeta - z(T_i)\right) - \kappa \geq 0, \\
\zeta \geq \log\left(\kappa \frac{P(0, T_{i+1})}{P(0, T_i)}\right) + z(T_i).
\end{aligned}$$

Moreover, the following substitutions are used:

$$\begin{aligned}
\zeta \quad &= \quad y\sqrt{2K(T_i, T_{i+1})} - K(T_i, T_{i+1}) + \nu(x(T_i), T_i, T_{i+1}) + z(T_i), \\
\xi \quad &= \quad \sqrt{\Sigma(T_i, T_{i+1})}\left(\frac{I(T_i, T_{i+1})}{\sqrt{2K(T_i, T_{i+1})\Sigma(T_i, T_{i+1})}} y + \sqrt{1 - \frac{I^2(T_i, T_{i+1})}{2K(T_i, T_{i+1})\Sigma(T_i, T_{i+1})}} h\right) - I(T_i, T_{i+1}) + x\phi(T_i, T_{i+1}).
\end{aligned}$$

This gives:

$$y \geq \frac{\log\left(\kappa\frac{P(0,T_{i+1})}{P(0,T_i)}\right) + K(T_i,T_{i+1}) - \nu(x(T_i),T_i,T_{i+1})}{\sqrt{2K(T_i,T_{i+1})}} =: \hat{d}_1(x(T_i)).$$

With these steps we obtain:

$$\begin{aligned}
\tilde{V}_{CR}^{C}(T_i,x(T_i),z(T_i)) &= \int_{\hat{d}_1(x(T_i))}^{\infty}\int_{\mathbb{R}} N\Bigg(\frac{P(0,T_i)}{P(0,T_{i+1})}\exp\Bigg(y\sqrt{2K(T_i,T_{i+1})} - K(T_i,T_{i+1}) + \\
&\quad \nu(x(T_i),T_i,T_{i+1})\Bigg) - \kappa\Bigg)P(T_i,T_{i+1},x(T_i))\frac{1}{2\pi}\exp\left(-\frac{1}{2}(h^2+y^2)\right)dhdy \\
&= \int_{\hat{d}_1(x(T_i))}^{\infty}\int_{\mathbb{R}} N\frac{1}{2\pi}\exp\Bigg(y\sqrt{2K(T_i,T_{i+1})} - K(T_i,T_{i+1}) + \nu(x(T_i),T_i,T_{i+1}) \\
&\quad -\frac{1}{2}(h^2+y^2)\Bigg)dhdy - NP(T_i,T_{i+1},x(T_i))\kappa\Phi(-\hat{d}_1(x(T_i))).
\end{aligned}$$

Substituting:

$$n = y - \sqrt{2K(T_i,T_{i+1})}$$

into this gives:

$$\begin{aligned}
\tilde{V}_{CR}^{C}(T_i,x(T_i),z(T_i)) &= \int_{\hat{d}_2(x(T_i))}^{\infty}\int_{\mathbb{R}} N\frac{1}{2\pi}\exp\left(-\frac{1}{2}(h^2+n^2)\right)dhdn - N\hat{P}(T_i,T_{i+1},x(T_i))\kappa\Phi(-\hat{d}_1(x(T_i))) \\
&= N(\Phi(-d_2(x(T_i))) - \hat{P}(T_i,T_{i+1},x(T_i))\kappa\Phi(-\hat{d}_1(x(T_i)))),
\end{aligned}$$

where

$$\hat{d}_2(x(T_i)) = \hat{d}_1(x(T_i)) - \sqrt{2K(T_i,T_{i+1})}.$$

With this derivation the value of a caplet at time T_i is obtained:

$$\begin{aligned}
\tilde{V}_{CR}^{C}(T_i,x(T_i),z(T_i)) &= N(\Phi(-\hat{d}_2(x(T_i))) - \hat{P}(T_i,T_{i+1},x(T_i))\kappa\Phi(-\hat{d}_1(x(T_i)))), \\
\hat{d}_1(x(T_i)) &= \frac{\log\left(\kappa\frac{P(0,T_{i+1})}{P(0,T_i)}\right) + K(T_i,T_{i+1}) - \nu(x(T_i),T_i,T_{i+1})}{\sqrt{2K(T_i,T_{i+1})}}, \\
\hat{d}_2(x(T_i)) &= \hat{d}_1(x(T_i)) - \sqrt{2K(T_i,T_{i+1})}.
\end{aligned}$$

In order to derive the present value of a caplet, the price at time T_i is considered as the payoff at time T_i. Then the pricing kernel has to be applied again:

$$\begin{aligned}
\tilde{V}_{CR}^{C}(0,0,0) &= \int\int_{\mathbb{R}^2} N\left(\Phi(-\hat{d}_2(\xi)) - \hat{P}(T_i,T_{i+1},\xi)\kappa\Phi(-\hat{d}_1(\xi))\right)P(0,T_i)\cdot \\
&\quad N_2\left(\frac{\xi + I(0,T_i)}{\sqrt{\Sigma(0,T_i)}}, \frac{\zeta + K(0,T_i) - \nu(0,0,T_i) - z(T_0)}{\sqrt{2K(0,T_i)}}\right)d\xi d\zeta.
\end{aligned}$$

Substituting:

$$\begin{aligned}
\xi &= y\sqrt{\Sigma(T_i,T_{i+1})} - I(0,T_i), \\
\zeta &= \sqrt{2K(0,T_i)}\left(\frac{I(0,T_i)}{\sqrt{2K(0,T_i)\Sigma(0,T_i)}}y + \sqrt{1 - \frac{I^2(0,T_i)}{2K(0,T_i)\Sigma(0,T_i)}}h\right) - K(0,T_i) + \nu(0,0,T_i) + z(T_0),
\end{aligned}$$

gives:

$$\begin{aligned}\tilde{V}_{CR}^{C}(0,0,0) &= \int_{\mathbb{R}} N\left(\Phi\left(-\hat{d}_2(y\sqrt{\Sigma(T_i,T_{i+1})}-I(0,T_i))\right)-\frac{P(0,T_{i+1})}{P(0,T_i)}\exp\Big(-yB(T_i,T_{i+1})\sqrt{\Sigma(0,T_i)}\\ &\quad -\frac{1}{2}B^2(T_i,T_{i+1})\Sigma(0,T_i)\Big)\kappa\Phi(-\hat{d}_1(y\sqrt{\Sigma(0,T_i)}-I(0,T_i)))\Big)P(0,T_i)\frac{1}{\sqrt{2\pi}}\exp\left(-\frac{1}{2}y^2\right)dy\\ &\overset{*}{=} NP(0,T_i)\Phi(-d_2)-NP(0,T_{i+1})\kappa\frac{1}{\sqrt{2\pi}}\exp\Big(-yB(T_i,T_{i+1})\sqrt{\Sigma(0,T_i)}\\ &\quad -\frac{1}{2}B^2(T_i,T_{i+1})\Sigma(0,T_i)-\frac{1}{2}y^2\Big)dy.\end{aligned}$$

With the substitution:

$$n=(y+B(T_i,T_{i+1})\sqrt{\Sigma(0,T_i)}),$$

we obtain:

$$\tilde{V}_{CR}^{C}(0,0,0) \overset{*}{=} N\left(P(0,T_i)\Phi(-d_2)-P(0,T_{i+1})\kappa\Phi(-d_1)\right),$$

where

$$\begin{aligned}d_2 &= \frac{\log\left(\frac{P(0,T_i)}{P(0,T_i)}\kappa\right)-\frac{1}{2}\left(B^2(T_i,T_{i+1})\Sigma(0,T_i)-K(T_i,T_{i+1})\right)}{\sqrt{B^2(T_i,T_{i+1})\Sigma(0,T_i)+2K(T_i,T_{i+1})}},\\ d_1 &= d_2+\sqrt{B^2(T_i,T_{i+1})\sqrt{\Sigma(0,T_i)}+2K(T_i,T_{1+2})}.\end{aligned}$$

Note that in * we made use of the property:

$$\int_{\mathbb{R}}\Phi(a+bx)\varphi(x)dx=\Phi\left(\frac{a}{\sqrt{1+b^2}}\right),$$

where $\Phi(\cdot)$ is a normal cumulative distribution function and $\varphi(\cdot)$ is a normal probability density function.

In this appendix the present value of a caplet on compounding rates is obtained:

$$\tilde{V}_{CR}^{C}(0,0,0) = N(P(0,T_i)\Phi(-d_2)-\kappa P(0,T_{i+1})\Phi(-d_1)),$$

where

$$\begin{aligned}d_2 &= \frac{\log\left(\kappa\frac{P(0,T_{i+1})}{P(0,T_i)}\right)-\frac{1}{2}\left(B^2(T_i,T_{i+1})\Sigma(0,T_i)+2K(T_i,T_{i+1})\right)}{\sqrt{B^2(T_i,T_{i+1})\Sigma(0,T_i)+2K(T_i,T_{i+1})}},\\ d_1 &= d_2+\sqrt{B^2(T_i,T_{i+1})\Sigma(0,T_i)+2K(T_i,T_{i+1})}.\end{aligned}$$

The present value of a floorlet on compounded rates can be obtained following the same steps but then with payoff function:

$$V_{CR}^{P}(T_{i+1},x(\cdot)) = N\tau\max\left(K-\frac{1}{\tau}\left(M(T_i,T_{i+1})-1\right),0\right).$$

D

Derivation of caplet and floorlet prices with the Black-Karasinski pricing kernel

This appendix provides details about an approximation of caplet/floorlet pricing formulae obtained with the Black-Karasinski pricing kernel. First, LIBOR caplets/floorlets are considered. Thereafter, also the pricing formula for caplets/floorlets on compounded rates is provided.

D.1. Black-Karasinski pricing kernel for LIBOR rates

This appendix is dedicated to price LIBOR caplets/floorlets with the Black-Karsinski pricing kernel. Following Turfus, 2021, Chapter 5, the below theorem provides a Green function to solve the pricing PDE given in Equation (4.2) for a low rate environment.

Theorem D.1 (Black-Karasinski pricing kernel)**.** *Suppose* $||\tilde{r}(t)|| = \mathcal{O}(\epsilon)$ *in* (4.1) *under some suitable norm for* $\epsilon \longrightarrow 0$*. The pricing kernel for* (4.2) *is then given by:*

$$G(x,t;\xi,T) = D(t,T)\sum_{n=0}^{\infty} G_n(x,t;\xi,T), \tag{D.1}$$

with $D(t,T) = \frac{P(0,T)}{P(0,t)}$*, where today's date is given by* 0*, and where* $G_n(x,t;\xi,T) = \mathcal{O}(\epsilon^n)$*. Further, the requirement that the calibrated model has to fit the forward interest rate curve implied by* $D(t,T)$ *is met by specifying a suitable asymptotic series for* $\tilde{r}(\cdot)$*, as follows:*

$$\tilde{r}(t) = \sum_{n=1}^{\infty} \tilde{r}_n(t), \tag{D.2}$$

with $||\tilde{r}_n(\cdot)|| = \mathcal{O}(\epsilon^n)$*. A solution to second-order in* ϵ *is provided by deriving:*

$$\begin{aligned}
G_0(x,t,\xi,T) &= \frac{1}{\sqrt{\Sigma(t,T)}}\varphi\left(\frac{\xi-\phi(t,T)x}{\sqrt{\Sigma(t,T)}}\right),\\
G_1(x,t;\xi,T) &= -\int_t^T \left(R_1(x,t,t_1)\mathcal{M}(t,t_1)-\bar{r}(t_1)\right)G_0(x,t;\xi,T)dt_1,\\
G_2(x,t;\xi,T) &= \int_t^T \left(R_1(x,t,t_1)\mathcal{M}(t,t_1)-\bar{r}(t_1)\right)\int_{t_1}^T \left(R_1(x,t,t_2)\mathcal{M}(t,t_2)-\bar{r}(t_2)\right)G_0(x,t;\xi,T)dt_2dt_1\\
&\quad -\int_t^T R_2(x,t,t_1)\mathcal{M}(t,t_1)G_0(x,t;\xi,T)dt_1,
\end{aligned}$$

where $\bar{r}(\cdot)$ is the instantaneous forward curve and we define:

$$\begin{aligned} R_n(x,t,t_1) &:= \tilde{r}_n(t_1)e^{\hat{\theta}(x,t,t_1)},\ n=1,2,\dots, && \text{(D.3)}\\ \hat{\theta}(x,t,t_1) &:= \phi(t,t_1)x-\frac{1}{2}\Sigma(0,t), && \text{(D.4)}\\ \mathcal{M}(t,t_1)g(x,\dots) &:= g(x+\Delta(t,t_1),\dots), && \text{(D.5)}\\ \Delta(t,t_1) &:= \frac{\Sigma(t,t_1)}{\phi(t,t_1)}, \end{aligned}$$

where $\phi(t,T)$ and $\Sigma(t,T)$ are defined as in Section 3.3.1.1. Truncation of (D.2) *at $n=2$ and the choice:*

$$\begin{aligned} \tilde{r}_1(t) &= \bar{r}(t),\\ \tilde{r}_2(t) &= \tilde{r}_2(t)\int_0^t \tilde{r}_1(t_1)\left(e^{\phi(t_1,t)\Sigma(0,t_1)}-1\right), \end{aligned}$$

ensures an exact calibration of the second-order Green's function to the forward curve represented by $D(t,T)$.

Proof. For a proof, we refer to Turfus, 2021, p. 55. □

Using the pricing kernel from Theorem D.1 the t-value of a derivative with payoff $V(T,x(T))$ can be derived by calculating the following integral:

$$V(t,x(t))=\int_{\mathbb{R}} V(T,\xi)G(x,t;\xi,T)d\xi.$$

Zero-coupon bond prices Before starting with the prices of caplets/floorlets, the value of a zero-coupon bond has to be obtained. The t-value of a zero-coupon bond is derived by applying the kernel approach to the payoff of 1 at the maturity T. Recall, $\hat{P}(t,T,x(t))\equiv P(t,T)$.

$$\begin{aligned} \hat{P}(t,T,x) &= D(t,T)\int_{\mathbb{R}} 1\cdot G(x,t,\xi,T)d\xi\\ &= D(t,T)\int_{\mathbb{R}} G_0(x,t;\xi,T)d\xi + D(t,T)\int_{\mathbb{R}} G_1(x,t;\xi,T)d\xi + D(t,T)\int_{\mathbb{R}} G_2(x,t;\xi,T)d\xi. \end{aligned}$$

For clarity, we break this calculation down in parts below.

$$D(t,T)\int_{\mathbb{R}} G_0(x,t;\xi,T)d\xi=\int_{\mathbb{R}}\frac{1}{\sqrt{\Sigma(t,T)}}\varphi\left(\frac{\xi-\phi(t,T)x}{\sqrt{\Sigma(t,T)}}\right)d\xi=D(t,T).$$

$$\begin{aligned} D(t,T)\int_{\mathbb{R}} G_1(x,t;\xi,T)d\xi &= D(t,T)\int_{\mathbb{R}} -\int_t^T (R_1(x,t,t_1)\mathcal{M}(t,t_1)-\bar{r}(t_1))\frac{1}{\sqrt{\Sigma(t,T)}}\varphi\left(\frac{\xi-\phi(t,T)x}{\sqrt{\Sigma(t,T)}}\right)dt_1d\xi\\ &= -D(t,T)\int_t^T\int_{\mathbb{R}} (R_1(x,t,t_1)\mathcal{M}(t,t_1)-\bar{r}(t_1))\frac{1}{\sqrt{\Sigma(t,T)}}\varphi\left(\frac{\xi-\phi(t,T)x}{\sqrt{\Sigma(t,T)}}\right)d\xi dt_1\\ &= -D(t,T)\int_t^T\int_{\mathbb{R}} (R_1(x,t,t_1)\mathcal{M}(t,t_1)-\bar{r}(t_1))\frac{1}{\sqrt{\Sigma(t,T)}}\varphi\left(\frac{\xi-\phi(t,T)x}{\sqrt{\Sigma(t,T)}}\right)d\xi dt_1\\ &= -D(t,T)\int_t^T (R_1(x,t,t_1)\mathcal{M}(t,t_1)-\bar{r}(t_1))dt_1\\ &= -D(t,T)\int_t^T (R_1(x,t,t_1)-\bar{r}(t_1))dt_1. \end{aligned}$$

$$
\begin{aligned}
D(t,T)\int_{\mathbb{R}} G_2(x,t;\xi,T)d\xi &= D(t,T)\int_{\mathbb{R}}\Bigg(\int_t^T (R_1(x,t,t_1)\mathcal{M}(t,t_1)-\bar{r}(t_1))\int_{t_1}^T (R_1(x,t,t_2)\mathcal{M}(t,t_2)-\bar{r}(t_2)) \\
&\quad G_0(x,t;\xi,T)dt_2dt_1 - \int_t^T R_2(x,t,t_1)\mathcal{M}(t,t_1)G_0(x,t;\xi,T)dt_1\Bigg)d\xi \\
&= D(t,T)\int_{\mathbb{R}}\int_t^T\int_{t_1}^T (R_1(x,t,t_1)\mathcal{M}(t,t_1)-\bar{r}(t_1))\,(R_1(x,t,t_2)\mathcal{M}(t,t_2)-\bar{r}(t_2))\cdot \\
&\quad G_0(x,t;\xi,T)dt_2dt_1d\xi - D(t,T)\int_{\mathbb{R}}\int_t^T R_2(x,t,t_1)\mathcal{M}(t,t_1)G_0(x,t;\xi,T)dt_1d\xi \\
&= D(t,T)\int_t^T\int_{t_1}^T\int_{\mathbb{R}} (R_1(x,t,t_1)\mathcal{M}(t,t_1)-\bar{r}(t_1))\,(R_1(x,t,t_2)\mathcal{M}(t,t_2)-\bar{r}(t_2))\cdot\cdot \\
&\quad G_0(x,t;\xi,T)d\xi dt_2dt_1 - D(t,T)\int_t^T\int_{\mathbb{R}} R_2(x,t,t_1)\mathcal{M}(t,t_1)G_0(x,t;\xi,T)d\xi dt_1 \\
&= D(t,T)\int_t^T\int_{t_1}^T (R_1(x,t,t_1)\mathcal{M}(t,t_1)-\bar{r}(t_1))\,(R_1(x,t,t_2)\mathcal{M}(t,t_2)-\bar{r}(t_2))\cdot \\
&\quad \int_{\mathbb{R}} G_0(x,t;\xi,T)d\xi dt_2dt_1 - D(t,T)\int_t^T R_2(x,t,t_1)\mathcal{M}(t,t_1)\int_{\mathbb{R}} G_0(x,t;\xi,T)d\xi dt_1 \\
&= D(t,T)\int_t^T\int_{t_1}^T (R_1(x,t,t_1)\mathcal{M}(t,t_1)-\bar{r}(t_1))\,(R_1(x,t,t_2)\mathcal{M}(t,t_2)-\bar{r}(t_2))\,dt_2dt_1 \\
&\quad -D(t,T)\int_t^T R_2(x,t,t_1)\mathcal{M}(t,t_1)dt_1 \\
&= D(t,T)\int_t^T\int_{t_1}^T R_1(x,t,t_1)\mathcal{M}(t,t_1)R_1(x,t,t_2)\mathcal{M}(t,t_2) - \bar{r}(t_1)R_1(x,t,t_2)\mathcal{M}(t,t_2) \\
&\quad -\bar{r}(t_2)R_1(x,t,t_1)\mathcal{M}(t,t_1) - \bar{r}(t_1)\bar{r}(t_2)dt_2dt_1 - D(t,T)\int_t^T R_2(x,t,t_1)dt_1 \\
&= D(t,T)\int_t^T\int_{t_1}^T R_1(x,t,t_1)\tilde{r}_1(t_2)\exp\left(\phi(t,t_2)(x+\frac{\Sigma(t,t_1)}{\phi(t,t_1)}) - \frac{1}{2}\phi^2(t,t_2)\Sigma(0,t)\right) \\
&\quad -\bar{r}(t_1)R_1(x,t,t_2) - \bar{r}(t_2)R_1(x,t,t_1) - \bar{r}(t_1)\bar{r}(t_2)dt_2dt_1 \\
&\quad -D(t,T)\int_t^T R_2(x,t,t_1)dt_1 \\
&= D(t,T)\int_t^T\int_{t_1}^T R_1(x,t,t_1)R_1(x,t,t_2)e^{\phi(t_1,t_2)\Sigma(t,t_1))} - \bar{r}(t_1)R_1(x,t,t_2) \\
&\quad -\bar{r}(t_2)R_1(x,t,t_1) - \bar{r}(t_1)\bar{r}(t_2)dt_2dt_1 - D(t,T)\int_t^T R_2(x,t,t_1)dt_1 \\
&= D(t,T)\int_t^T (R_1(x,t,t_1)-\bar{r}(t_1))\int_{t_1}^T (R_1(x,t,t_2)-\bar{r}(t_2))\,dt_2dt_1 \\
&\quad +D(t,T)\int_t^T R_1(x,t,t_1)\int_{t_1}^T R_1(x,t,t_2)\left(e^{\phi(t_1,t_2)\Sigma(t,t_1)}-1\right)dt_2dt_1 \\
&\quad -D(t,T)\int_t^T R_2(x,t,t_1))dt_1.
\end{aligned}
$$

As a result, the t-value of a zero-coupon bond with maturity T is given by:

$$\begin{aligned}
\hat{P}(t,T,x) &= D(t,T) + P_1(t,T,x) + P_2(t,T,x) + \mathcal{O}(\epsilon^3),\\
\hat{P}_1(t,T,x) &= -D(t,T)\int_t^T R_1(x,t,t_1) - \bar{r}(t_1)dt_1,\\
\hat{P}_2(t,T,x) &= D(t,T)\int_t^T (R_1(x,t,T) - \bar{r}(t_1))\int_{t_1}^T R_1(x,t,t_2) - \bar{r}(t_2)dt_2dt_1\\
&\quad + D(t,T)\int_t^T R_1(x,t,t_1)\int_{t_1}^T R_1(x,t,t_2)\left(e^{\phi(t_1,t_2)\Sigma(t,t_1)} - 1\right)dt_2dt_1\\
&\quad - D(t,T)\int_t^T R_2(x,t,t_1)dt_1.
\end{aligned}$$

Note, that x in the zero-coupon bond formula corresponds to the value of the process $x(t)$ at time t.

LIBOR caplet/floorlet prices Let us consider a LIBOR caplet over the period $[T_i, T_{i+1}]$ with strike K and notional N. In order to obtain the t-value of this caplet with the Black-Karasinski pricing kernel, first the T_i-value of the caplet needs to be determined. This value is given by:

$$V^C(T_i, x(T_i)) = N\max\left(1 - \kappa\hat{P}(T_i, T_{i+1}, x(T_i)), 0\right), \tag{D.6}$$

where $\kappa = (1 + \tau K)$. We seek for a formula of the t-value of this caplet with second-order accuracy with respect to ϵ. This is obtained by applying the pricing kernel to the T_i-value of the caplet. The approximation which is derived below, is valid for a low rate environment. Suppose that strike K is of order $\mathcal{O}(\epsilon)$, such that the strike is in line with the LIBOR payment. The corresponding integral which needs to be calculated goes over the range of $[-\infty, \infty]$ for the value of $x(T_i)$. Since the payoff of the LIBOR caplet consists of a max-function in (D.6), the range of the integral can simply be reduced and start from the point where this max-function has a positive value. This can be done due to the monotonicity of $\hat{P}(T_i, T_{i+1}, x(T_i))$. The values of $x(T_i)$ for which the max-function is positive satisfy the following inequalities:

$$\begin{aligned}
1 - \kappa\hat{P}(T_i, T_{i+1}, x(T_i)) &\geq 0\\
\hat{P}(T_i, T_{i+1}, x(T_i)) &\leq \kappa^{-1}\\
D(T_i, T_{i+1}) + \hat{P}_1(T_i, T_{i+1}, x(T_i)) + \hat{P}_2(T_i, T_{i+1}, x(T_i)) &\leq \kappa^{-1}
\end{aligned}$$

The critical value of x^* to remove this max-function can be found by solving the equation:

$$D(T_i, T_{i+1}) + \hat{P}_1(T_i, T_{i+1}, x^*) + \hat{P}_2(T_i, T_{i+1}, x^*) = \kappa^{-1}. \tag{D.7}$$

Remark, the background idea is similar to the Jamshidian trick, see Andersen and Piterbarg, 2010. To obtain the second-order approximation, the payoff of the LIBOR caplet is split into two parts and the pricing kernel is applied in the following way:

$$\begin{aligned}
V^C(t,x) &= \int_{\mathcal{R}} V(\xi,T)G(x,t;\xi.T)d\xi\\
&= D(t,T_i)\int_{\mathbb{R}} \hat{V}_1(\xi)G_0(x,t;\xi,T_i) + \hat{V}_1(\xi)G_1(x,t;\xi,T_i) + \hat{V}_2(\xi)G_0(x,t;\xi,T_i)d\xi + \mathcal{O}(\epsilon^3),
\end{aligned}$$

where

$$\begin{aligned}
\hat{V}_1(\xi) &:= \left(1 - \kappa D(T_i, T_{i+1})(1 + \hat{P}_1(T_i, T_{i+1}, \xi))\right)\mathbb{1}_{\xi > x^*},\\
\hat{V}_2(\xi) &:= -\kappa D(T_i, T_{i+1})\hat{P}_2(T_i, T_{i+1}, \xi)\mathbb{1}_{\xi > x^*},
\end{aligned}$$

with $V_n(\xi) = \mathcal{O}(\epsilon^n)$, since we assume:

$$1 - \kappa D(T_i, T_{i+1}) = 1 - (1 + \tau K)D(T_i, T_{i+1}) = \tau K D(T_i, T_{i+1}) = \mathcal{O}(\epsilon).$$

As a result, the t-value of a LIBOR caplet is given by:

$$
\begin{aligned}
V^C(t,x) \quad = \quad & (D(t,T_i) - \kappa D(t,T_{i+1}))\,\Phi(-d_1(x^* - \phi(t,T_i)x,t,T_1)) \\
& +\kappa D(t,T_{i+1}) \int_{T_i}^{T_{i+1}} R_1(x,t,u)\Phi(-d_2(x^* - \phi(t,T_i)x,t,T_i,u))\\
& -\bar{r}(u)\Phi(-d_1(x^* - \phi(t,T_i)x,t,T_i))du \\
& -(D(t,T_i) - \kappa D(t,T_{i+1})) \int_t^{T_i} R_1(x,t,u)\phi(-d_2(x^* - \phi(t,T_i)x,t,T_i,u)) \\
& -\bar{r}(u)\Phi(-d_1(x^* - \phi(t,T_i)x,t,T_i))du \\
& -\kappa D(t,T_{i+1}) \int_{T_i}^{T_{i+1}} R_1(x,t,v) \int_t^v e^{\phi(u,v)\Sigma(t,v)} R_1(x,t,u)\Phi(-d_2^*(x^* - \phi(t,T_i)x,t,T_i,u,v)) \\
& -\bar{r}(u)\Phi(-d_1^*(x^* - \phi(t,T_i)x,t,T_i,u,v))dudv \\
& +\kappa D(t,T_{i+1}) \int_{T_i}^{T_{i+1}} R_1(x,t,v) \int_t^v R_1(x,t,u)\Phi(-d_2(x^* - \phi(t,T_i)x,t,T_i,u)) \\
& -\bar{r}(u)\Phi(-d_1(x^* - \phi(t,T_i)x,t,T_i))dudv \\
& +\kappa D(t,T_{i+1}) \int_{T_i}^{T_{i+1}} R_2(x,t,v)\Phi(-d_2(x^* - \phi(t,T_i)x,t,T_i,v))dv + \mathcal{O}(\epsilon^3),
\end{aligned}
$$

where, for $v \geq T_i$ and $u \in (t,v]$, we define:

$$
\begin{aligned}
d_1(\xi,t,T_i) \quad &:= \quad \frac{\xi}{\sqrt{\Sigma(t,T_i)}}, \\
d_2(\xi,t,T_i,w) \quad &:= \quad d_1(\xi - \phi(T_i \wedge w, T_i \vee w)\Sigma(t,T_i \wedge w),t,T_i), \\
d_1^*(\xi,t,T_i,u,v) \quad &:= \quad d_1(\xi - \phi(T_i,v)\Sigma(u \wedge T_i,T_i),t,T_i), \\
d_2^*(\xi,t,T_i,u,v) \quad &:= \quad d_2(\xi - \phi(T_i,v)\Sigma(u \wedge T_i,T_i),t,T_i,u).
\end{aligned}
$$

The binary operators $\wedge$ and $\vee$ denote the minimum and maximum, respectively.

Then, for $t = 0$ and $x = 0$, the present value of the LIBOR caplet is given by:

$$
\begin{aligned}
V^C(0,0) \quad = \quad & (D(0,T_i) - \kappa D(0,T_{i+1}))\,\Phi(-d_1(x^*,0,T_i)) \\
& -D(0,T_i) \int_0^{T_i} \bar{r}(u)\left(\Phi(-d_2(x^*,0,T_i,u)) - \Phi(-d_1(x^*,0,T_i))\right) du \\
& +\kappa D(0,T_{i+1}) \int_0^{T_{i+1}} \bar{r}(u)\left(\Phi(-d_2(x^*,0,T_i,u)) - \Phi(-d_1(x^*,0,T_i))\right) du \\
& -\kappa D(0,T_{i+1}) \int_{T_i}^{T_{i+1}} \bar{r}(v) \int_0^v \bar{r}(u) e^{\phi(u,v)\Sigma(0,u)} \left(\Phi(-d_2^*(x^*,0,T_i,u,v)) - \Phi(-d_2(x^*,0,T_i,v))\right) dudv \\
& +\kappa D(0,T_{i+1}) \int_{T_i}^{T_{i+1}} \bar{r}(v) \int_0^v \bar{r}(u) \Big(\Phi(-d_1^*(x^*,0,T_i,u,v)) - \Phi(-d_2(x^*,0,T_i,v)) \\
& +\Phi(-d_2(x^*,0,T_i,u)) - \Phi(-d_1(x^*,0,T_i)) \Big) dudv + \mathcal{O}(\epsilon^3).
\end{aligned}
$$

Moreover, using the put-call parity, the present value of a LIBOR floorlet is easy to obtain:

$$
\begin{aligned}
V^P(0,0) \quad = \quad & (\kappa D(0,T_{i+1}) - D(0,T_i))\,\Phi(d_1(x^*,0,T_i)) \\
& + D(0,T_i)\int_0^{T_i} \bar{r}(u)\,(\Phi(d_2(x^*,0,T_i,u)) - \Phi(d_1(x^*,0,T_i)))\,du \\
& - \kappa D(0,T_{i+1})\int_0^{T_{i+1}} \bar{r}(u)\,(\Phi(d_2(x^*,0,T_i,u)) - \Phi(d_1(x^*,0,T_i)))\,du \\
& + \kappa D(0,T_{i+1})\int_{T_i}^{T_{i+1}} \bar{r}(v)\int_0^{v} \bar{r}(u)e^{\phi(u,v)\Sigma(0,u)}\left(\Phi(d_2^*(x^*,0,T_i,u,v)) - \Phi(d_2(x^*,0,T_i,v))\right)dudv \\
& - \kappa D(0,T_{i+1})\int_{T_i}^{T_{i+1}} \bar{r}(v)\int_0^{v} \bar{r}(u)\Big(\Phi(d_1^*(x^*,0,T_i,u,v)) - \Phi(d_2(x^*,0,T_i,v)) \\
& + \Phi(d_2(x^*,0,T_i,u)) - \Phi(d_1(x^*,0,T_i))\Big)dudv + \mathcal{O}(\epsilon^3).
\end{aligned}
$$

D.2. Black-Karasinski pricing kernel for compounded rates

This appendix is dedicated to price caplets/floorlets on compounded rates using the kernel approach. Following Turfus, 2021, Chapter 13, the below theorem yields the Green function corresponding to the pricing PDE given in Equation (4.4) for a low rate environment.

Theorem D.2. *The pricing kernel for the extended Black-Karasinski pricing equation from* (4.4) *can be asymptotically, for* $||\bar{r}(\cdot)|| = \mathcal{O}(\epsilon)$*, represented as:*

$$
\tilde{G}(x,z,t;\xi,\zeta,T) = D(t,T)\sum_{j=0}^{\infty}\tilde{G}_j(x,z,t;\xi,\zeta,T), \tag{D.8}
$$

with $||G_j(\cdot;\cdot)|| = \mathcal{O}(\epsilon^j)$*,*

$$
\begin{aligned}
\tilde{G}_0(x,z,t;\xi,\zeta,T) \quad = \quad & \frac{1}{\sqrt{\Sigma(t,T)}}\varphi\left(\frac{\xi-\phi(t,T)x}{\sqrt{\Sigma(t,T)}}\right)\delta(\zeta-z), \\
\tilde{G}_1(x,z,t;\xi,\zeta,T) \quad = \quad & Z_0(t,T)(1-\partial_z\tilde{G}_0(x,z,t;\xi,\zeta,T) - \int_t^T \bar{r}(t_1)e^{\hat{\theta}(x,t,t_1)}\left[1-\partial_z\tilde{G}_0(x,z,t;\xi-\Sigma(t,t_1),\zeta,T)\right]dt_1, \\
\tilde{G}_2(x,z,t;\xi,\zeta,T) \quad = \quad & \frac{1}{2}Z_0^2(t,T)(1-\frac{\partial}{\partial z})^2\tilde{G}_0(x,z,t;\xi,\zeta,T) \\
& - \int_t^T (Z_0(t,T)\bar{r}(t_1)(1-\partial_z)+\tilde{r}_2(t_1))e^{\hat{\theta}(x,t,t_1)}(1-\partial_z)\tilde{G}_0(x,z,t;\xi-\Sigma(t,t_1),\zeta,T) \\
& + \int_t^T \bar{r}(t_2)e^{\theta(x,t,t_2)}\int_t^{t_2}\bar{r}(t_1)e^{\hat{\theta}(x,t,t_1)+\phi(t_1,t_2)\Sigma(t,t_1)}(1-\partial_z)^2\cdot \\
& \tilde{G}_0\left(x,z,t;\xi-\sum_{i=1}^{2}\Sigma(t,t_i),\zeta,T\right)dt_1dt_2,
\end{aligned}
$$

where ∂_z *denotes the differential operator with respect to* z*,* $\delta(\cdot)$ *is the Dirac delta function and* $Z(t,T)$ *is defined as:*

$$
Z(t,T) = \int_t^T \bar{r}(s)ds.
$$

Proof. For a proof, we refer to Turfus, 2021, Chapter 13. □

Using this second-order approximation of the above pricing kernel, the t-value of a caplet on compounded rates between $[T_i.T_{i+1}]$ can be obtained. Then, the approximate price of a caplet on compounded rate can be calculated according to the below theorem. The approximation is due to a truncation of the pricing kernel and due to freezing $F_2(T_i,T_{i+1})$ at the value of $\hat{K}(T_i,T_{i+1})$, see both formulae below, to obtain an analytically tractable value of the caplet at time T_i.

Theorem D.3. *For the Black-Karasinski short-rate process, governed by* (4.1)*, the present value, at time* 0*, of a caplet with a compounded rate underlying, strike* K *and payment period* $[T_i, T_{i+1}]$ *is given to an approximation by:*

$$V_{CR}^{C}(0,0) \approx V^{C}(0,0) + \Delta V_{CR}^{C}(0,0), \tag{D.9}$$

where

$$\begin{aligned}
V^{C}(0,0) &= (D(0,T_i) - \kappa D(0,T_{i+1}))\Phi(-d_1(x^*,0,T_i)) \\
&\quad -D(0,T_i)\int_0^{T_i} \bar{r}(t_1)(\Phi(-d_2(x^*,0,T_i,t_1)) - \Phi(-d_1(x^*,0,T_1)))dt_1 \\
&\quad +\kappa D(0,T_{i+1})\int_0^{T_{i+1}} \bar{r}(t_1)(\Phi(-d_2(x^*,0,T_i,t_1)) - \Phi(-d_1(x^*,0,T_1)))dt_1 \\
&\quad -\kappa D(0,T_{i+1})\int_{T_i}^{T_{i+1}} \bar{r}(t_2)\int_0^{t_2} \bar{r}(t_1)e^{\phi(t_1,t_2)\Sigma(0,t_1)}(\Phi(-d_2^*(x*,0,T_i,t_1,t_2)) \\
&\quad -\Phi(-d_2(x^*,0,T_i,t_1)))dt_1dt_2 \\
&\quad +\kappa D(0,T_{i+1})\int_{T_i}^{T_{i+1}} \bar{r}(t_2)\int_0^{t_2} \bar{r}(t_1)(\Phi(-d_1^*(x^*,0,T_i,t_1,t_2)) - \Phi(-d_2(x^*,0,T_i,t_2)) \\
&\quad +\Phi(-d_2(x^*,0,T_i,t_1)) - \Phi(-d1(x^*,0,T_i)))dt_1dt_2,
\end{aligned}$$

with x^* *as defined in* (D.7) *and*

$$\begin{aligned}
d_1(\xi,t,T_i) &:= \frac{\xi + \hat{K}(T_i,T_{i+1})}{\sqrt{\Sigma(t,T_i) + 2\hat{K}(T_i,T_{i+1}}}, \\
d_2(\xi,t,T_i,w) &:= d_1(\xi - \phi(T_i \wedge w, T_i \vee w)\Sigma(t,T_i \wedge w) - 2\hat{K}(T_i,T_{i+1})), \\
\hat{K}(T_i,T_{i+1}) &:= \int_{T_i}^{T_{i+1}} \bar{r}(t_2)\int_{T_i}^{t_2} \bar{r}(t_1)e^{\Delta x*(T_i,t_1,t_2)}(e^{\phi(t_1,t_2)\Sigma(T_i,t_1)} - 1)dt_1dt_2, \\
\Delta x^*(T_i,t_1,t_2) &:= \phi(T_i,t_1)\phi(T_1,t_2)\Sigma(0,T_1).
\end{aligned} \tag{D.10}$$

The formula for $\Delta V_{CR}^{C}(0,0)$ *is given by:*

$$\begin{aligned}
\Delta V_{CR}^{C}(0,0) &= \frac{D(0,T_i)}{\hat{K}(T_i,T_{i+1})}\int_{T_i}^{T_{i+1}} \bar{r}(t_2)\int_{T_i}^{t_2} \bar{r}(t_1)e^{\Delta x*(T_i,t_1,t_2)}(e^{\phi(t_1,t_2)\Sigma(T_i,t_1)} - 1)\cdot \\
&\quad [\varphi(-d_2(x^* - \Delta x^*(T_i,t_1,t_2),0,T_1)) - \varphi(-d_2(x*,0,T_i))]\,dt_2dt_2.
\end{aligned}$$

The errors in the term $V^{C}(0,0)$ *are of order* $\mathcal{O}(\epsilon^2)$ *with* $\epsilon = ||\tilde{r}(\cdot)||$ *and the errors in the term* $\Delta V_{CR}^{C}(t_0)$ *are of order* $\mathcal{O}(\Sigma^2(T_i,T_{i+1}))$*.*

Proof. The proof of this statement is technically involved and requires detailed insight into perturbation analysis, which is beyond the scope of the thesis. Therefore, herewith we sketch the steps of the proof of the pricing kernel approach for caplets on compounded rates under the Black-Karasinski model. It is assumed that all perturbations are of sufficient accuracy. However, we do not validate or challenge the accuracy of the approximations. In the below, we follow Turfus, 2021, Chapter 13 and refer for further details therein.

It is more convenient to work with an alternative representation of the pricing kernel that is obtained as a by-product of (D.8), see Turfus, 2021, p. 173. This alternative representation is given by:

$$\begin{aligned}
\tilde{G}(x,z,t;\xi,\zeta,T) &= D(t,T)e^{-F_1(x,t,T)(1-\partial_z)}\tilde{G}_0(x,z,r;\xi,\zeta,T) \\
&\quad +D(t,T)\sum_{n=1}^{\infty}(-1)^n(1-\partial_z)^n\int_t^T\int_t^{t_n}\ldots\int_t^{t_2}\Bigg(\prod(R(x,t,t_i)\mathcal{M}(t,t_i) - \bar{r}(t_i)) \\
&\quad -\prod_{i=1}^{n}(R(x,t,t_i) - \bar{r}(t_i))\Bigg)dt_1\ldots dt_n\tilde{G}_0(x,z,t;\xi,\zeta,T),
\end{aligned} \tag{D.11}$$

where the operator $\mathcal{M}(t,t_1)$ is given in Equation (D.5) and we define:

$$\begin{aligned} R(x,t,t_1) &:= \tilde{r}(t_1)e^{\theta(x,t,t_1)}, \\ F_1(x,T_i,T_{i+1}) &:= \int_{T_1}^{T_{i+1}} R(x,T_i,t_1) - \tilde{r}(t_1))dt_1, \\ F_2(x,T_i,T_{i+1}) &:= \int_{T_i}^{T_{i+1}} R(x,T_i,t_2) \int_{T_i}^{t_2} R(x,T_i,t_1) \left(e^{\phi(t_1,t_2)\Sigma(T_i,t_1)} - 1\right) dt_1 dt_2. \end{aligned} \tag{D.12}$$

Analogously to Section 3.3.1.2, the time t-value of a caplet on compounded rates is obtained in two steps. First, the time T_i-value is determined by applying the pricing kernel to the payoff of the caplet. Second, the pricing kernel is applied again, but then to the T_i-value of the caplet, to derive the time t-value of the caplet.

Using the above alternative representation of the pricing kernel given in (D.11), the T_i-value of the caplet can be calculated by applying the kernel approach. Similar to the Hull-White model case, the payoff of caplets on compounded rates is given by Equation (3.15) with $z(t)$ as in Equation (4.3). Notice that this payoff is independent of ξ. Therefore, the integral over the kernel (D.11) with respect to ξ can be calculated separately to obtain the T_i-value of the caplet. Notice, in the $\overset{*}{=}$-steps below, the Taylor expansion of an exponential function is used. Recall, ∂_z and ∂_z^2 denote the first and second order partial derivative operators with respect to z, respectively. Furthermore, the following exponential representations of differential operators acting on a Gaussion distribution function are used:

$$\begin{aligned} e^{a\partial_z} l(z) &= l(a+z), \\ e^{a\partial_z^2} l(z) &= {}^{1} \quad \frac{1}{\sqrt{4\pi}} \int_{-\infty}^{\infty} l(z - y\sqrt{a}) e^{-\frac{1}{4}y^2} dy. \end{aligned}$$

$$\begin{aligned} &\int_{\mathbb{R}} \tilde{G}(x,z,T_i;\xi,\zeta,T_{i+1})d\xi \\ =\ & D(T_i,T_{i+1}) \left(e^{-F_1(x,T_i,T_{i+1})(1-\partial_z)} + F_2(x,T_i,T_{i+1})(1+\partial_z)^2 + \mathcal{O}(\epsilon^3)\right) \int_{\mathbb{R}} \tilde{G}_0(x,z,T_i;\xi,\zeta,T_{i+1})d\xi \\ \overset{*}{=}\ & D(T_i,T_{i+1}) \Big(1 - F_1(x,T_i,T_{i+1})(1-\partial_z) + F_2(x,T_i,T_{i+1})(1+\partial_z)^2 + \\ & \mathcal{O}((-F_1(x,T_i,T_{i+1})(1-\partial_z))^2) + \mathcal{O}(\epsilon^3)\Big) \int_{\mathbb{R}} \tilde{G}_0(x,z,T_i;\xi,\zeta,T_{i+1})d\xi \\ \overset{*}{=}\ & D(T_i,T_{i+1}) e^{-F_1(x,T_i,T_{i+1})(1-\partial_z) + F_2(x,T_i,T_{i+1})(1+\partial_z)^2} \int_{\mathbb{R}} \tilde{G}_0(x,z,T_i;\xi,\zeta,T_{i+1})d\xi + \mathcal{O}(\epsilon^3) \\ =\ & P(T_i,T_{i+1},x) e^{F_2(x,T_i,T_{i+1})\partial_z^2} \int_{\mathbb{R}} \tilde{G}_0(x, z + F_1(x,T_i,T_{i+1}) - 2F_2(x,T_i,T_{i+1}), T_i;\xi,\zeta,T_{i+1})d\xi + \mathcal{O}(\epsilon^3). \end{aligned}$$

With this observation, the T_i-value of the caplet on compounded rates is given by:

$$V_{CR}^{C}(T_i,x) = \Phi(-\tilde{d}_2(x,T_i,T_{i+1})) - \kappa P(x,T_i,T_{i+1})\Phi(-\tilde{d}_1(x,T_i,T_{i+1})), \tag{D.13}$$

where $\tilde{d}_1$ and $\tilde{d}_2$ are defined as:

$$\tilde{d}_1(x,T_i,T_{i+1}) := \frac{x^* - x - F_2(x,T_i,T_{i+1})}{\sqrt{2F_2(x,T_i,T_{i+1})}}, \tag{D.14}$$

$$\tilde{d}_2(x,T_i,T_{i+1}) := \tilde{d}_1(x,T_i,T_{i+1}) + \sqrt{2F_2(x,T_i,T_{i+1})}, \tag{D.15}$$

with x^* as defined in (D.7). Further to this, in the expression of $F_2(x,T_i,T_{i+1})$, see Equation (D.12), $R(x,T_i,t_1)$ and $R(x,T_i,t_2)$ can be replaced by $R_1(x,T_i,t_1)$ and $R_1(x,T_i,t_2)$, as defined in Equation (D.3), while keeping second-order accuracy. The calculation of the convexity correction term $F_2(x,T_i,T_{i_1})$, corresponding to the compounding period, is complex as it depends on value of x. However, one

[1] Weierstrass transform, for more information we refer to Zayed, 2019.

would prefer this to be analytically tractable. Therefore, we freeze $F_2(x,T_i,T_{i+1})$ in Equations (D.14) and (D.15) at the representative value $\hat{K}(T_i,T_{i+1})$ defined in (D.10) which gives:

$$\begin{aligned}\bar{d}_1(x,T_i,T_{i+1}) &:= \frac{x^* - x - \hat{K}(T_i,T_{i+1})}{\sqrt{2\hat{K}(T_i,T_{i+1})}},\\ \bar{d}_2(x,T_i,T_{i+1}) &:= \bar{d}_1(x,T_i,T_{i+1}) + \sqrt{2\hat{K}(T_i,T_{i+1})}.\end{aligned}$$

By such replacement an error is made. A correction of this error can be derived by considering a Taylor expansion of the T_i-value of a caplet with respect to $F_2(x,T_i,T_{i+1}) - \hat{K}(T_i,T_{i+1})$, resulting in an approximation of the T_i-value of the caplet:

$$\begin{aligned}V^C_{CR}(T_i,x) &\approx \Phi(-\bar{d}_2(x,T_i,T_{i+1})) - \kappa P(x,T_i,T_{i+1})\Phi(-\bar{d}_1(x,T_i,T_{i+1}))\\ &\quad -\frac{F_2(x,T_i,T_{i+1}) - \hat{K}(T_i,T_{i+1})}{2\hat{K}(T_i,T_{i+1})}\Big(\bar{d}_1(x,T_i,T_{i+1})\varphi\left(-\bar{d}_2(x,T_i,T+i+1)\right)\\ &\quad +\kappa D(T_i,T_{i+1})\bar{d}_2(x,T_i,T_{i+1})\varphi\left(-\bar{d}_1(x,T_i,T_{i+1})\right)\Big)\\ &\approx \Phi(-\bar{d}_2(x,T_i,T_{i+1})) - \kappa P(x,T_i,T_{i+1})\Phi(-\bar{d}_1(x,T_i,T_{i+1}))\\ &\quad +\frac{F_2(x,T_i,T_{i+1}) - \hat{K}(T_i,T_{i+1})}{\hat{K}(T_i,T_{i+1})}\frac{x - x^*}{\sqrt{2\hat{K}(T_i,T_{i+1})}}\varphi(-\bar{d}_2(x,T_i,T_{i+1})),\end{aligned} \tag{D.16}$$

where the fact that $\varphi(-\bar{d}_2) = \kappa D(T_i,T_{i+1})\varphi(-\bar{d}_1)$ is used. The final step to obtain the t-value of the caplet, is applying the pricing kernel to the expression given in Equation (D.16). This results in:

$$V^C_{CR}(0,0) \approx V^C(0,0) + \Delta V^C_{CR}(0,0),$$

where $V^C(0,0)$ is given by setting $t=0$ and $x=0$ in Equation (D.17) and $\Delta V^C_{CR}(0,0)$ is given in Equation (D.18).

$$\begin{aligned}V^C(x,t) &= \left(D(t,T_i) - \kappa D(t,T_{i+1})\right)\Phi(-d_1(x^* - \phi(t,T_i)x,t,T_i))\\ &\quad -D(t,T_i)\int_t^{T_i} R_1(x,t,t_1)\Phi(-\bar{d}_2(x^* - \phi(t,T_i)x,t,T_i,t_1)) - \bar{r}(t_1)\Phi(-d_1(x^* - \phi(t,T_i)x,t,T_i))dt_1\\ &\quad +\kappa D(t,T_{i+1})\int_t^{T_{i+1}} R_1(x,t,t_1)\Phi(-d_2(x^* - \phi(t,T_i)x,t,T_i,t_1)) - \bar{r}(t_1)\Phi(-d_1(x^* - \phi(t,T_i)x,t,T_i))dt_1\\ &\quad -\kappa D(t,T_{i+1})\int_{T_i}^{T_{i+1}} R_1(x,t,t_2)\int_t^{t_2} e^{\phi(t_1,t_2)\Sigma(t,t_1)}R_1(x,t,t_1)\Phi(-d_2^*(x^* - \phi(t,T_i)x,t,T_i,t_1,t_2))\\ &\quad -\bar{r}(t_1)\Phi(-d_1^*(x^* - \phi(t,T_i)x,t,T_i,t_1))dt_1dt_2\\ &\quad +\kappa D(t,T_{i+1})\int_{T_i}^{T_{i+1}} R_1(x,t,t_2)\int_t^{t_2} R_1(x,t,t_1)\Phi(-d_2(x^* - \phi(t,T_i)x,t,T_i,t_1))\\ &\quad -\bar{r}(t_1)\Phi(-d_1(x^* - \phi(t,T_i)x,t,T_i))dt_1dt_2\\ &\quad +\kappa D(t,T_{i+1})\int_{T_i}^{T_{i+1}} R_2(x,t,t_1)\Phi(-d_2(x^* - \phi(t,T_i)x,t,T_i,t_1))dt_1\end{aligned} \tag{D.17}$$

$$\begin{aligned}\Delta V^C_{CR}(0,0) &= D(0,T_i)\int\int_{\mathbb{R}^2} G_0(0,0,0;\xi,\zeta,T_i)\Delta V_{caplet}(\xi,T_i)d\zeta d\xi\\ &= \frac{D(0,T_i)}{K(T_i,T_{i+1})}\int_{\mathbb{R}}\varphi\left(\frac{\xi}{\sqrt{\Sigma(0,T_i)}}\right)\left(\frac{F_2(\xi,T_i,T_{i+1})}{K(T_i,T_{i+1})} - 1\right)\frac{\xi - x^*}{\sqrt{2K(T_i,T_{i+1})}}\varphi(-\bar{d}_2(\xi,T_i,T_{i+1}))d\xi\\ &= \frac{D(0,T_i)}{K(T_i,T_{i+1})}\int_{T_i}^{T_{i+1}}\bar{r}(t_2)\int_{T_i}^{t_2}\bar{r}(t_1)e^{\Delta x^*(T_i,t_1,t_2)}\left(e^{\phi(t_1,t_2)\Sigma(T_i,t_1)} - 1\right)\cdot\\ &\quad \left(\varphi(-d_2(x^* - \Delta x^*(T_i,t_1,t_2),0,T_i)) - \varphi(-d_2(x^*,0,T_i))\right)dt_1dt_2.\end{aligned} \tag{D.18}$$

□

E

Results comparative study

Maturity	HW imp vol	BK imp vol	Diff imp vol	HW price	BK price	Diff price
$1Y$	13,4	14,5	-1,04	$2,23 \cdot 10^{-3}$	0,01	$-3,34 \cdot 10^{-3}$
$2Y$	18,7	18,7	0,02	0,65	0,64	$3,31 \cdot 10^{-3}$
$3Y$	29,5	27,7	1,73	7,71	6,77	0,94
$4Y$	42,3	40,9	1,41	26,09	25,00	1,10
$5Y$	47,9	50,2	-2,33	45,77	47,81	-2,04
$6Y$	53,5	56,1	-2,58	65,86	68,28	-2,42
$7Y$	59,5	57,0	2,45	83,79	81,38	2,42
$8Y$	61,8	58,3	3,51	96,50	92,89	3,61
$9Y$	60,2	61,0	-0,83	104,39	105,27	-0,88
$10Y$	59,3	61,8	-2,50	111,92	114,65	-2,73
$11Y$	58,0	59,6	-1,65	116,14	117,99	-1,85
$12Y$	57,2	57,8	-0,51	113,38	113,98	-0,60
$13Y$	54,8	53,9	0,91	112,98	111,90	1,09
$14Y$	53,9	53,6	0,24	115,10	114,82	0,29
$15Y$	52,5	51,6	0,86	113,57	112,50	1,07

(a) Results for the 0.5% strike model

Table E.1: The forward Bachelier implied volatilities, in bps, from the Hull-White and Black-Karasinksi model with corresponding model prices. The forward implied volatilities correspond to caplets with a tenor of $1Y$ and notional of 10.000. (Continues on next page)

Maturity	HW imp vol	BK imp vol	Diff imp vol	HW price	BK price	Diff price
$1Y$	24,4	27,9	-3,44	$3,81 \cdot 10^{-4}$	$2,94 \cdot 10^{-3}$	$-2,56 \cdot 10^{-3}$
$2Y$	34,1	34,1	0,03	0,52	0,52	$2,58 \cdot 10^{-3}$
$3Y$	39,9	40,0	-0,07	3,75	3,77	-0,02
$4Y$	46,6	45,5	1,15	13,01	12,31	0,70
$5Y$	49,8	50,7	-0,83	25,91	26,58	-0,68
$6Y$	53,0	54,0	-1,03	40,49	41,47	-0,97
$7Y$	56,4	55,4	0,95	54,17	53,20	0,97
$8Y$	58,2	57,0	1,19	65,32	64,03	1,29
$9Y$	58,5	58,8	-0,34	74,37	74,76	-0,39
$10Y$	58,8	59,6	-0,77	82,80	83,70	-0,90
$11Y$	58,9	60,3	-1,31	88,64	90,23	-1,59
$12Y$	59,8	60,1	-0,34	88,91	89,34	-0,43
$13Y$	59,1	59,3	-0,18	90,98	91,21	-0,23
$14Y$	59,3	59,0	0,29	94,82	94,43	0,38
$15Y$	58,9	57,5	1,38	95,32	93,46	1,86

(b) Results for the 1% strike model

Maturity	HW imp vol	BK imp vol	Diff imp vol	HW price	BK price	Diff price
$1Y$	30,1	32,8	-2,75	$5,40 \cdot 10^{-6}$	$4,28 \cdot 10^{-5}$	$-3,73 \cdot 10^{-5}$
$2Y$	41,9	41,9	0,00	0,16	0,16	$-1,03 \cdot 10^{-5}$
$3Y$	47,3	48,1	-0,76	1,74	1,88	-0,14
$4Y$	52,8	52,1	0,73	7,19	6,88	0,31
$5Y$	55,4	55,7	-0,26	16,06	16,23	-0,17
$6Y$	56,8	56,9	-0,16	26,08	26,21	-0,13
$7Y$	56,8	56,7	0,14	34,51	34,38	0,13
$8Y$	57,3	57,0	0,31	42,74	42,42	0,32
$9Y$	58,2	58,3	-0,07	51,35	51,43	-0,08
$10Y$	59,0	59,2	-0,20	59,41	59,65	-0,24
$11Y$	59,2	59,7	-0,52	64,98	65,61	-0,63
$12Y$	59,3	58,9	0,31	65,15	64,75	0,39
$13Y$	58,3	58,2	0,16	66,98	66,78	0,21
$14Y$	58,0	58,2	-0,18	70,22	70,46	-0,24
$15Y$	57,4	57,2	0,20	70,73	70,46	0,28

(c) Results for the 1.5% strike model

Maturity	HW imp vol	BK imp vol	Diff imp vol	HW price	BK price	Diff price
$1Y$	34,1	$1,09 \cdot 10^{-2}$	34,06	$3,89 \cdot 10^{-8}$	0,00	$3,89 \cdot 10^{-8}$
$2Y$	47,5	47,5	$1,86 \cdot 10^{-3}$	0,04	0,04	$1,34 \cdot 10^{-5}$
$3Y$	53,4	54,0	-0,69	0,80	0,87	-0,07
$4Y$	59,2	58,1	1,08	4,27	3,96	0,31
$5Y$	62,0	62,5	-0,47	10,73	10,97	-0,25
$6Y$	62,4	62,6	-0,18	18,00	18,13	-0,13
$7Y$	60,5	60,3	0,16	23,24	23,11	0,13
$8Y$	59,6	59,0	0,62	28,89	28,33	0,57
$9Y$	60,1	60,1	-0,06	35,68	35,73	-0,06
$10Y$	60,4	60,8	-0,46	42,23	42,74	-0,51
$11Y$	60,3	61,4	-1,09	47,02	48,28	-1,26
$12Y$	60,3	59,7	0,56	47,66	46,99	0,67
$13Y$	59,5	59,4	0,02	49,65	49,63	0,02
$14Y$	59,1	59,3	-0,12	52,68	52,83	-0,15
$15Y$	58,6	58,0	0,56	53,50	52,78	0,72

(d) Results for the 2% strike model

Table E.1: (Continue) The forward Bachelier implied volatilities, in bps, from the Hull-White and Black-Karasinksi model with corresponding model prices. The forward implied volatilities correspond to caplets with a tenor of $1Y$ and notional of 10.000.

Bibliography

Albrecher, H., Binder, A., Lautscham, V., & Mayer, P. (2013). *Introduction to quantitative methods for financial markets*. Springer Science & Business Media.

Andersen, L., & Piterbarg, V. (2010). *Interest rate modeling*. Atlantic Financial Press.

Björk, T. (2004). *Arbitrage theory in continuous time* (Second Edition). Oxford University Press.

Brigo, D., & Mercurio, F. (2007). *Interest rate models- theory and practice: With smile, inflation and credit* (Second Edition). Springer Finance.

Clifford, P., Wang, Y., Zaboronski, O., & Zhang, K. (2010). Pricing options using trinomial trees.

Craig, W. (2018). *A course on partial differential equations*. American Mathematical Soc.

Delbaen, F., & Schachermayer, W. (2006). *The mathematics of arbitrage*. Springer.

Glasserman, P. (2004). *Monte carlo methods in financial engineering*. Springer Science & Business Media.

Higham, D. (2004). *An introduction to financial option valuation*. Cambridge University Press.

Hoorens, B. (2011). *On the cheyette short rate model with stochastic volatility* (Master's thesis). Delft University of Technology.

Iwashita, Y. (2014). Smile interpolation and extrapolation. *Technical Report 25, Open Gamma*.

Kirkwood, J. (2003). *Mathematical physics with partial differential equations*. Elsevier.

Klassen, T. (2001). Simple, fast, and flexible pricing of asian options. *Journal of Computational Finance*, *4*(3), 89–124.

Korn, R., Korn, E., & Kroisandt, G. (2010). *Monte carlo methods and models in finance and insurance* (First Edition). CRC Press.

Korn, R., & Stefanie, M. (2010). Binomial trees in option pricing—history, practical applications and recent developments. *Recent developments in applied probability and statistics* (pp. 59–77). Springer.

Kostiuk, A. (2004). *Multilevel constructions* (Doctoral dissertation). Technische Universität Kaiserslautern.

Oosterlee, C., & Grzelak, L. (2020). *Mathematical modeling and computation in finance*. World Scientific Publishing Europe Ltd.

Rice, J. (2007). *Mathematical statistics and data analysis* (Third Edition). Brooks/Cole, Cengage Learning.

Seifried, F. (2013). Interest rate theory: Financial mathematics ii. *Department of Mathematics University of Kaiserslautern*.

Shreve, S. (2004). *Stochastic calculus for finance ii; continuous-time models*. Springer.

Sterling, C. C., & Hári, N. (2007). Interest rate models; the hull-white model. *ING Bank Quantitative Analytics Team CMRM Trading*.

Turfus, C. (2019). Closed-form arrow-debreu pricing for the hull-white short rate model. *Quantitative Finance*, *19*(12), 2087–2094.

Turfus, C. (2020a). Analytic pricing of options on compounded rates. https://www.researchgate.net/publication/339739447_Analytic_Pricing_of_Options_on_Compounded_Rates

Turfus, C. (2020b). Caplet pricing with backward-looking rates. *Available at SSRN 3527091*.

Turfus, C. (2021). *Perturbation methods in credit derivatives: Strategies for efficient risk management* (First Edition). Wiley.

White, R., & Iwashita, Y. (2014). Eight ways to strip your caplets: An introduction to caplet stripping. *Technical Report 24, Open Gamma*.

Zayed, A. I. (2019). *Handbook of function and generalized function transformations*. CRC press.